Universität Bremen

Unraveling the Chukchi Shelf sediments: insights into past ice sheet extent and gas migration

---

Dissertation zur Erlangung des Titels Dr. rer. nat.

Thesis submitted in fulfillment of the requirements for the degree of Doctor of Natural Science (Dr.rer.nat.)

vorgelegt von:

Carsten Lehmann

February 2024

Faculty of Geoscience
University of Bremen

ALFRED-WEGENER-INSTITUT
HELMHOLTZ-ZENTRUM FÜR POLAR-
UND MEERESFORSCHUNG

HELMHOLTZ

Betreuer/Supervisor:
Prof. Dr. Wilfried Jokat

Gutachter / *Reviewer*:

Prof. Dr. Wilfried JOKAT
Alfred Wegener Institute Helmholtz Centre
for Polar and Marine Research
Am Alten Hafen 26
27568 Bremerhaven

Dr. Matthias FORWICK
UiT The Arctic University of Norway
Institutt for geovitenskap
Postboks 6050 Langnes
NO-9037 Tromsø

Tag des Kolloquiums / *Date of Colloquium*: 15.12.2023

Acknowledgments

At this point, it is my turn to thank the many people who supported me during my doctoral studies. A text can never reflect the gratitude for this help and support.

First and foremost, I would like to thank my supervisor Prof. Dr. Wilfried Jokat. He helped me in every step of this work with his vast knowledge of marine geophysics methods. He also answered my questions with passion and it did not matter how stupid the question was. He also mentally supported me through all the review processes and kept me on track. A special thanks also goes to Dr. Matthias Forwick for his interest in this work and willingness to co-review my thesis.

I would like to thank my office twin, Dr. Ursula Schlager. Together we endured all the problems of writing and data processing, were among the last people in the office during the COVID crisis, had long and interesting conversations about everything imaginable, and took many coffee breaks. She also gave me a lot of advice for this work. The same goes for my office mates Banafsheh Najjarifarizhendi, Johanna Gille-Petzold and Michaela Meier, who were always available for an encouraging chat or discussion.

I would also like to thank the entire geophysics department at the Alfred Wegener Institute for their support, helpful advice and discussions during the many lunch breaks, and excellent tips on how to improve my paper.

Special thanks to Bernard Coakley and the captain and crew of the R/V Marcus G. Langseth for the successful deployment of the instruments and data recovery, and to the U.S. National Science Foundation for funding the cruise MGL1112.

Finally, I would like to thank my entire family for their support throughout all phases of my work.

"Line 141: I would reconsider using very uncommon collocation "geoscientific knowledge": mixing greek and latin roots might not be the best wording choice."

Unknown Reviewer

(2021)

To my grandfather (*1927 - †2023)

Contents

List of Figures

List of Tables

Abstract

Marine geophysical methods can image the sedimentary deposits on the shelf areas and continental slopes. From the structures of these deposits, conclusions can be drawn about the existence of permafrost, gas and its migration through the sedimentary layers, and the past existence, extensions, and movements of ice sheets. Insights into past climatic conditions can be incorporated into numerical climate models and help to model the evolution of climate in the future. This work focuses on the depositional history of sediments on the outer Chukchi Shelf and the adjacent Chukchi Borderland. More broadly, the deposition of and erosion by ice masses resting on the seafloor during glacial periods, in particular a possible ice sheet along the Beringia continental margin, are investigated. For this purpose, reprocessed seismic reflection data recorded in 2011 as part of a research project on the tectonic past of the Chukchi Shelf by the research vessel *Marcus G. Langseth* are used.

Based on a seismostratigraphic analysis it was possible for the first time to describe a glacial unconformity on the Chukchi Shelf, which, comparable to an unconformity in the Barents Sea, indicates erosion of sediments by an ice sheet. Furthermore, characteristic seafloor structures are visible on the entire northern shelf area up to the continental margin of the Chukchi Shelf as well as the southern Chukchi Borderland. These indicate multiple ice masses advancing from different directions and at different times.

Along the Beringian continental margin the glacial deposits, which were pushed over the shelf edge by an ice sheet, show different thicknesses. In the central part of the continental margin between 165° E and 161°W, in extension of glacial troughs such as Scoresby Sound, massive glacial sediment deposits up to 450 m thick can be described. Away from these areas, there is no evidence of comparably thick glacial deposits in the seismic data. This allows conclusions to be drawn about the extent of an ice sheet on the Beringian continental margin as well as the flow dynamics of ice streams.

Furthermore, migration structures of rising methane are recognizable in the seismic data. Together with accumulations of gases in shallow sediments, these indicate the escape of methane into the water column. Due to the iceberg-fissured seafloor and the narrow strip of recorded multibeam echo sounder data on the seafloor, no surface features typical of gas seepage, such as pockmarks, can be identified. Furthermore, the seismic velocities indicate that there are no large-scale areas of marine permafrost (left) on the Chukchi Shelf.

In summary, these results reflect the glacial past of overlying ice masses and the potential for further methane outgassing on the shelf. The results obtained provide the basis for further geologic studies on this previously understudied continental margin.

Zusammenfassung

Marine geophysikalische Methoden können die Sedimentablagerungen auf den Schelf-gebieten und Kontinentalhängen darstellen. Aus den Strukturen dieser Ablagerun-gen können Rückschlüsse auf die Existenz von Permafrost, Gas und dessen Migration durch die Sedimentschichten und die frühere Existenz, Ausdehnungen und Bewegun-gen von Eisschilden gezogen werden. Erkenntnisse über die klimatischen Bedingun-gen in der Vergangenheit können in numerische Klimamodelle einfließen und helfen, die Entwicklung des Klimas in der Zukunft zu modellieren. Diese Arbeit fokussiert sich auf die Ablagerungsgeschichte von Sedimenten auf dem äußeren Tschukchen-schelf und des angrenzenden Tschukchen Grenzlands. Im weiteren Sinne werden die Ablagerungen von und Erosion durch während der Eiszeiten auf dem Meeres-boden aufliegenden Eismassen, insbesondere eines möglichen Eisschilds entlang des Kontinentalrands von Beringia, untersucht. Hierzu werden reprozessierte seismische Reflexionsdaten verwendet, welche 2011 im Rahmen eines Forschungsprojekts zur tektonischen Vergangenheit des Tschukschen Shelfs durch das Forschungsschiff *Marcus G. Langseth* aufgezeichnet wurden.

Aufgrund einer seismostratigraphischen Analyse ist es erstmals gelungen eine glazia-le Diskordanz auf dem Tschukschen Schelf zu beschreiben, welche, vergleichbar zu einer Diskordanz in der Barentssee, auf Erosion von Sedimenten durch ein Eisschild hinweist. Weiterhin sind auf dem gesamten nördlichen Schelfbereich bis zum Kon-tinentalrand des Tschukchen Schelfs sowie dem südlichen Tschukschen Grenzland charakteristische Strukturen des Meeresbodens sichtbar. Diese deuten auf mehrere, aus unterschiedlichen Richtungen und zu unterschiedlichen Zeiten vorstoßende Eis-massen hin.

Entlang des Beringischen Kontinentalrands zeigen die glazialen Ablagerungen, wel-che von einem Eisschild über die Schelfkante geschoben wurden, unterschiedliche Mächtigkeiten. Im zentralen Bereich des Kontinentalrands zwischen 165° E und 161°W, in Verlängerung glazialer Tröge wie dem Scoresby Sund, können massive glaziale Sedimentablagerungen von bis zu 450 m Mächtigkeit beschreiben werden. Abseits dieser Bereiche gibt es in den seismischen Daten keine Hinweise auf vergleich-bar mächtige, glaziale Ablagerungen. Dies lässt Rückschlüsse auf die Ausdehnung eines Eisschildes auf dem Beringischen Kontinentalrand sowie die Fließdynamiken der Eisströme zu.

Des weiteren sind in den seimischen Daten Migrationsstrukturen von aufsteigendem Methan erkennbar. Zusammen mit Akkumulationen von Gasen in flachen Sedimen-ten deuten diese auf das Austreten von Methan in die Wassersäule hin. Aufgrund

des von Eisbergen zerfurchten Meeresbodens und des schmalen Streifens der aufgezeichneten Fächerecholotdaten auf dem Meeresboden sind keine für den Gasaustritt typischen Oberflächenformen wie Pockmarks zu identifizieren. Weiterhin zeigen die seismischen Geschwindigkeiten, dass auf dem Tschukschen Schelf keine großflächigen Gebiete marinen Permafrosts (mehr) existieren.

Zusammenfassend spiegeln diese Ergebnisse die glaziale Vergangenheit von aufliegenden Eismassen und das Potenzial für weitere Methanausgasungen auf dem Schelfbereich wider. Die erzielten Ergebnisse bilden die Grundlage für weitere geologische Studien an diesem bisher wenig beachteten Kontinentalrand.

1. Introduction

Ongoing climate change affects the entire world and will affect it even more in the future (IPCC, 2021). Predicting the effects of climate change on current climate conditions relies on numerical models that consider, among other things, the cryosphere and natural gas seeps from submarine regions (Randall et al., 2007). These models are not only based on current conditions such as the extent and dynamics of ice sheets and permafrost regions, but also require information of their past geometries (Randall et al., 2007). In addition, it is also important to study methane sources and locate areas where methane leaks from the seafloor into the water column, as methane is a major contributor to global warming (Kerr, 2010). Significant methane sources are located in submarine areas of the Arctic Ocean (Fleischer et al., 2001; Kerr, 2010; Shakhova et al., 2010). Historically, studies in the Arctic Ocean have been difficult due to widespread thick, year-round sea ice (Kristoffersen et al., 2011). As a result, the geoscientific database is sparse not only for the deep-sea basins but also for the shelf areas surrounding the Arctic basins (Kristoffersen et al., 2011). The retreat of sea ice due to global warming in recent decades and improved technical equipment now allow more extensive scientific cruises to these previously difficult or inaccessible areas of the Arctic Ocean.

One of the areas surrounding the Arctic Ocean is Beringia, a biogeographic region between the Lena River in Siberia and the Mackenzie River in Canada (Figure 1.1) (Elias & Brigham-Grette, 2013). It has the world's largest epicontinental area (Jakobsson, 2002). Beringia includes the Chukchi and Kamchatka peninsulas in eastern Siberia and Alaska and the Yukon region in North America. It also includes the shelf areas of what are now the East Siberian, Chukchi, Bering, and Beaufort Seas. The Bering Strait divides Beringia in Siberia and Alaska and connects the Bering Sea in the Northern Pacific Ocean with the Chukchi Sea in the Arctic Ocean. The shallow Bering Strait emerged several times during Quaternary (2.58 Myrs – today) eustatic sea-level falls from the waxing and waning of ice sheets (Elias & Brigham-Grette, 2013; Hopkins, 1959). The existence of an ice sheet during Plio-Pleistocene glaciations in the Beringian region, particularly in the extensive and shallow northern shelf areas of the East Siberian and Chukchi seas, has long been debated (e.g., Brigham-Grette & Gualtieri, 2004; Grosswald & T. Hughes, 2002). The presence of glacial seafloor features such as mega scale glacial lineations,

moraines and grounding zone wedges on the Chukchi Shelf, Chukchi Borderland and the East Siberian Shelf are now considered evidence for the existence of such an ice sheet (Figure 1.1,Dove et al., 2014; S. Kim et al., 2021; Niessen et al., 2013; O´Regan et al., 2017). In addition, the existence of three glacial troughs on the northern continental margins also supports the former existence of such an ice sheet (Dove et al., 2014; S. Kim et al., 2021; O´Regan et al., 2017). However, it is not known when this ice sheet existed, how large its extent was, and in what direction its ice streams flowed. These questions are partly the subject of the present work.

The shelf regions of East Siberia and the Chukchi seas release large amounts of methane to the atmosphere (Li et al., 2017; Shakhova et al., 2005; Shakhova et al., 2010). In part, this is the result of thawing of submarine permafrost, biogenic methane production in shallow sediments, and/or migration of methane of thermogenic origin from deeper sediment layers to the seafloor (Li et al., 2017; Matveeva et al., 2015; Shakhova et al., 2010). During the last century, the shelf regions in the Chukchi region have been of commercial interest (Craddock & Houseknecht, 2016; Homza et al., 2019b). The oil and gas industry explored the American part of the Chukchi Shelf. The results report a huge hydrocarbon potential and a high possibility for gas release on the Chukchi Shelf south of 73° N due to the observation of widespread gas filled pockets (Bogoyavlenskiy & Kishankov, 2020; Hill et al., 2007; Homza et al., 2019b). Furthermore, authigenic carbonate formation was reported on the Chukchi Shelf north of 73° N as well as gas hydrate in gas mounds with an underlying bottom simulating reflection at the flank of the Chukchi Rise (Choi et al., 2022; Y.-G. Kim et al., 2020; Kolesnik et al., 2014). Analyses of the gas hydrates revealed a thermogenic origin at depths greater than 1 km (S. Kim et al., 2021). However, the gas migration pathways and their distribution between the Chukchi Shelf north of 73° and the Chukchi Borderland have not yet been described and are investigated in this thesis.

Despite the commercial exploration of the Chukchi Shelf region, the outer continental polar margins remain poorly resolved with geophysical data. In 2011, the R/V Marcus G. Langseth collected geophysical data in the outer Chukchi region (Figure 1.1c) to investigate the tectonic history and relationship between the Chukchi Shelf and the Chukchi Borderland (Coakley, 2011a; Coakley, 2011b; Ilhan & Coakley, 2018). The geophysical data (e.g., marine seismic data, bathymetry data, and sub bottom profiler data) recorded during the cruise were used to examine the topography of the seafloor and underlying sedimentary structures of the Chukchi region. The widespread influence of grounded ice was previously identified in the bathymetric and sub bottom profiler data (Dove et al., 2014). However, bathymetric and sub
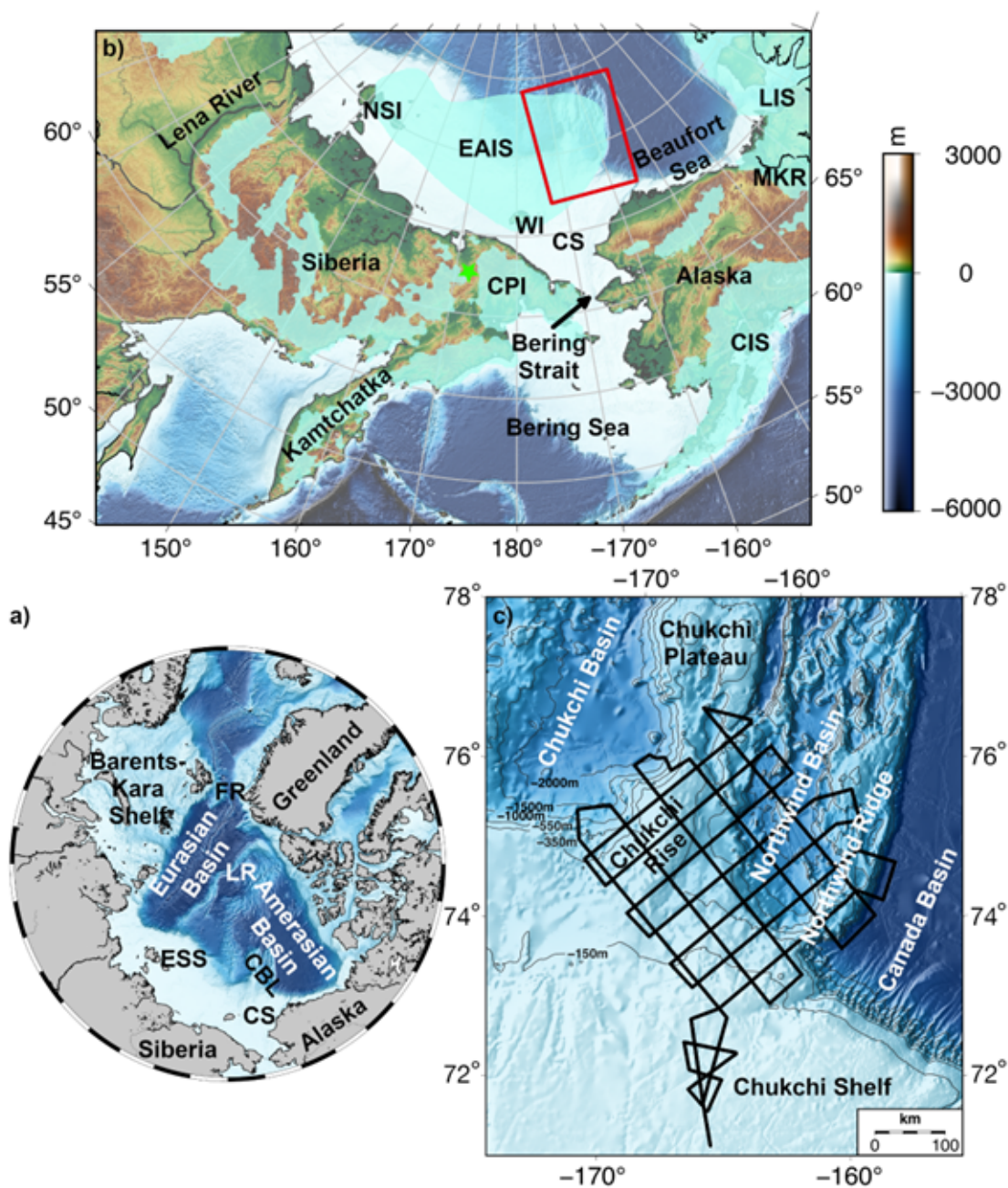
Figure 1.1. – Overview maps of a) the Arctic Ocean, b) the Beringian Region and c) the seismic grid of MGL1112 used in this study. Light blue shaded areas in b) represent suggested ice coverage independent of time, red star location of lake El'gygytgyn. Abbreviations: CBL - Chukchi Borderland, CIS – Cordilleran ice sheet, CPI - Chukchi Peninsula, CS - Chukchi Shelf, ESIS - East Siberian Ice Sheet, ESS - East Siberian Shelf, FR - Fram Strait, LIS - Laurentide Ice Sheet, LR - Lomonosov Ridge, MKR - Mackenzie River, NSI - New Siberian Islands, WI - Wrangel Island

bottom profiler data only map the topography of the seafloor and are not capable of resolving sedimentary structures at depths greater than 100 m below the seafloor (Dove et al., 2014). The recorded seismic data image deeper sedimentary sections and can, therefore, be used to study tectonic features such as faults and folds, as well as direct hydrocarbon indicators and glacial landforms (J. A. Dowdeswell et al., 2016; Nanda, 2021).

1.1. Outline of this thesis

This work is based primarily on the seismic dataset of the outer Chukchi Shelf and Chukchi Borderland obtained during cruise MGL1112 of the R/V Marcus G. Langseth in 2011 (Figure 1.1c). In addition, eight published seismic lines are used to map the slopes of the continental margin from the Lomonosov Ridge to the Beaufort Sea (Niessen et al., 2013; Nikishin et al., 2017; Triezenberg et al., 2016). The objective of this work is to examine the sedimentary structures to infer the possible existence and extent of past ice sheets on the Beringian Margin, as well as current gas and fluid migration and the existence of permafrost on the Chukchi Margin. The key questions are summarized in Section 1.2.

In Chapter 2, I briefly summarize the current knowledge of the geologic background of the Chukchi Shelf and Chukchi Borderland and introduce the discussion of the possible existence of an ice sheet on the northern Beringian Margin.

Marine seismic data, bathymetry data, and sub bottom profiler data are investigated in this thesis. However, multi-channel seismic data form the backbone of this work. Before these data can be interpreted, they must be processed. Processing increases the signal-to-noise ratio and provides an interpretable image of the subsurface. An overview of the data sets and seismic processing is provided in chapter 3.

The geophysical data were combined to provide an interpretable picture of the sedimentary structures of the seafloor and subsurface. Three articles were written for scientific journals to present the main results of this work. An overview of my contributions to each publication can be found in Chapter 4, and the articles can be found in Chapters 5 through 7.

The results of this study were summarized in the conclusions in chapter 8. The last chapter 9 of this thesis gives an outlook on possible future geoscientific investigations on the Chukchi Margin to gain further knowledge based on the results of this thesis.

1.2. Research Questions

1.2.1. Ice sheets on the outer Chukchi Shelf and the southern Chukchi Borderland

Ice sheets erode and shape subglacial sediments (J. A. Dowdeswell et al., 2016 and references therein). Bathymetric studies of the outer Chukchi Shelf reveal the widespread influence of grounded ice masses on the seafloor in this region (e.g., Dove et al., 2014; Jakobsson et al., 2005; Jakobsson et al., 2008; S. Kim et al., 2021; Polyak et al., 2007; Polyak et al., 2001). These comprise glacial erosion and glacial landforms such as mega scale glacial lineations and recessional moraines (Dove et al., 2014; Jakobsson et al., 2005; Jakobsson et al., 2008; S. Kim et al., 2021; Polyak et al., 2007; Polyak et al., 2001). However, glacial landforms on the seafloor show only the effect of the last glacial grounding event since subsequent ice sheets can overprint landforms of preceding ice sheets (Batchelor et al., 2013a). Studies of sub bottom profiler data indicate a layer of glacially shaped sediments covering the outer shelf regions (Dove et al., 2014; S. Kim et al., 2021). Due to the limited penetration depth of the echosounder data, these studies are restricted to the very shallow sediments of a few tens of meters (Dove et al., 2014; Jakobsson et al., 2016a). Therefore, the influence of grounded paleo ice masses on deeper sediments is investigated in this publication using seismic reflection data.

Research questions:
Which glacial landforms can be identified in geophysical data?
How are glacial sediments and landforms distributed along the Chukchi Shelf and Borderland?
Do the data reveal any evidence for an ice sheet in the Chukchi region?

1.2.2. Extent and dynamic of the East Siberian Ice Sheet

Ice sheets are capable of altering the surface of the Earth (J. A. Dowdeswell et al., 2016 and references therein). Depending on the frequency and duration of glaciation, the flow velocity of ice streams, and the available sediment reservoir, large amounts of sediment were subglacially eroded by ice sheets (Dahlgren et al., 2005; Laberg et al., 2012). These transported sediments were deposited on the shelf slope, and the shelf expanded basinward. Along the Greenland and Norwegian margins, for example, glacially transported sediments extended the continental margin by ~80 km and ~150 km, respectively (Nielsen et al., 2005; Rise et al., 2005). However, along the Beringian Margin, such glacially transported sediments have been poorly studied to this day.

Research questions:

Were glacial sediments deposited along the Beringian Margin?

Can lateral thickness variations of glacially transported sediments be determined to investigate the dynamics of the ice sheet?

Can these results be used to further constrain the extent of a former Beringian Ice Sheet?

Can the changes on the continental shelf caused by a Beringian Ice Sheet be compared to the Norwegian and Greenland continental margins in terms of duration and dynamics of glaciation(s)?

1.2.3. Migration of hydrocarbons and permafrost on the outer Chukchi Shelf

Methane is considered a significant contributor to climate change (Kerr, 2010). It is released naturally on land and on Arctic shelves by thawing permafrost, decay of gas hydrates, and upward migration from deep reservoirs (J.-H. Kim et al., 2020; Matveeva et al., 2015; Shakhova et al., 2010). The East Siberian and Western Chukchi shelves are believed to release large amounts of methane into the atmosphere (Bogoyavlenskiy & Kishankov, 2020; Li et al., 2017; Shakhova et al., 2005; Shakhova et al., 2010). Geoscientific studies have identified several areas in the Chukchi region that indicate the presence of shallow accumulated gas (Bogoyavlenskiy & Kishankov, 2020; Hill et al., 2007). Numerous gas inclusions are reported on the Chukchi Shelf south of 73° (Bogoyavlenskiy & Kishankov, 2020; Hill et al., 2007). At 74°7.2' N and 166°00.0' W, Kolesnik et al. (2014) described the presence of authigenic carbonate formations in dredged sediments. In addition, gas hydrates in sediment cores from gas mounds on the western flank of the Chukchi Shelf suggest a thermogenic origin at depths greater than 1 km (J.-H. Kim et al., 2020; Y.-G. Kim et al., 2020). However, the distribution and pathways of the upwelling gas as well as the possible extent of permafrost have not been described on the outer Chukchi Shelf yet.

Research questions:

Do seismic data show the (upward) migration structures of gas on the outer Chukchi Shelf?

Are the reported gas hydrates and migrations limited to the known locations or do more spots exist?

Do our seismic data show large submarine permafrost structures that could release large amounts of methane into the atmosphere through thawing?

2. A brief journey through the geologic history of the Chukchi Shelf and Chukchi Borderland

2.1. The Chukchi Region

The Arctic Ocean is surrounded by the landmasses of North America and Eurasia (Figure 1.1a). It is connected to the Atlantic Ocean through the deep Fram Strait and to the Pacific Ocean by the shallow Bering Strait (Figure 1.1a). The Arctic Ocean comprises two major basins, the younger Eurasian Basin and the older Amerasian Basin. Both are separated by the Lomonosov Ridge. The Eurasian Basin was formed by seafloor spreading that began to separate the Lomonosov Ridge from the Barents-Kara Shelf 56 Ma (Jokat et al., 1995; Kristoffersen et al., 1990; Vogt et al., 1979). This interpretation is based on magnetic spreading anomalies in the Eurasian Basin (Vogt et al., 1979). The Amerasian Basin was formed in the Jurassic to Early-Cretaceous (Grantz et al., 2011). However, its tectonic evolution is not well understood and still controversial (Grantz et al., 2011; Hutchinson et al., 2017; Ilhan & Coakley, 2018; Lawver et al., 1990). Especially, the location and development of the Chukchi Borderland cannot be fully explained by existing models of the opening of the Amerasian Basin (Hutchinson et al., 2017; Ilhan & Coakley, 2018; Lawver et al., 1990).

The Chukchi Shelf is part of the circum-Arctic continental shelf and located north of the Bering Strait bounded between Alaska and East Siberia. It encompasses an area of 620,000 km^2 with a width of up to 900 km (Jakobsson, 2002). The water depth ranges between <50 m and ~550 m, with a mean water depth of 80 m (Jakobsson, 2002). The Chukchi Shelf is partly prolonged northwards by the Chukchi Borderland which comprises the Chukchi Rise, Chukchi Plateau, the Northwind Basin and the Northwind Ridge (Figure 1.1c) (Hall et al., 1990). In total, the Chukchi Borderland covers ~420,000 km^2 (Hall et al., 1990). It consists of extended continental crust forming high standing continental blocks (Brumley et al., 2015; Hall et al., 1990; Ilhan & Coakley, 2018). The shallow plateaus of the Chukchi Borderland are at water depths of 246 m to 1000 m (Hall et al., 1990; Hunkins et al., 1962). They rise up to

3400 m above the surrounding deep-sea basins which are the Canada Basin (up to 3900 m water depth), the Mendeleev Abyssal Plain (up to 2900 m water depth) and the Chukchi Abyssal Plain (up to 2100 m water depth) (Hall et al., 1990; Johnson et al., 1990). The Northwind Basin has water depths up to 2110 m with seamounts reaching to water depths shallower than 1000 m (Hall et al., 1990).

2.1.1. Sediments on the Chukchi Shelf

The sediments covering the Chukchi Shelf are up to 18 km thick deposited since the late Devonian(?) (Sherwood et al., 2002; Homza et al., 2019b; Piskarev et al., 2018). Of these, the Cenozoic sediments, which reach a thickness of up to 9 km on the Chukchi Shelf southwest of the research area (Piskarev et al., 2018), are the focus of this work. The Cretaceous and Tertiary rocks overlying a Lower Cretaceous unconformity are assigned to the Brookian Megasequence (125 Myrs to 2.6 Myrs) (Sherwood et al., 2002). The Brookian Megasequence sediments consist of sediments derived from the Chukotka and Brooks Ranges in Siberia and Alaska, respectively. These sediments are separated by a 66-million-year-old Middle Brookian unconformity that divides the megasequence into the upper and lower Brookian Megasequence (Hegewald, 2012; Houseknecht & Bird, 2011; Moore et al., 1994; Sherwood et al., 2002). The sediments were deposited in large, northward-migrating clinoform complexes that were influenced by sea-level fluctuations and tilting from the inner shelf to the continental margin (Freiman et al., 2019; Houseknecht & Bird, 2011). In addition, the Brookian megasequence contains organic-rich, mostly marine sections that are good source rocks for oil and gas (Homza & Bergman, 2019).

Quaternary sediments covering the Chukchi Shelf are only 2 m thick in places on the inner shelf south of 71° N, but become thicker northward toward the margin (Houseknecht et al., 2016). Due to the lack of long sediment cores, their thickness on the outer shelf is not known. The few existing cores, up to 50 m in length, show sediments consisting mainly of conglomerate, (shallow) marine and non-marine sandstone, siltstone, and mudstone (Houseknecht et al., 2016; Sherwood et al., 2002). Sedimentation was influenced by eustatic fluctuating sea levels of up to 120 m, which led to flooding and drying of the Bering Strait, and by the intrusion of Pacific water currents into the Arctic Ocean in the past and present (Jakobsson et al., 2017; Matveeva et al., 2015). Furthermore, sediments were reworked by grounded ice masses, especially on the outer shelf areas close to the continental margin (see next section for more details).

2.2. History of the Beringian Ice Sheets

Continental glaciation around the Arctic Ocean is thought to have begun during the Ice Age around the Plio-Pleistocene transition ($\sim$2.6 Ma)(Jansen et al., 2000; Nielsen et al., 2005; Rise et al., 2005). However, the existence of ice sheets covering Beringia or at least parts of it during the Quaternary remains controversial (e.g., Brigham-Grette & Gualtieri, 2004; Grosswald & T. Hughes, 2002; Niessen et al., 2013; Zhang et al., 2020).
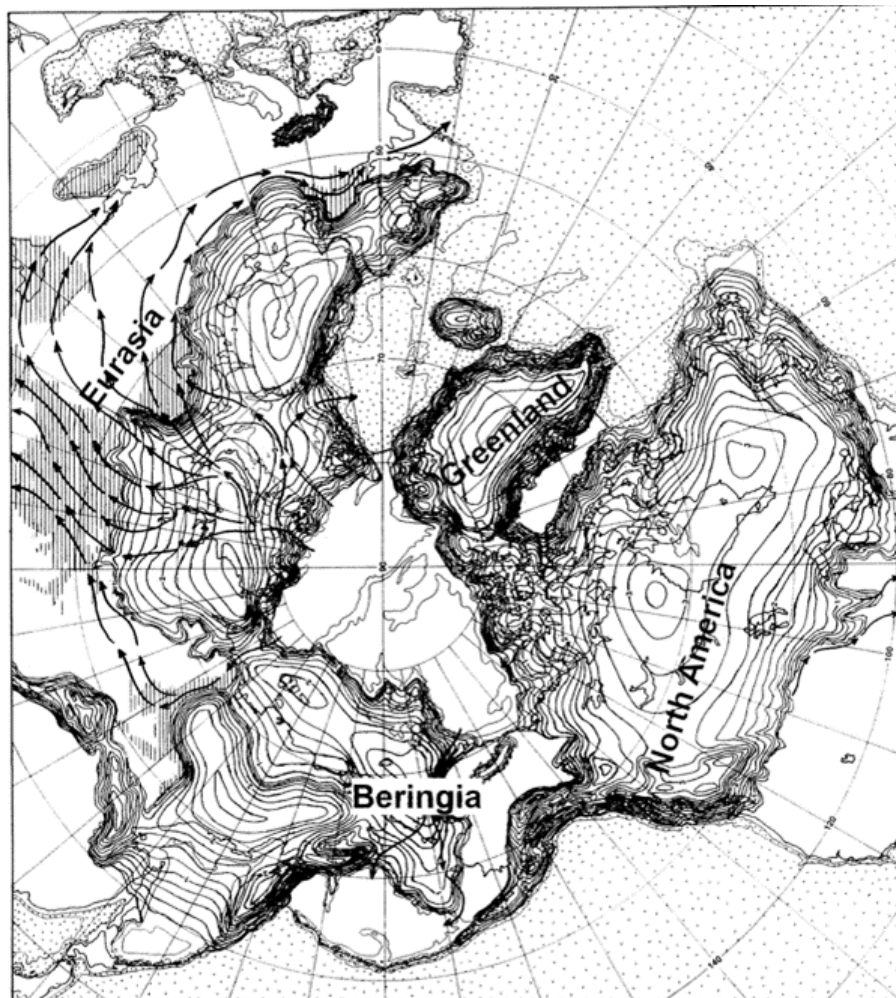
Figure 2.1. – Numerical reconstructions of Circum-Arctic ice sheets during the LGM with an ice sheet over Beringia. Ice sheet contours are given in 200 m interval. Modified after Grosswald & T. Hughes (2002)

In 1897, Baron Eduard Gustav von Toll assumed that at some time the New Siberian Islands were covered by an ice cap (Von Toll, 1897). Since then, the assumed maximum extent of the ice cap became larger and larger, and some authors hypothesized that large parts of Beringia were covered by an ice sheet (Grosswald, 1998; Gross-

wald & T. Hughes, 2002; T. Hughes et al., 1977; Zhang et al., 2018; Zhang et al., 2020). In addition, some authors speculated that such an ice sheet existed during the Last Glacial Maximum (LGM) (Figure 2.1) and that it was partially connected to a floating ice shelf in the Arctic Ocean (Grosswald, 1998; Grosswald & T. Hughes, 2002; T. Hughes et al., 1977). The strongest proponents of a Beringian Ice Sheet argued, based on satellite images, that the valleys in eastern Siberia follow a north-south direction and were formed by ice streams from north to south over Beringia (Grosswald, 1998). Further, they assumed ice domes on the shelf areas of the East Siberian and the Chukchi Sea interpreted from ice-shoved features (Grosswald, 1998; Grosswald & T. J. Hughes, 1995; Grosswald & T. Hughes, 2002). Numerical models showed that the existence of such an ice sheet was quite possible during the Quaternary (Colleoni et al., 2016; Grosswald & T. Hughes, 2002; Zhang et al., 2018; Zhang et al., 2020).

In contrast, the opponents of a Beringian Ice Sheet denied the existence of a continental ice sheet not only during the LGM and claimed that Beringia was never extensively glaciated (Barr & C. D. Clark, 2012; Brigham-Grette & Gualtieri, 2004; Glushkova, 2011; Kaufman et al., 2011; Melles et al., 2012). They assumed an alpine glaciation that never covered the Beringian continental lowlands (Barr & C. D. Clark, 2012; Glushkova, 2011; Kaufman et al., 2011). The strongest evidence for the absence of a Beringian Ice Sheet was found in Lake El'gygytgyn in northeastern Siberia (Figure 1.1b). The lake sediments show a constant lacustrine sediment deposition over 2.8 Myrs and indicate partial perennial ice cover of the lake, but no evidence of overconsolidation of the lake bottom caused by a thick ice sheet (Melles et al., 2012). Furthermore, there is no evidence of glacial rebound along Beringia's coasts (Heiser, 1997). Opponents of the Beringian Ice Sheet explain the moraines in Chukotka, Alaska, and in mountain valleys and some valley foothills as formed by glaciers (Barr & C. D. Clark, 2012; Glushkova, 2011; Kaufman et al., 2011), some of which also reached the now-flooded shelf areas (Brigham-Grette, 2001). The most extensive ice advance of glaciers was dated to pre-LGM times based on these moraines (Barr & C. D. Clark, 2012; Glushkova, 2011; Kaufman et al., 2011). Such an absence of an ice sheet at least during the LGM is further supported by mammoth bones and plant remains scattered across Beringia and Wrangel Island (Brigham-Grette & Gualtieri, 2004).

However, the rejection of a Beringian Ice Sheet again does not fit with the studies that show evidence for a more extensive grounding of ice masses on the northern Beringian shelves prior to the LGM (Dove et al., 2014; Hunkins et al., 1962; Jakobsson et al., 2014; Jakobsson et al., 2008; S. Kim et al., 2021; O´Regan et al., 2017).

The earliest documented evidence for grounded ice in the shelf region was provided by research camps on large ice floes that reported a scoured seafloor of the Chukchi Plateau in over 300 m water depth (Hunkins et al., 1962). Over decades, more and more data have been collected showing the widespread remnants of grounded ice masses along the entire Beringian continental margin. In the 21st century, the found mega-scale glacial lineations and moraines on the seafloor were interpreted as formed by continental margin-parallel ice advances from the Laurentide Ice Sheet (Engels et al., 2008) and/or speculatively formed by an ice sheet on the Chukchi Shelf (Polyak et al., 2007; Polyak et al., 2001). Jakobsson et al. (2008) published a different interpretation of these seafloor features suggesting that an ice rise with divergent ice flow directions had developed on the Chukchi Plateau. Niessen et al. (2013) published clear evidence in bathymetric and sub bottom echosounder data for an ice sheet grounded near the Arlis Plateau in up to 1200 m of water depth. From these and the previous reported seafloor features, they suggested the extent of a likely East Siberian Ice Sheet (ESIS) on the continental shelf (Figure 1.1b) and suspected several glacial advances of an ice sheet from the East Siberian Shelf (Niessen et al., 2013). Numerical models showed that the formation of such an ice sheet was possible (Colleoni et al., 2016). Further evidence for an ice sheet was provided by three later published bathymetric troughs on the continental shelf margin and subglacial features such as retreat moraines and large-scale lineations distributed over the outer Chukchi Shelf and the Chukchi Borderland (Dove et al., 2014; S. Kim et al., 2021; O´Regan et al., 2017). In addition, onshore geological studies on Wrangel Island and the New Siberian Islands (NSI) support the existence of an ice sheet on the shelf (Gualtieri et al., 2005; Nikolskiy et al., 2017). These studies reported glacial sediments and moraines on the northern NSI (Nikolskiy et al., 2017), and elevated shorelines and glacial till on Wrangel Island (Gualtieri et al., 2005; Gualtieri et al., 2003). Despite all the evidence found to date for Beringian Margin glaciation, estimation of the timing of glaciation(s) is complicated by the lack of sediment cores greater than ∼10 m in length on the shelf. The few existing piston and gravity cores yield evidence for ice grounding events during LGM (33 kyrs - 20 kyrs BP), marine isotope stage (MIS) 4 (71 kyrs - 57 kyrs BP), and MIS 6 (191 kyrs - 130 kyrs BP) (Joe et al., 2020; Park et al., 2017; Polyak et al., 2007; Wang et al., 2013; Ye et al., 2020). The earliest presumed glaciation of the Beringian Margin occurred in MIS 12 (478 kyrs - 424 kyrs BP) (Dong et al., 2017).

3. Methods

This study is mainly based on data collected by the R/V Marcus G. Langseth during cruise MGL1112 in September and October 2011. The aim of the project was to study the tectonic relationship between the Chukchi Shelf and the Borderland (Coakley, 2011b; Ilhan & Coakley, 2018). I reprocessed the data and used them to study sediments influenced by grounded ice, gas migrations in the sediments and the possible existence of permafrost. In this chapter, a brief introduction to the various hydro-acoustic methods used and the processing of the seismic reflection data is given.
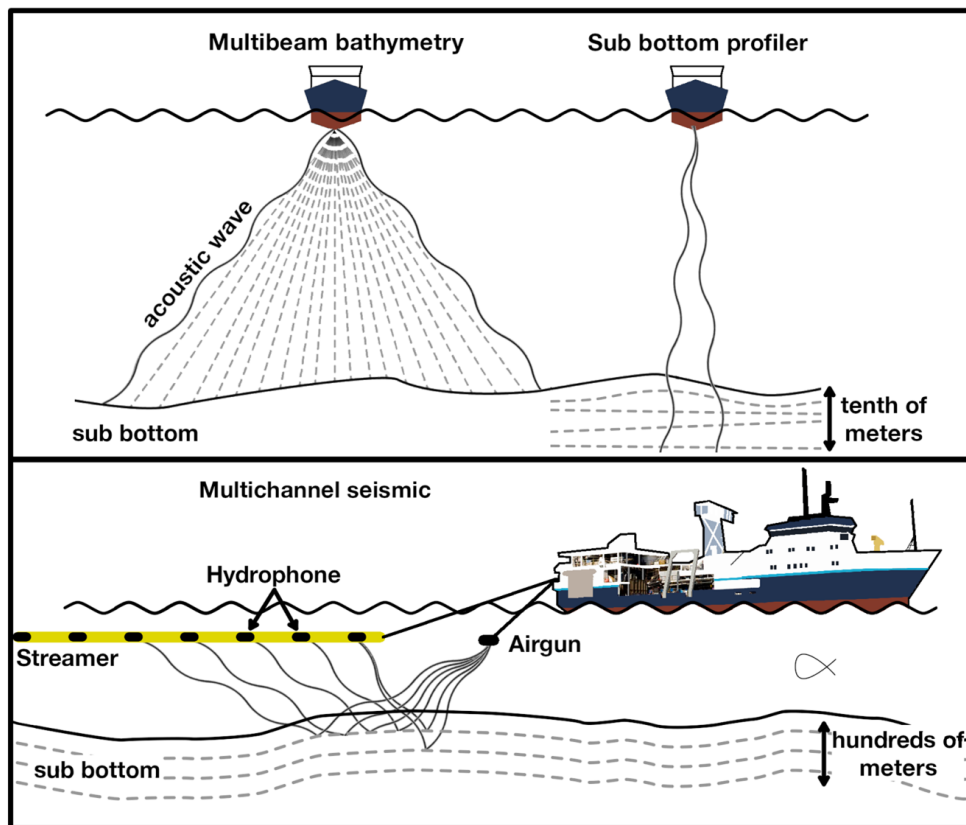
Figure 3.1. − Schematic principle of the hydroacoustic methods used, which also indicates the depth of penetration.

Hydro-acoustic methods such as multibeam bathymetry, seismic and sub bottom

profiler are used in marine environments to investigate the seafloor and its sub bottom (Jakobsson et al., 2016a; Nanda, 2021; Sheriff & Geldart, 1995). The main principle is based on the generation of a pulse-like acoustic wave (Figure 3.1). The generated acoustic wave propagates through liquid and solid media and is transmitted, reflected and refracted at interfaces of different media and/or different densities (Lurton, 2010). The travel time of the signal from the transmitter to the receiver and the amplitude of the returning signal are recorded with a receiver. The depth of the reflecting surface can then be calculated from the two-way travel times (TWT) together with the velocities of the water column and the subsurface. The penetration depth into the underlying medium and resolution of structures is dependent on the used frequency of the acoustic signal (Lurton, 2010). A higher frequency leads to higher resolution, but lower penetration depth, and vice versa (Lurton, 2010). More detailed information about hydroacoustic methods can be found in the literature (e.g., Jakobsson et al., 2016a; Lurton, 2010; Nanda, 2021; Yilmaz, 2001).

3.1. Multibeam bathymetric data

The multibeam technique aims to map the seafloor. The signal is transmitted and recorded in an across-track fan with several individual beams of acoustic waves (Figure 3.1). With modern multibeam systems, these fans reach typically opening angles between 130° and 150° with individual beam opening angles of 0.5° to 5° (Jakobsson et al., 2016a). The coverage width of the surveyed seafloor depends on the fan opening angle and the water depth. The water depth is determined from the acoustic velocity in water and the measured TWT of the signal reflected at the seafloor. During the entire cruise MGL1112, the hull mounted Knudsen EM122 12 kHz multibeam echo sounder was used for mapping the seafloor. The processing was performed on board with MB Systems. Grids were generated with a 50 x 50 m resolution.

3.2. Sub bottom profiler data

In contrast to multibeam echo sounders, sub bottom profilers (also called sediment profilers or sediment echosounders) are designed to study shallow sediments below the seafloor. They operate at frequency ranges between 1 and 20 kHz, with the commonly used frequency being 3.5 kHz (Jakobsson et al., 2016a). The signal should be emitted as vertically as possible below the vessel. The penetration depth of the signal is up to 100 m in sediments, but drops to a few tens of meters in more consolidated sediments, e.g., in formerly glacially covered areas (Jakobsson et al., 2016a). A Knudsen 3260 echo sounder system is installed on the R/V Marcus G. Langseth, which operated at a frequency of 3.5 kHz during cruise MGL1112.

3.3. Seismic data

Seismic reflection data are widely used to identify structures in the subsurface, especially in oil and gas exploration (Sheriff & Geldart, 1995). Various acoustic sources such as airguns, sparker, sleeve guns or boomers are used in marine settings. Here, I concentrate on airguns which were the source during MGL1112. Such airguns are towed behind the ship and generate acoustic waves with peak frequencies between 20 Hz and 100 Hz. The acoustic waves are generated hereby from compressed air which rapidly displaces the surrounding water. The returning reflected signal is recorded with hydrophones in streamers (Figure 3.1). Based on the travel times of the reflections and the seismic velocities, geological layers in the subsurface can be mapped. The recorded raw seismic data must be extensively processed to improve the signal-to-noise ratio by removing artifacts and by filtering, and to correct for the geological structure of the subsurface. Only after that the seismic data can be carefully interpreted.

The recorded grid of cruise MGL1112 comprises ~5300 km 2D multi-channel seismic (MCS) data (Figure 1.1c)(Coakley, 2011a; Coakley, 2011b). The acoustic waves were generated every 37.5 m with a tuned array of 10 Bolt airguns. Total volume of the guns was 1850 cubic inch (~30 l). However, differential GPS losses forced on some lines a change from the distance interval shooting to a time interval shooting of 12 s to keep the shot interval of ~37.5 m. A 5850 m long streamer with 468 hydrophones at 12,5 m group spacing was used to record the returning acoustic waves.

Additional published seismic reflection data were used for further interpretations along the Beringian Margin. Specific information on the data used is provided in the scientific article in chapter 6.

3.4. Seismic Data Processing

Originally, the seismic reflection data of MGL1112 were processed with a 25 m Common Depth Point (CDP) interval and interpreted for the tectonic evolution of the Chukchi Borderland by Ilhan & Coakley (2018). However, the CDP interval of the 25 m is too large to resolve near-surface sedimentary structures. Therefore, I reprocessed the extensive seismic dataset with a CDP interval of 6.25 m to refine the shallower sedimentary structures. The processing was performed as described in Yilmaz (2001).The data were processed with the seismic processing software Paradigm. The workflow image in Figure 3.2 was used to process seismic data of MGL1112.

The recorded seismic data were demultiplexed to convert the acquired data from
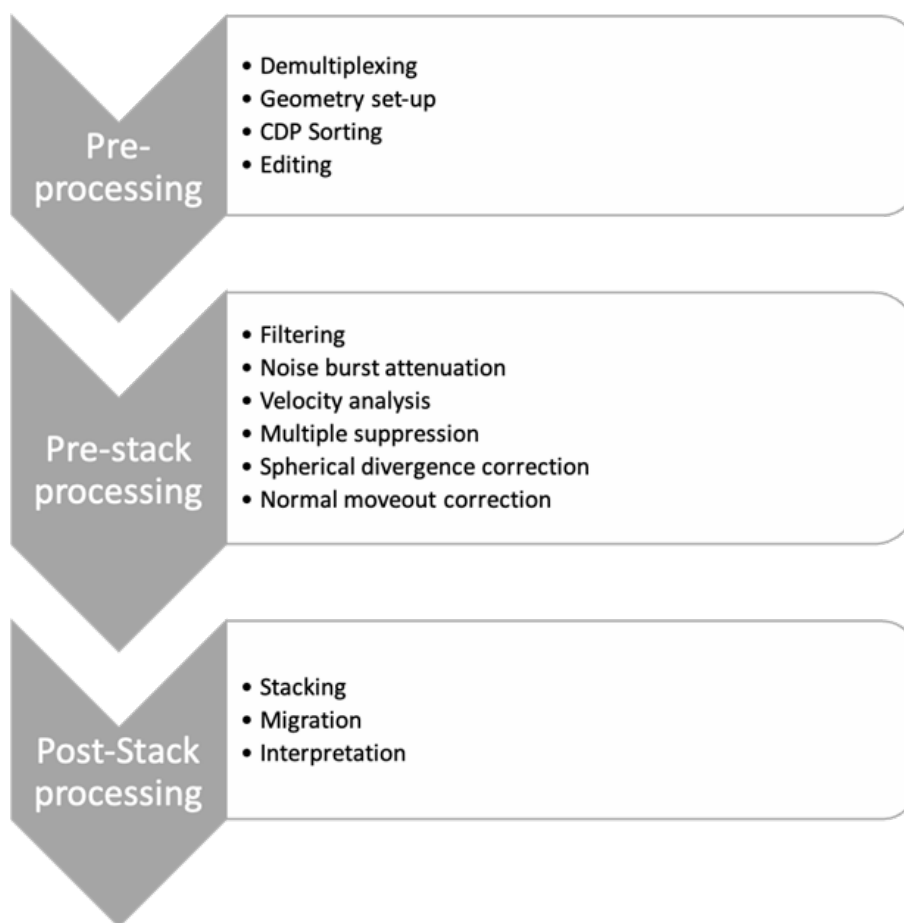
Figure 3.2. – Processing steps for seismic data.

storage format to readable seismic shot gathers. Afterwards, these shot gathers were tied to the navigation data, i.e., to latitude, longitude, course, and water depth. The shot gathers were resorted to CDP-gathers with a 6.25 m interval.

After CDP sorting, the seismic data were edited, i.e., noisy traces and bad or dead channels were removed. In addition, a noise burst filter was applied to suppress spikes. A band pass filter of 10 - 120 Hz with flanks from 5 and to 140 Hz was applied. Frequencies below 5 Hz and above 140 Hz were muted out. An interactive velocity analysis was performed to obtain a velocity model for each seismic reflection profile. Afterwards, a multiple suppression algorithm was applied which is explained in greater detail in section 3.4.2. Spherical divergence correction and normal moveout (NMO) correction with the obtained velocities were applied to the multiple suppressed data and the data were stacked. These stacks were migrated with an FK Kirchhoff migration. At last, a mean filter for smoothing was applied.

3.4.1. Weak seafloor reflection

In parts of the study area with water depths less than $100\,\mathrm{m}$ ($\sim$$130\,\mathrm{ms}$ TWT), seafloor and shallow sediment reflections are weak or not visible in the seismic data (Figure 3.3). This is the result of the interference of the direct wave with the seafloor and shallow subsurface reflections. Left panel of figure 5 shows a common shot gather (shot 1250 of profile 01C). At near offset traces, the seafloor reflection is indistinguishable from the direct wave. In the NMO-corrected CDP gather (Figure 3.3, right panel), which contains traces of shot 1250, the signal of the seafloor reflection at $100\,\mathrm{ms}$ is almost invisible on the first 3 traces. On larger offsets, the signals mixes and a low-frequency signal is produced.

Figure 3.3. – Interfering direct wave and seafloor reflection in shot 1250 (left) and CDP 7970 (right).

To avoid the problem of the interfering signals, a wider distance between the first channels and the gun source (offset) would be necessary. With a given water depth (h), assumed water sound velocity (v) and the duration of the source signal (t), the minimum offset (x) needed to avoid an interference between the direct wave signal and the reflection signal can be calculated:

$$x = \frac{4h^2 - t^2 \cdot v^2}{2t \cdot v} \tag{3.1}$$

Hence, for a water depth of h=$100\,\mathrm{m}$, an assumed water sound velocity of v=$1500\,\mathrm{m/s}$ and a source signal length of t=$20\,\mathrm{ms}$ the minimum offset calculates to $\sim$$651\,\mathrm{m}$ which is larger than the offset used for data acquisition during MGL1112 ($226\,\mathrm{m}$). Therefore, a different offset between the source and streamer must be used to resolve shallow sediments if seismic data are to be collected at these water depths.
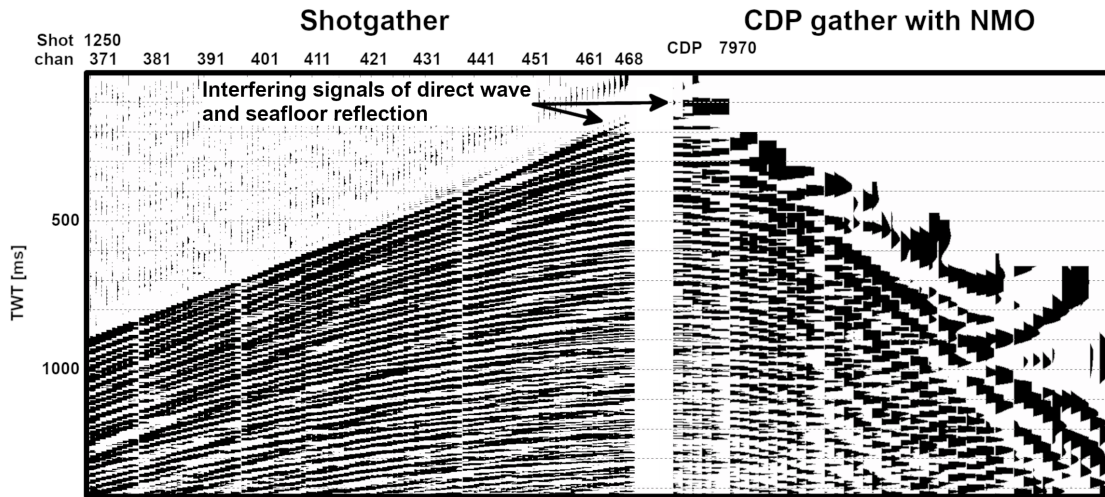
3.4.2. Multiple attenuation

This section describes methods for suppressing multiple reflections. Multiple reflections are secondary reflections with interbed and intrabed ray paths from more than one reflecting interface in the subsurface (Figure 3.4). The order of such a multiple depends on the number of reflections at an upper surface. A first-order surface multiple is reflected only once at an upper surface, e.g., the water surface (Figure 3.4b); a second-order multiple is reflected twice (Figure 3.4c). Multiple suppression/attenuation is important because the multiple signals can interfere with the primary signal, resulting in a poor signal-to-noise ratio or causing the data interpretation to be challenging because the multiple signal could be misinterpreted as a primary reflection (Yilmaz, 2001).
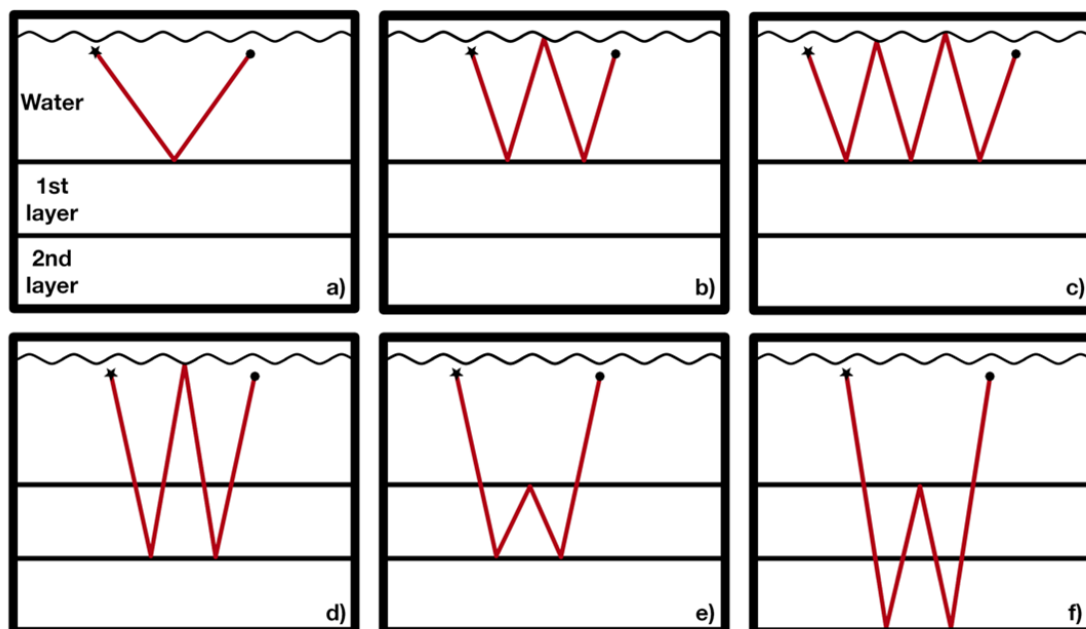
Figure 3.4. – Figure 6 Primary and multiple reflections. Stars indicate airgun source and black dot the receiver. (a) A primary reflection; (b) a first-order seafloor multiple; (c) a second-order seafloor multiple; d) a first-order free-surface multiple; (e) a first-order interbed multiple, f) first order intrabed multiple.

The simplest first order multiple in marine seismic is the so-called seafloor multiple (Figure 3.4b): The acoustic wave is reflected twice at the seabed and once with a downward reflection at the sea surface. The result is a signal that reaches the receiver with twice the time of the seafloor reflection. The seafloor multiple is usually the strongest multiple due to the high impedance contrast between the water column and the seafloor. The suppression of such multiples becomes more difficult with an irregular sub surfaces (Nanda, 2021). Especially on the Chukchi Shelf, in

water depths shallower than 350 m, it was difficult to remove the seafloor multiple. Reflections of the densely iceberg-scoured seafloor resulted in many diffraction hyperbolas in both the primary and the multiple reflections. These hyperbolas are common artifacts in formerly glaciated regions and are out-of-plane reflections related to the relatively narrow depressions of iceberg scours (Jakobsson et al., 2016a; Yilmaz, 2001). Such out of plane reflections result in a shift in the apex of the diffraction hyperbola and thus a shift in the periodicity of the multiple.

However, for a correct interpretation it is essential to remove the multiples from the data. Therefore, I tested several methods for multiple attenuation:

a) Predictive deconvolution
b) Radon transformation
c) F-k filtering
d) Surface related multiple prediction
e) Karhunen-Loeve transformation.

In the following, the results of the different methods are discussed on the example of one CDP after a short explanation of those methods. Detailed explanations are given in e.g., Sheriff & Geldart, 1995; Verschuur, 2013; Yilmaz, 2001. The input data for the multiple methods are shown in panels I of Figure 3.5 a and b. The seafloor signal arrives at ~400 ms. Mulitple signals are the down dipping reflections at ~800 ms, ~1200 ms and ~1600 ms, respectively. The signal of the first multiple has a strength of ~-5 dB.
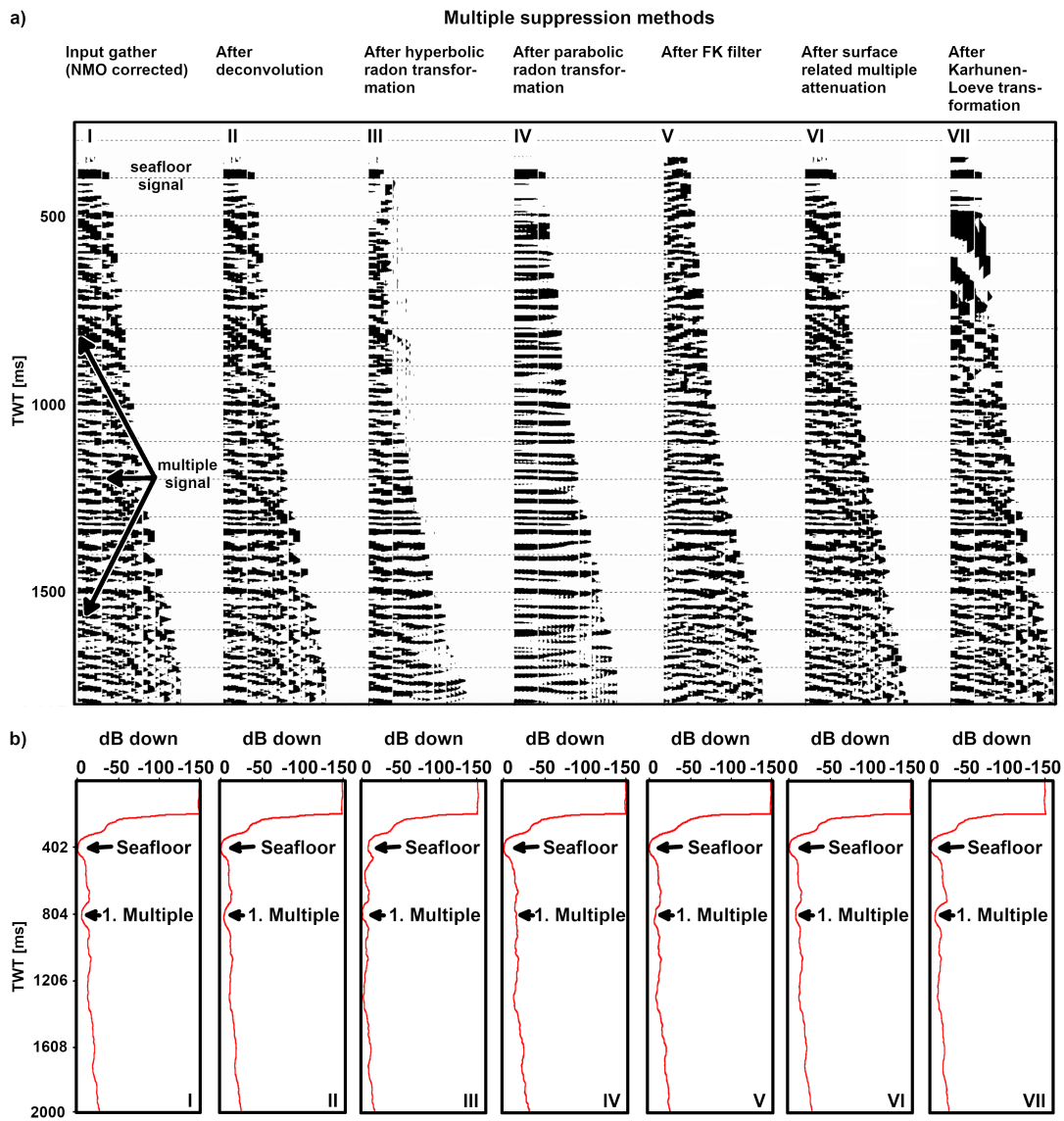
Figure 3.5. – Multiple attenuation for CDP 22000 on profile 01E. a) Results of different multiple attenuation methods. b) showing the time variant energy distribution of the CDP 22000 in dB

a) Predictive deconvolution

In general, the deconvolution process aims to remove a previous convolution process (Yilmaz, 2001). In seismic reflection data, the convolution process results from the convolution of the acoustic source signal with the earth's reflectivity (Yilmaz, 2001). In seismic processing, the predictive deconvolution process removes periodic signals like reverberations and multiples (Verschuur, 2013; Yilmaz, 2001). An autocorrelation is used to determine the operator lengths, which is the signal length of the wavelet, and the prediction length, which is the time between the primary signal and the multiple signal.

The panel II in figure 3.5 shows the predictive deconvolution result for CDP 22000 of line 01E. The seafloor is imaged at $\sim$400 ms and the first multiple occurs at $\sim$800 ms. The deconvolution result is not significantly different from the input data. The reflections up to 100 ms below the seafloor show low frequency noise. Further, multiple parabolas are still imaged. This is confirmed by the gain analysis below (Figure 3.5b), which shows a similar decrease in multiple energy as in the input CDP ($\sim$-5 dB). Only a temporal shift of the peak of the multiple energy by a few milliseconds is observed.

b) Radon transformation:

Radon Transformation is a method to suppress coherent events such as multiples almost artifact free. Hereby, the data in the x-t (offset-time) domain are transformed into the tau-p domain (Yilmaz, 2001; Verschuur, 2013), where tau is the intercept time at zero offset and p the ray parameter. In the tau-p domain, certain signals such as primary and multiple signals, direct arrivals, ground-roll, airwave are mapped into separate regions (Verschuur, 2013). The separation of the different wave types makes elimination of a certain wave type possible. The transformation into the tau-p domain is possible via linear, parabolic or hyperbolic transformation (Verschuur, 2013; Yilmaz, 2001).

hyperbolic: Reflections in seismic CDP gathers are imaged as hyperbolic events (Yilmaz, 2001). Due to the different velocities, simultaneously arriving primary and multiple signals have different dips in the x-t domain. Hyperbolic reflections are mapped as ellipses in the tau-p domain and both signals are imaged separately in the tau-p domain after a hyperbolic radon transformation. The hyperbolic Radon transformation is defined by:

$$u(q, \tau) = \sum_x d(x, \tau^2 + qx^2) \tag{3.2}$$

$u(q, \tau)$ is the radon transformed seismogram and $d(x, t)$ the original seismogram where two-way traveltime $t = \tau^2 + qx^2$. q is $\frac{1}{v}$ and v is the stacking velocity. τ is the two-way zero-offset time, x is the offset.

By choosing velocity limits that are slightly higher and slower the velocity of the primary signal, it is possible to transform only certain reflections in the forward Radon transform. Therefore, multiples are not transformed into the tau-p domain. After transforming back to the t-x domain, the multiple signals are filtered out.

Panel III in figure 3.5a shows the result of the hyperbolic Radon transformation. Downward sloping multiple signals are suppressed especially after 1000 ms TWT and the flattened, NMO-corrected primary signal remains. Before 1000 ms TWT, however, it is not possible to see a coherent primary signal for near-offset traces with sequence numbers <4. For sequence numbers >4, the traces show an attenuated to no signal. Moreover, the decaying multiple signal is still preserved at 800 ms. Even the amplitudes show a ~10 dB increased multiple signal at 800 ms compared to the seafloor.

Parabolic: Multiple reflections are mapped as parabolic events in NMO-corrected CDP gathers (Hampson, 1986). The parabolic Radon transform sums the amplitude along these parabolas and maps these events in the tau-p domain as focused points. Via a forward and reverse parabolic Radon transformation with defined velocities, e.g., from the velocity analysis, the NMO-corrected primary signal can be filtered out and a seismogram containing only multiples is created. This seismogram is subtracted from the NMO-corrected seismogram and the primary signal is preserved. The parabolic Radon transformation is defined by:

$$u(q, \tau) = \sum_x d(x, \tau + qx^2) \tag{3.3}$$

Here, in $d(x, t)$ the travel time t is substituted by $\tau + qx^2$.
The result of the parabolic radon transformation is a flattened primary signal with suppressed dipping multiple signal (panel IV in figure 3.5a). In the amplitude energy analysis, the peak of multiple energy at 800 ms has disappeared and decreased to ~-15 dB (panel IV Figure 3.5b). However, reflections in a range of 400 ms to 500 ms TWT are also weakened compared to the input data (panel I in Figure 3.5b).

c) F-k filtering

A two-dimensional Fourier transformation is used to transform data from the x-t (offset-time) in the f-k (frequency-wavenumber) domain. It is defined as:

$$f_{k,l} = \sum_{m=0}^{M-1} \sum_{n=0}^{N-1} F_{m,n} \cdot e^{-2\pi i \frac{mk}{M}} e^{-2\pi i \frac{nl}{N}} \text{ for } k = 0, ..., M-1 \text{ and } l = 0, ...N-1 \quad (3.4)$$

f is transformed matrix with size of M x N. k and l are rows and columns, respectively. F are the data in the x-t domain.

Multiple signals have a slower seismic velocity than the primary signal recorded at the same time and still dip downward after a NMO correction (Figure 3.6a). Therefore, it is possible to overcorrect the data in the x-t domain in such a way that the primary signal is overcorrected (dip upwards) and the multiple signal is undercorrected (dip downwards) (Figure 3.6b). The different gradients of coherent signals can be distinguished in the f-k domain. The primary signals with an upward dip (decreasing travel time with increasing offset) are shown in the negative wavenumber region (Figure 3.6b). In contrast, the multiples have a downward dip (increasing travel time with decreasing offset) and are displayed in the range of positive wavenumbers (Figure 3.6b). After muting the positive wavenumbers in the f-k domain (Figure 3.6c), the remaining signal is transformed back to the x-t domain (Figure 3.6d).

Panel V in figure 3.5 shows the multiple suppression with f-k filtering. Multiple signals at 800 ms and 1200 ms could be nearly suppressed (Figure 3.5b, panel V). The peak energy of the first multiple at ~800 ms is reduced to ~-10 dB compared to the seafloor energy at ~400 ms TWT. The multiple energy almost meets the surrounding primary signal energy. However, the seismic sections still show many multiple artifacts (e.g., dipping signal after 1400 ms TWT) and a distorted seafloor reflection compared to the input data.

d) Surface Related Multiple Attenuation
A different way to suppress multiples is the surface-related multiple attenuation. Surface-related multiples (Figure 3.4b, c, d) are typically the strongest multiple events present in the seismic data and can be considered as two primary ray paths connected at the point of surface reflection (Verschuur, 2013). Verschuur et al. (1992) stated that these multiples can be predicted by the convolution and summation of common source and common receiver gathers. The advantage is that no knowledge of the subsurface structure, such as velocities, is required (Verschuur, 2013).

A multiple model for each shot gather is calculated by Taylor expansions of the

multiple prediction operator:

$$P_0 = P - \left(\frac{R}{S(\omega)}\right)[P]^2 + \left(\frac{R}{S(\omega)}\right)^2 [P]^3 + ... = T_0 + T_1 + T_2 + ... \qquad (3.5)$$

The matrix P_0 represents multiple-free data. The zero-order Taylor term $T_0 = P$ in the expansion is the seismic input data itself, containing both the primary reflections and multiples of different orders. The first order Taylor term T_1 ($T_1 = -\frac{R}{S(\omega)}P^2$) contains the first order multiples and all other higher order multiples except the primary reflection. R is the reflection coefficient at the free surface. $S(\omega)$ is the frequency function of the source signal, which is usually set to a spike function. This leads to a bias in the predicted multiple events as the predicted multiples have the correct two-way travel time but have different amplitudes and wavelet shapes than in the input data. Therefore, the multiples are subtracted from the original shot gather data by a least-squares matching filter.

This process is computationally intensive and the maximum frequency should be reduced before multiple prediction. Theoretically, a zero offset of the shot-gathering data is required, and the shot interval must be equal to the receiver interval. Since the data do not have a zero offset, the missing offsets must be extrapolated before prediction. To achieve an equal shot-receiver interval, the algorithm in ECHOS copies the nearest tracks and places them at the location of missing traces.

The result of the surface related multiple attenuation is imaged in panel VI of figure 3.5a. Optically the multiple at 800 ms was slightly suppressed in the seismogram compared to the input traces (Figure 3.5a, panel I). Few improvements of the primary signal are also observable in the seismogram at 900 ms (Figure 3.5a, panel VI). The amplitude analysis supports the slight improvement but still shows a peak maximum of $\sim$-10 dB at the multiple arrival time around 800 ms (Figure 3.5b, panel VI).
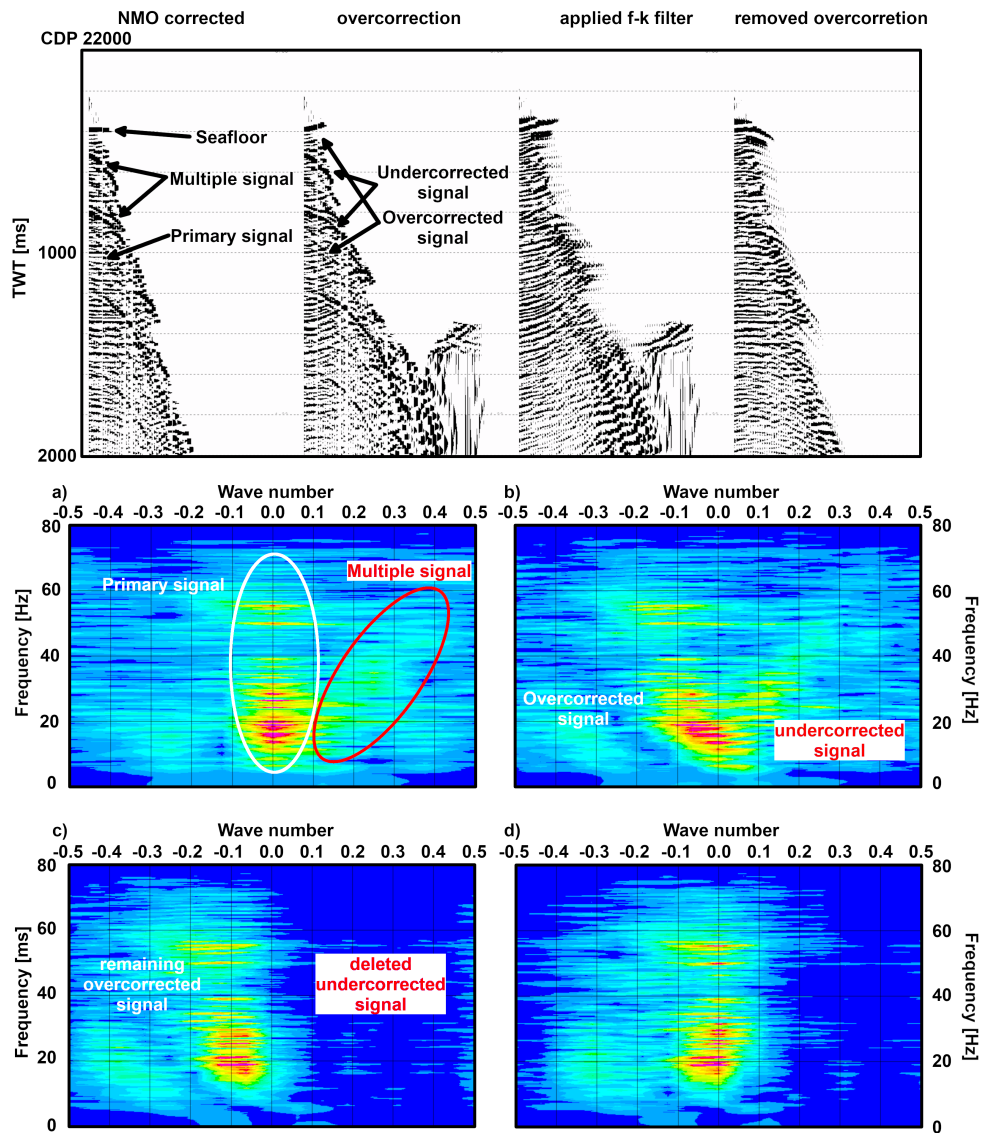
Figure 3.6. − Steps of overcorrection and result of f-k multiple filtering. Upper panels show seismogram of one CDP. Lower panels show to upper panels corresponding energy in f-k domain.

e) Karhunen-Loeve transformation

The basic concept of the Karhunen-Loeve transformation is the different move-out of multiple and primary signals (Al-Yahya, 1991). After NMO correction, the Karhunen-Loeve transform is applied to seismic trace gathers and forms a covariance matrix from the dot products of all the pairs of traces in the gather (Al-Yahya, 1991). Then it computes eigenvalues and eigenvectors for this matrix. The data are transformed back to the x-t domain by storing only the two main eigenvectors. This results in preserving only the flat events.

The result of the multiple suppression using the Karhunen-Loeve transformation is imaged in panel VII of figure 3.5a. The first change compared to the input data, is the strong dipping artifact after 500 ms. Below 700 ms no improvement to the input data could be achieved. This is also evident in the amplitude energy analysis with a peak of ∼-5 dB at 800 ms (Figure 3.5b, panel VII). In addition, the analysis also shows a higher amplitude reduction of ∼-20 dB between the primary signal and the seafloor and first multiple peaks at 400 ms and at 800 ms, respectively.

Results of Multiple Attenuation

The multiple attenuation results shown so far represent only one CPD of profile 01E and thus only one point of the profile. Since the different methods showed different results and sometimes visually strong improvements, a comparison of the different methods in a stacked section is useful. The NMO-corrected and stacked section without multiple suppression is shown in figure 3.7. The resulting stacks of the different applied methods are shown in Figures. 3.8 - 3.13. The seafloor of the stacked section in profile 01E is densely plowed by icebergs. This is evident from many overlapping hyperbolas which are also visible in the first seafloor multiple mapped from CDP 23000 at ∼1000 ms and ∼1500 ms TWT, over ∼500 ms TWT and ∼1000 ms TWT in the central stack to ∼600 ms TWT and ∼1200 ms TWT at CDP 13000 in Figures 3.7 - 3.13). The multiple is highlighted with a red stippled line in figure 3.7 for better visibility.

As can be seen, the multiples are not suppressed in any of the stacks (Figures 3.8 - 3.13). In particular, the predictive deconvolution (Figure 3.8), the parabolic Radon transform (Figure 3.10), and the Karhunen-Loeve transform (Figure 3.13) show a thicker seafloor reflection representing lower frequencies. The hyperbolic radon transform reduced the energy of the primary signal (Figure 3.9). The surface-related multiple attenuation reduced many of the diffraction branches but left clearly visible multiple artifacts in the stack (Figure 3.12). The best result was obtained with the f-k filter (Figure 3.11). However, the multiples are still not completely suppressed

and diffraction branches are still visible. Therefore, further steps were necessary to achieve multiple suppression for the final, almost multiple free stack. Since the f-k filter already provided a good multiple suppression, it was combined with a preceding f-k coherence dip filter. The coherence dip filter improved the coherence of the overcorrected signals and already removed some extremely undercorrected multiple signals before using the f-k filter. However, since primary and multiple signals have the same dips at near offsets, it is often not possible to distinguish between the two. For this purpose, the near offsets were muted to improve the multiple suppression result. A final improvement was the use of a mean filter applied to the migrated stack (Figure 3.14) to attenuate steep diffraction branches. Examples of other tested combinations of multiple suppression methods with poor results are listed in the Appendix (Figures A.1 - A.5).
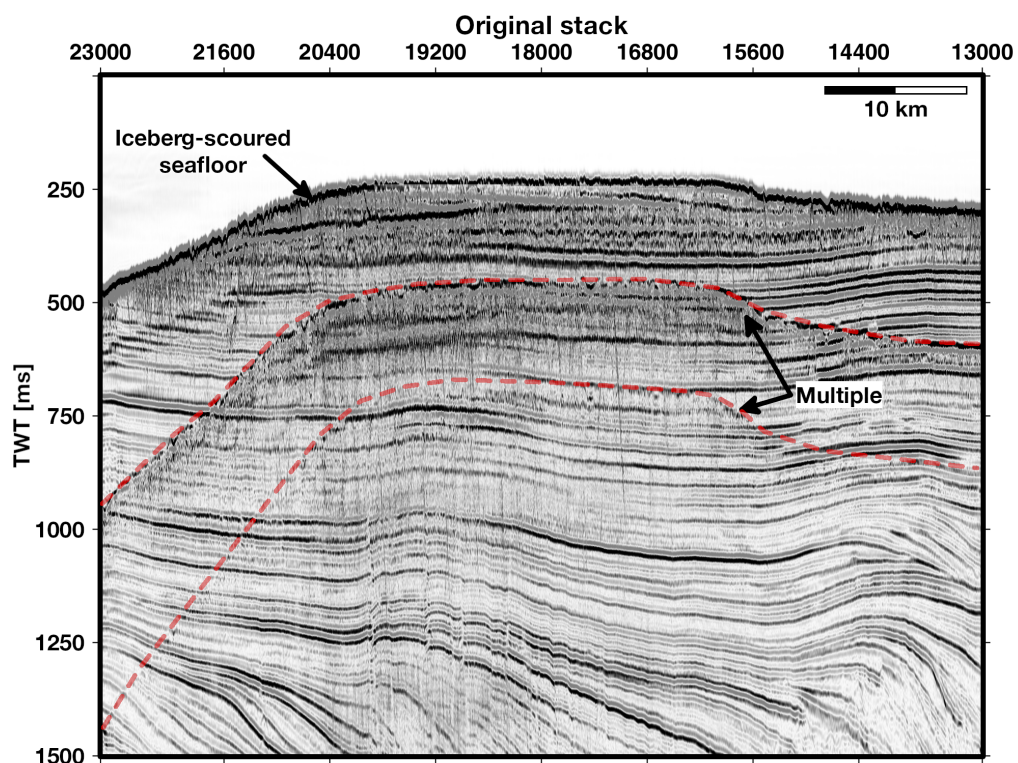
Figure 3.7. − Stacked section of profile 01E before multiple attenuation.

After Deconvolution

23000   21600   20400   19200   18000   16800   15600   14400   13000

Low frequent shallow reflections

Multiple artifacts

TWT [ms]

250

500

750

1000

1250

1500
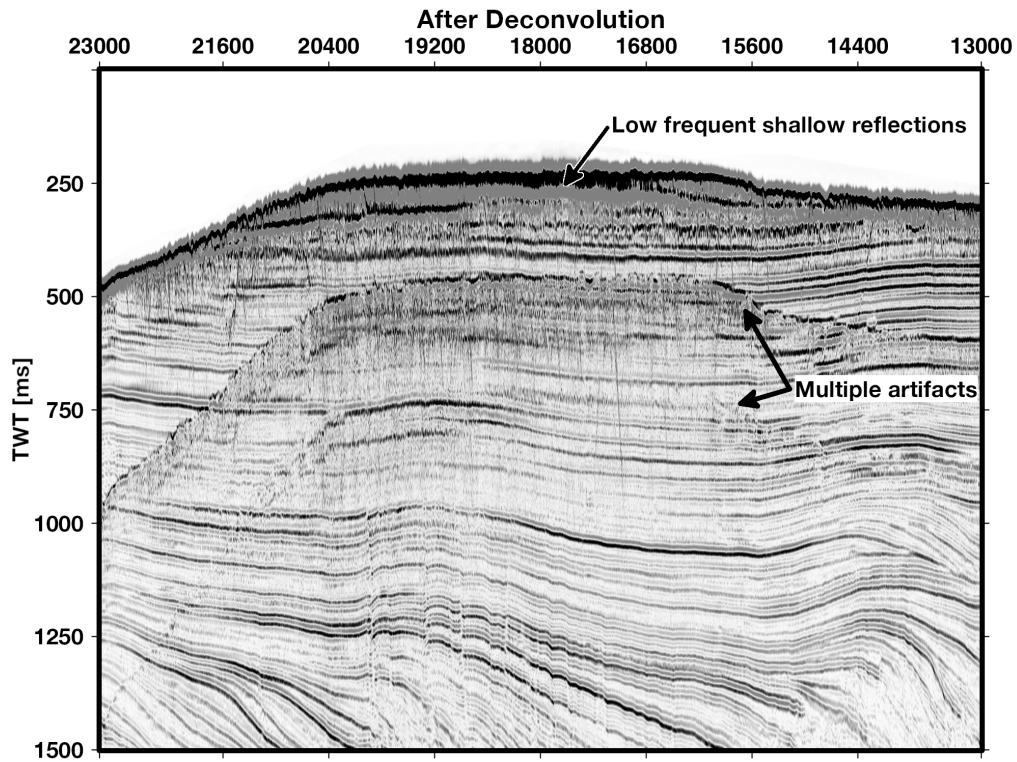
Figure 3.8. – Stacked section of profile 01E after a predictive deconvolution.

After hyperbolic radon transformation

23000   21600   20400   19200   18000   16800   15600   14400   13000

Reduction of primary signal

Multiple artifacts

TWT [ms]

250

500

750

1000

1250

1500
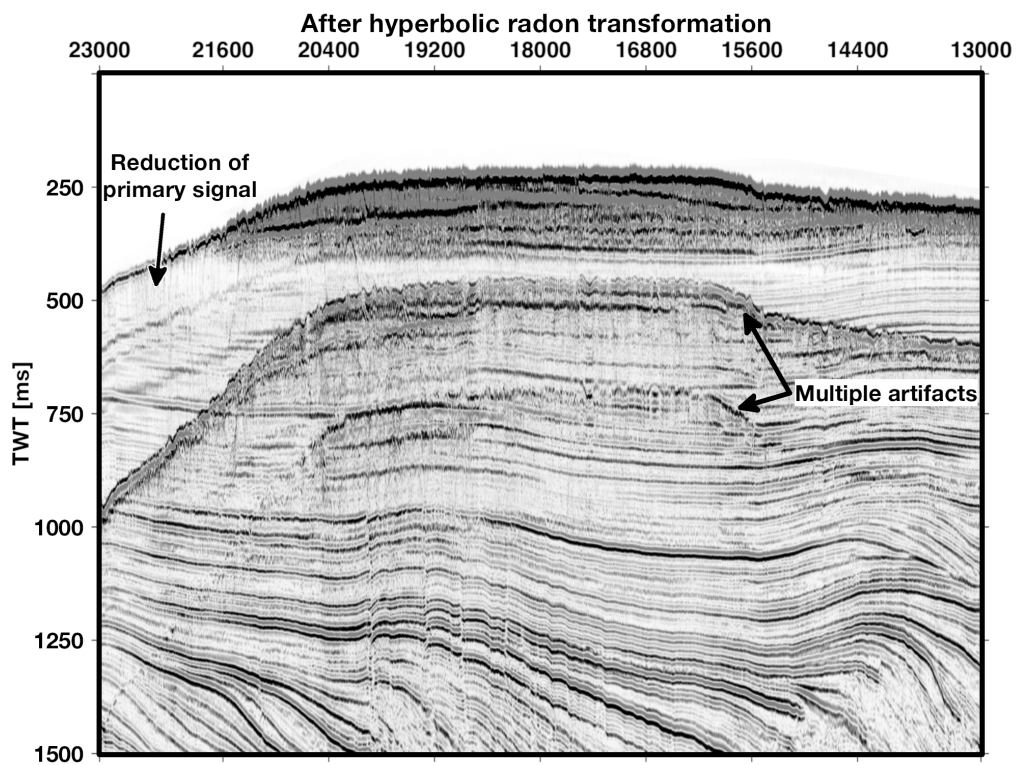
Figure 3.9. – Stacked section of profile 01E after hyperbolic multiple attenuation.

After parabolic radon transformation
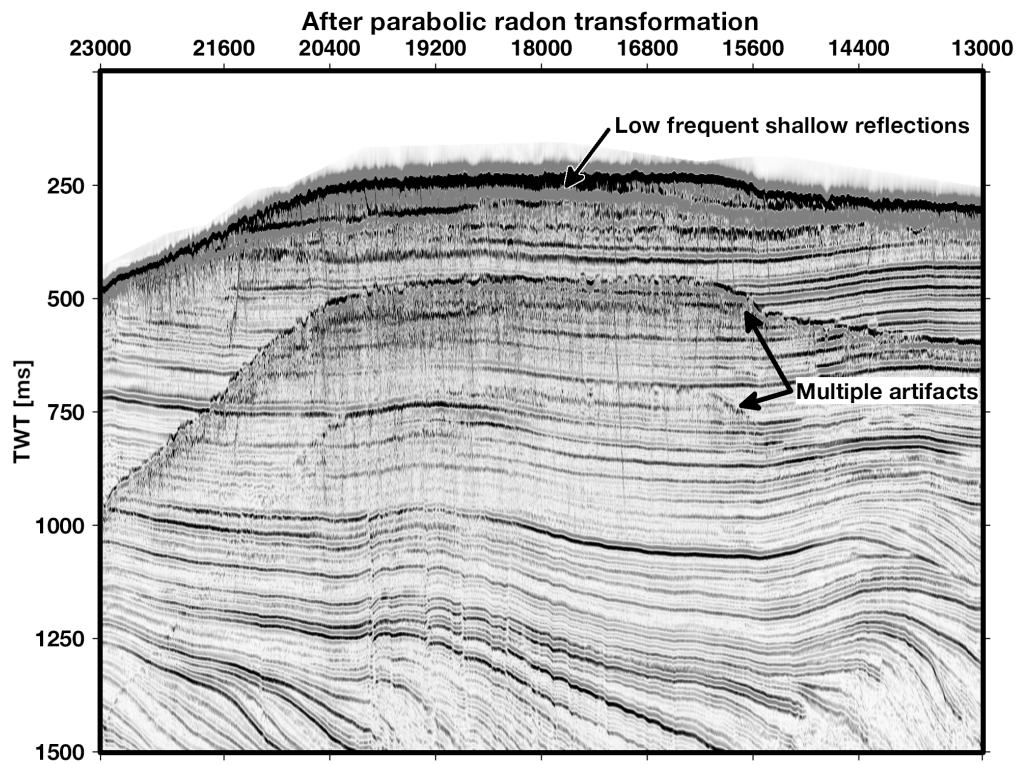
Figure 3.10. − Stacked section of profile 01E after parabolic multiple attenuation.

After FK transformation
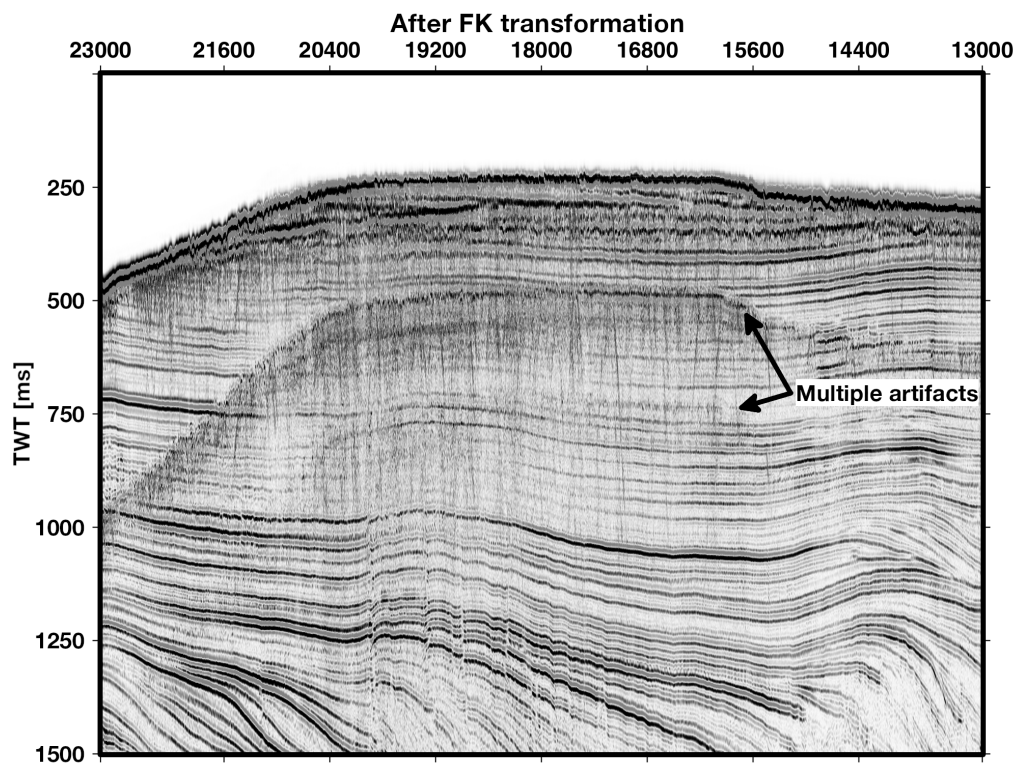
Figure 3.11. − Stacked section of profile 01E after an f-k filter.
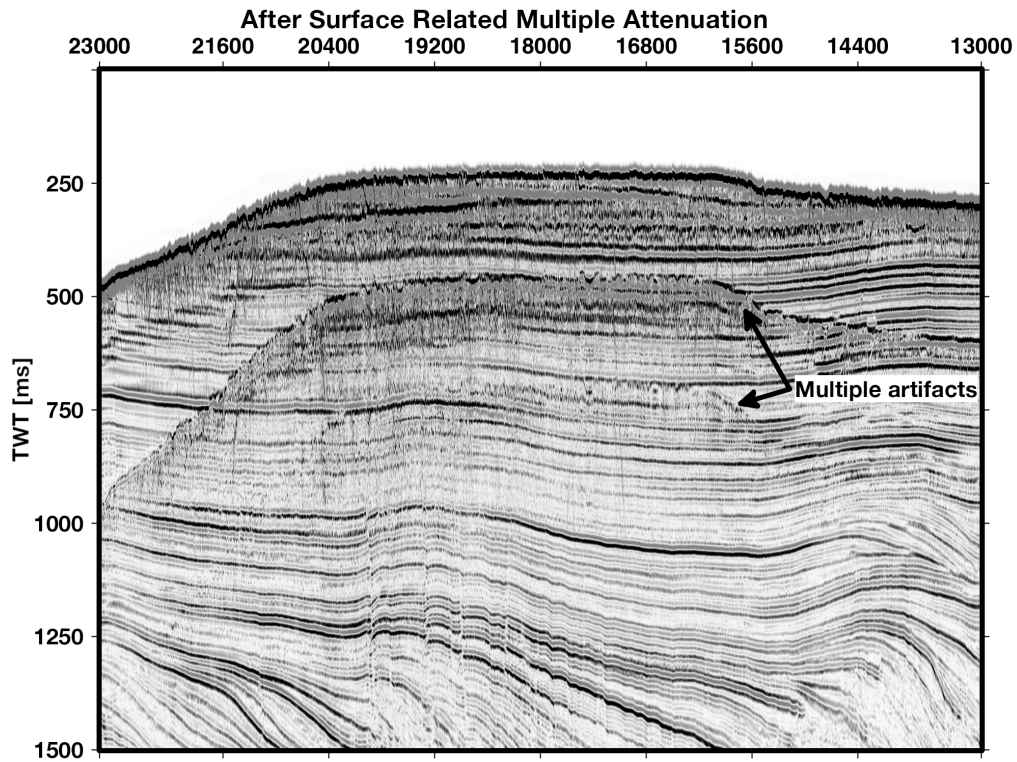
Figure 3.12. − Section of profile 01E after the SRMA.
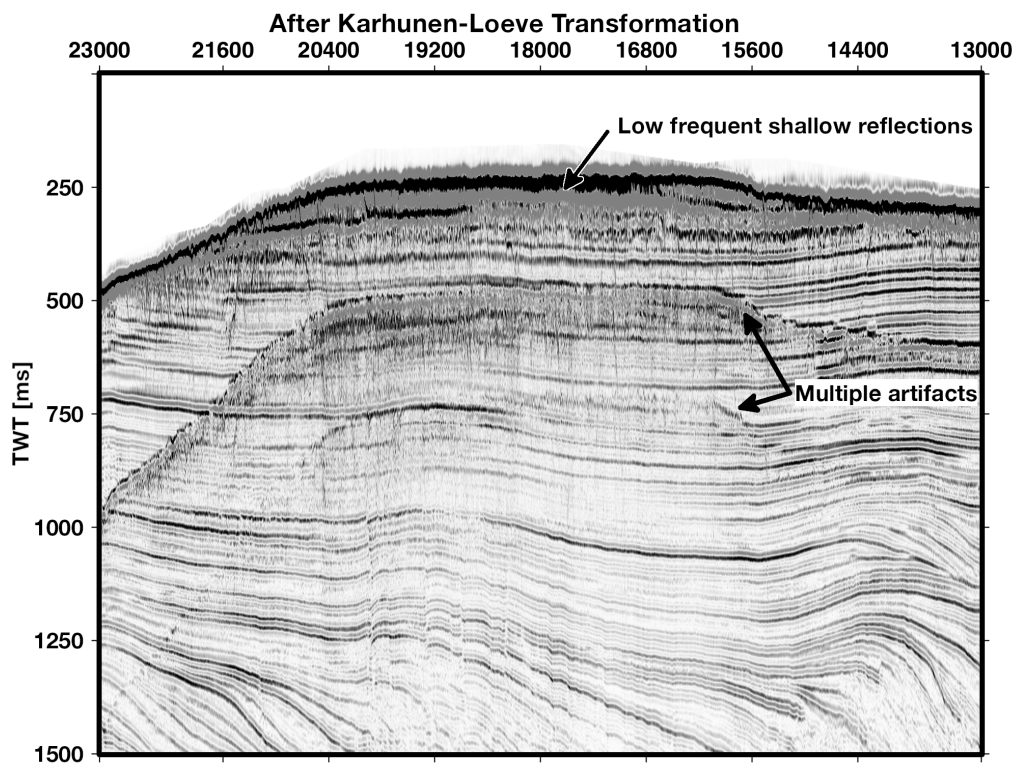
Figure 3.13. − Section of profile 01E after a Karhunen-Loeve transformation.
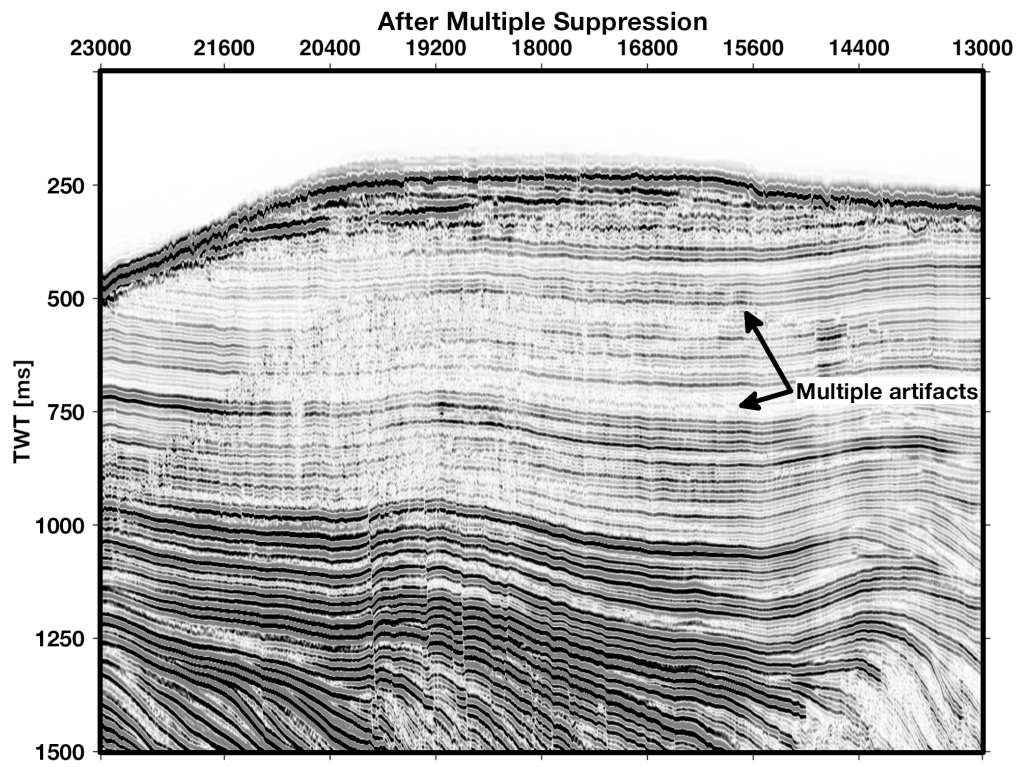
Figure 3.14. – Final stack of profile 01E after multiple suppression, migration and mean filter.

4. Contributions to scientific journals

4.1. Glacial sediments on the outer Chukchi Shelf and Chukchi Borderland in seismic reflection data

Authors: Carsten Lehmann[1], Wilfried Jokat[1,3], Bernard Coakley[2]
[1]Alfred-Wegener-Institute, Helmholtz Centre for Polar and Marine Research (AWI), Am Alten Hafen 26, 27568 Bremerhaven, Germany,
[2]Geophysical Institute, University of Alaska Fairbanks, 2156 Koyukuk Drive, Fairbanks, AK 99775, USA
[3]Geoscience Department, University of Bremen, Klagenfurter Str. 4, 28359 Bremen, Germany.

In this paper, MCS, bathymetric and sediment echo sounder data acquired during the MGL1112 cruise are used to investigate glacial structures distributed over the Chukchi Shelf and Chukchi Borderland. The work provides information on the distribution and thickness of glacial landforms and sedimentary structures in the Chukchi region and attempts to draw conclusions on its glacial history. A possible connection between the glacial landforms and a hypothetical 1 km thick pan-Arctic ice shelf is briefly discussed.

Wilfried Jokat supervised my scientific work at AWI and proofread the article. Bernard Coakley planned and conducted cruise MGL1112 and improved the manuscript with his helpful comments. I processed and interpreted the MCS data. I wrote the manuscript and prepared all the figures for this article.

4.2. Seismic constraints for ice sheets along the northern margin of Beringia

Authors: Carsten Lehmann[1,2], Wilfried Jokat[1,2]
[1]Alfred-Wegener-Institute, Helmholtz Centre for Polar and Marine Research (AWI), Am Alten Hafen 26, 27568 Bremerhaven, Germany,
[2] University of Bremen, Geoscience Department, Klagenfurter Str. 4, 28359 Bremen

Along the Beringian Margin, several MCS profiles from cruise MGL1112 and previously published profiles map the continental slopes. These profiles are used to determine the thickness of deposited glacial sediments on the continental slopes. The results are used to study the extent of former ice sheets as well as their dynamics. The results are compared to the formerly glaciated continental margins of East Greenland and Norway.

I processed the MCS data and interpreted them. Based on the interpretation, I wrote the manuscript and prepared all the figures. Wilfried Jokat supervised my work at AWI and improved the article with his comments.

4.3. Evaluation of Methane Release Potential on the Chukchi Shelf with Seismic Data

Authors: Carsten Lehmann[1,2], Wilfried Jokat[1,2]
[1]Alfred-Wegener-Institute, Helmholtz Centre for Polar and Marine Research (AWI), Am Alten Hafen 26, 27568 Bremerhaven, Germany,
[2]University of Bremen, Geoscience Department, Klagenfurter Str. 4, 28359 Bremen

The article provides new insights into the existence of migration structures and possible gas seepage areas on the Chukchi Margin. It also provides information about the possible existence of permafrost in this region. For this purpose, I analyze seismic data of MGL1112 and describe distinct sedimentary structures and velocities of

sediments shallower than 2500 ms TWT. The results are compared with other shelf areas of the Arctic Ocean.

The MCS data were processed and interpreted by myself. Likewise, I wrote the manuscript and created all figures. This was done under the supervision of Wilfried Jokat, who also improved the article with his comments.

5. Glacial sediments on the outer Chukchi Shelf and Chukchi Borderland in seismic reflection data

Carsten Lehmann[1,3], Wilfried Jokat[1,3], Bernard Coakley[2]

[1] Alfred-Wegener-Institute, Helmholtz Centre for Polar and Marine Research (AWI), Am Alten Hafen 26, 27568 Bremerhaven, Germany,

[2] Geophysical Institute, University of Alaska Fairbanks, 2156 Koyukuk Drive, Fairbanks, AK 99775, USA

[3] Geoscience Department, University of Bremen, Klagenfurter Str. 4, 28359 Bremen, Germany.

Corresponding author: Carsten Lehmann (clehmann@awi.de)

Abstract

The up to 900 km broad shelves off East Siberia and northwest off Alaska, including the Chukchi Shelf and Borderland, are characterized by shallow water in the periphery of the Arctic Ocean, north of the Bering Strait. Seafloor investigations revealed the widespread presence of glacial bedforms, implying the former existence of grounded ice in this region. We discuss the erosion and deposition around and beneath ice sheets/shelves using a regional grid of 2D seismic reflection data, acquired in 2011 from R/V Marcus G. Langseth across the outer 75 km of the Chukchi Shelf and the adjacent Chukchi Borderland. A high amplitude glacial base (GB) reflection extends over large parts of the shelf, separating glacial from preglacial strata. We define eleven seismic reflection characters, that we use to infer distinct depositional environments of glacial sediments. Thick well stratified sediments overlying the GB reflection in the south may have been impacted by fewer advance-retreat cycles than those near the northeastern and western shelf breaks. Here, the GB reflection pinches out at the seafloor next to reworked and eroded areas. Numerous meltwater channels, some up to several kilometers wide, together with grounding

zone wedges and recessional moraines are hints for ice sheets in the Chukchi Region. These ice sheets built up a huge grounding zone wedge of 48 km x 75 km on the Chukchi Rise. More grounding zone wedges on the western sides of bathymetric highs of the Chukchi Borderland along with mega scale glacial lineations indicate later ice shelf advances from east during the late Quaternary. However, in the absence of deep sediment cores, the timing or origin of the ice grounding events cannot be fully reconstructed.

5.1. Introduction

Ice sheets and their attached ice shelves play an important role in Earth's climate system (IPCC, 2018). The extent and geometry of ancient ice sheets and shelves and their evolution provide important constraints for numerical climate and glacio-isostatic models of the past, present and the future (Brigham-Grette, 2013; Stokes & Tarasov, 2010; Stokes et al., 2005). Determining the distribution of ice sheets on the continental shelves surrounding the Arctic Ocean is partly made difficult by sea ice cover, which hinders systematic geophysical investigations. This is especially true for the northern Chukchi Sea, a region of rapid ongoing changes in sea ice distribution over an up to 900 km broad, shallow continental shelf. This shelf and the adjacent Chukchi Borderland are of particular interest for regional glaciation studies because they appear to have been covered by an ice sheet-shelf system prior to the Last Glacial Maximum (LGM) (Brigham-Grette, 2013; Dove et al., 2014; Niessen et al., 2013).

Previous multibeam bathymetric seafloor mapping has revealed the widespread impact of icebergs/sheets reaching to water depths of 1200 m along the Arctic Ocean´s continental margins and across submarine ridges (e.g., Dove et al., 2014; Gebhardt et al., 2011; Jakobsson, 2016; Kristoffersen et al., 2004; Niessen et al., 2013). Together with sub-bottom profiler data, they reveal preserved glacial landforms on the seafloor, including Mega-Scale Glacial Lineations (MSGL), drumlins, ice-marginal Grounding Zone Wedges (GZW), and moraines. All of these are diagnostic features of paleo-ice stream processes (Ottesen & J. A. Dowdeswell, 2006; Ottesen et al., 2005; Stokes & C. D. Clark, 1999). Multibeam and sub-bottom profile data, however, have no or limited depth penetration and image only the surface and the very shallow sub-surface of these regions (Batchelor et al., 2013a; Dove et al., 2014; J. A. Dowdeswell et al., 2007), which represent for the most part the last ice mass grounding event. Multi-channel seismic reflection data can reveal the structure and extent of deeper horizons, and can be used to constrain the geometry and chronology of even older ice sheets/shelves (J. A. Dowdeswell et al., 2007).

This paper describes and interprets the geomorphic structures and seismic character of the sediments left behind by ice sheets and ice shelves at the northern part of the Chukchi Shelf and the adjacent Chukchi Borderland in water shallower than 750 m. For this, we use reprocessed 2D seismic reflection data supported by sub-bottom profiler (SBP) data to better resolve the shallow structures.
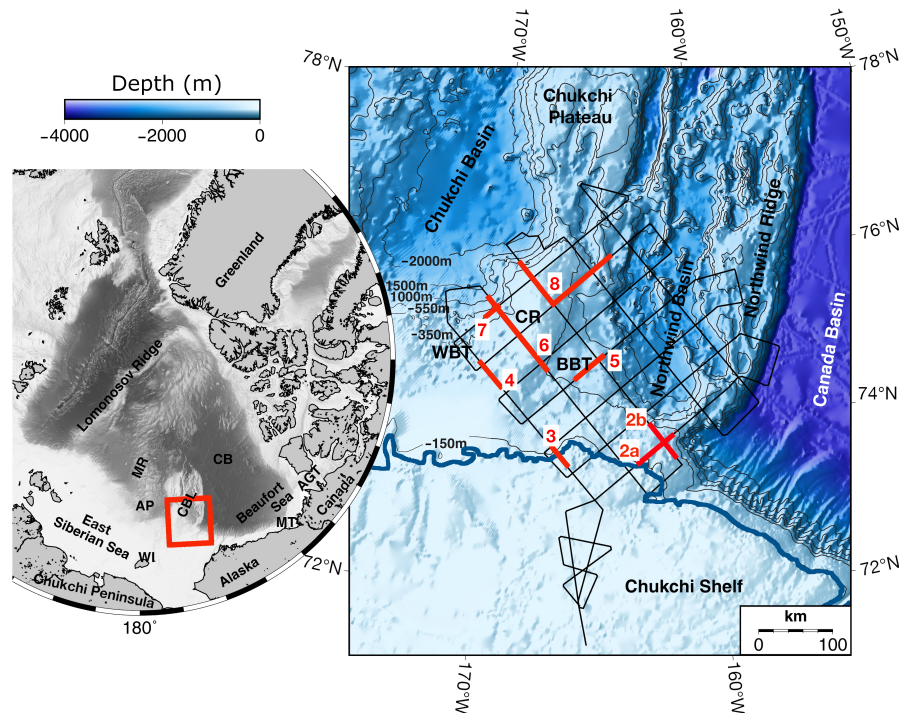
Figure 5.1. – Study area: Bathymetric map IBCAO v3.0 (Jakobsson et al., 2012) showing the locations of seismic reflection profiles. Locations for Figs. 5.2-5.8 shown in red. Blue thick line indicates 130 m isobath which is likely the shoreline during the LGM sea-level lowstands (P. U. Clark et al., 2009). Massive iceberg scouring occurs between the -150 m and -350 m contour lines (Dove et al., 2014). The main shelf break depth along the Chukchi Borderland is represented by the -550 m contour line. Abbreviations: AGT – Amundsen Gulf Trough, AP – Arlis Plateau, BBT – Broad Bathymetric Trough, CB – Canada Basin, CBL – Chukchi Borderland, CR – Chukchi Rise, MR – Mendeleev Ridge, MT – Mackenzie Trough, WBT – Western Bathymetric Trough, WI – Wrangel Island

5.2. Study area and previous work

The Chukchi Shelf is an up to ∼900 km wide continental shelf in the Arctic Ocean, located north of Chukchi Peninsula in Siberia and northwest of Alaska (Figure 5.1). From the Bering Strait connecting the Chukchi and Bering seas, the seafloor continuously deepens from less than 50 m to $450 - 750$ m at the northern Chukchi shelf break. This shallow margin is prolonged northwards by the Chukchi Borderland, which comprises the Northwind Ridge, Chukchi Rise, and Chukchi Plateau (Figure

5.1). These plateaus rise as much as 3400 m above the deep abyssal plains of the Canada Basin, reaching a minimum water depth of approximately 300 m (Hall et al., 1990). The Chukchi Borderland is considered to consist of high standing continental blocks (Brumley et al., 2015; Hall et al., 1990).

Numerous studies have focused on the impact of ice sheets and ice shelves on the Chukchi margin (e.g., Dove et al., 2014; Hunkins et al., 1962; Jakobsson et al., 2008; S. Kim et al., 2021; Polyak et al., 2007). Early depth recorder data revealed a very rough seafloor at depths of less than 350 m on the Chukchi Plateau interpreted to be incised by icebergs (Hunkins et al., 1962). Swath bathymetric data from the Chukchi margin show a widespread impact of not only icebergs but also grounded ice sheets/shelves such as glaciogenic bedforms like MSGL and morainic ridges (Dove et al., 2014; Jakobsson et al., 2008; S. Kim et al., 2021; Polyak et al., 2001). These bedforms suggest a complex glacial history with origins from an ice shelf emanated from the northwestern margin of the Laurentide Ice Sheet and/or a likely regional ice sheet on the Chukchi Shelf (Dove et al., 2014; Jakobsson et al., 2008; S. Kim et al., 2021; Polyak et al., 2001). Multiple indications for ice stream activity were found in glacial eroded bathymetric troughs, namely the Broad Bathymetric Trough (BBT) and the Western Bathymetric Trough (WBT) on the eastern and western flanks of the Chukchi Rise, respectively (Dove et al., 2014; S. Kim et al., 2021). In deeper water, prograding glacial wedges were identified at the western shelf edges of the Chukchi Rise (Hegewald & Jokat, 2013b; Ilhan & Coakley, 2018; S. Kim et al., 2021). Indications for a wider glacial history in this region are observed on the East Siberian margin and on the Arlis Plateau (Figure 5.1) (Jakobsson et al., 2016b; Joe et al., 2020; Niessen et al., 2013) and along the Beaufort-Alaska margin to the east (Engels et al., 2008). It has been suggested that these ice sheets may have been part of an extensive glacial complex associated with a kilometer-thick ice shelf that completely covered the central Arctic Ocean at one point in time (T. Hughes et al., 1977; Jakobsson et al., 2016b). In summary, the current, sparse knowledge on the glacial history of the Chukchi margin provides ample evidence for ice sheet/shelf impact but is not sufficient to understand the extent, timing and interaction(s) of glaciations in this of region.

5.3. Data and Methods

A regional grid of 5,300 km of 2D multi-channel seismic (MCS) profiles were acquired by R/V Marcus G. Langseth (Figure 5.1) across the Chukchi Shelf and Chukchi Borderland in 2011 to investigate the tectonic evolution and seismic stratigraphy (Coakley, 2011a; Coakley, 2011b). Additionally, sub-bottom profiler and swath

bathymetric data were recorded throughout the entire cruise.

As seismic source, a tuned airgun array of ten Bolt guns with a total volume of 1,830 cubic inches ($\sim$30 l) was used. Its frequency spectrum ranges between 5 Hz and 125 Hz. A 5850 m-long SentinelTM streamer with 468 hydrophones and 12.5 m hydrophone spacing was used to image the subsurface. Source and streamer were towed at 6 m and 9 m depth, respectively. The shot spacing on most profiles was distance-controlled to 37.5 m. Returning signals were recorded for 10 s at a sampling rate of 2 ms. Satellite differential GPS losses in parts of the survey grid made a distance defined shot interval impossible to achieve on some profiles. On these profiles, the seismic energy was released time-controlled every 12.8 s, which resulted in a shot spacing of approximately 37.5 m.

The MCS data were first processed with 25 m bins by ION Geophysical and interpreted for studying the tectonic evolution of the Chukchi Borderland by Ilhan & Coakley (2018). We reprocessed the seismic profiles to resolve small-scale structures in the shallow parts of the sedimentary column. For the reprocessing, MCS data were common depth point (CDP) sorted into 6.25 m bins resulting in a maximum fold of 78. Seismic data processing included attenuation of random, linear and coherent noise, in particular the seafloor multiple. For noise reduction, we applied bandpass filtering, velocity analysis, noise attenuation (high amplitude noise bursts, etc.), f-k dip multiple filtering (one coherence filter to weaken the multiple and a f-k filter on overcorrected CDP gathers), spherical spreading corrections, stacking and, finally, time migration and a mean filter. A distance of over 200 m between source and first channel combined with a binning of only 6.25 m results in negative interference between the direct wave and the seafloor reflection over shallow areas ($<$100 m water depth). Consequently, the seafloor reflection is weak or completely suppressed in the stack, and so we rely on sub-bottom profiler data for our interpretation of shallow structures in these areas. To estimate the shallow sediment thicknesses in meters, we applied a mean velocity of 1.7 km/s for the glacial sediments, based on a model by Hegewald (2012). Water depths were calculated with a mean velocity of 1.5 km/s. Using these velocities, and a peak frequency of 30 Hz for the sediments, the vertical resolution of our seismic data is about 12.5 m at the seafloor and 14 at the base of the shallow sediments we focus on. The seismic data are displayed in Two-Way-Traveltime (TWT) below the sea surface. The available sediment cores in the research area are too short to provide age constraints for the upper pre-glacial sedimentary units.

The sub-bottom profiler (SBP) data were acquired using a Knudsen Chirp 3260

echosounder with a source frequency range of 2 to 6 kHz. The SBP data penetrated the sediments between 10 to 100 m.
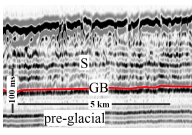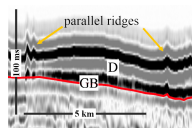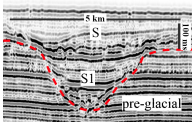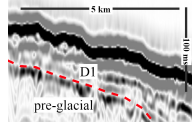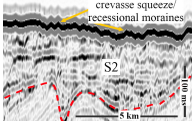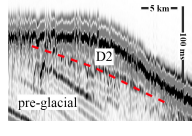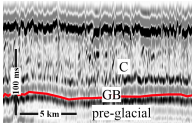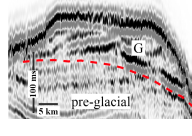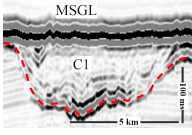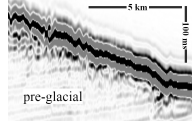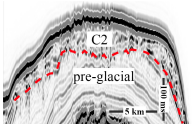
The multibeam bathymetric data were recorded during the cruise using a 12 kHz Kongsberg EM122. After editing and gridding the multibeam data with MB-System (Rembert, 2012) and the Generic Mapping Tool (GMT) (Wessel & Smith, 1998), the data were visualized using QGIS.

5.4. Results

As a first step for the subsequent interpretation, we identified and classified sedimentary structures potentially caused by ice sheets or ice streams, and mapped their areal extents within the study area. The description of analyzed MCS data is split into two areas. The first is located south of ∼75° N on the Chukchi Shelf and Northwind Ridge down to water depths of 750 m, the second one north of 75° N on the Chukchi Rise and surrounding shelf breaks. Eleven seismic characters relevant for this study are described in Table 5.1. Examples are shown in figures 5.2 - 5.8. The distribution maps of these characters are shown in Figures 5.9 and 5.10.

The abbreviations for the characters are chosen after their main reflection pattern and their origin, respectively, similar to Batchelor et al. (2013b) and Batchelor et al. (2013a). Based on the acoustic reflection pattern, stratified characters are denoted with S, S1, and S2. Chaotic characters are separated into the three categories C, C1, and C2. Predominately (semi-)transparent seismic characters are titled D, D1, and D2. Morphological structures such as a sedimentary wedge on the Chukchi Rise and truncated layers topped by laminated sediments are labelled G and T, respectively. Acoustically well-layered strata below the defined characters are collectively termed 'pre-glacial'. A prominent high amplitude reflection is considered to separate pre-glacial strata from glacial influenced sediments. Here, we name it the glacial base reflection (GB, see more details in the next sections). An age for the top of the pre-glacial sediments is not available because available sediment cores do not penetrate pre-glacial strata.

Table 5.1. – Classification of seismic characters identified from 2D seismic profiling of the Chukchi Shelf and Chukchi Rise. Red line represents the glacial base reflection (GB). Where the high amplitude glacial base reflection is absent, the stippled red line indicates the correlated boundary between pre-glacial and glacial sediments. The characters abbreviations are chosen after the predominant seismic reflection pattern of the characters and their, morphology and stratigraphy (see text for more details).

Seismic Abbreviation	Seismic Example	Character Description	Seismic Abbreviation	Seismic Example	Character Description
stratified			**(semi-)transparent**		
S		stratified, low to medium amplitude, topped by thin transparent layer	D		No internal reflections, partly accumulated to asymmetric wedge
S1		stratified, high to medium amplitude, infill channels	D1		stratified with lobate-shape geometry, occurs at shelf edges
S2		Mixture of stratified and chaotic characters, fills channels	D2		No internal reflections, deposited close to truncated areas
chaotic C		Chaotic, with medium to low amplitude	G		semitransparent, dipping internal reflections, asymmetric geometry
C1		stratified, high to medium amplitude, infill channels	T		truncated pre-glacial reflectors covered by laminated sediments
C2		Chaotic character, wedge-like body on a bathymetric high			

5.4.1. Chukchi Shelf and slope

A prominent smooth, continuous, high amplitude GB reflection is present in MCS data at 250 ms − 400 ms TWT south of 73° N to 1000 ms TWT on a profile east of the Chukchi Rise (Figures 5.2a, 5.3, 5.4, 5.5, 5.9a). On all other profiles the GB reflection pinches out at the seafloor in water depths of 300 − 350 m (400 − 450 ms TWT; for example, at the "truncation point" labelled in Figure 5.2a). This

reflection marks the transition from deeper, stratified deposits, marked by medium-to-high amplitude reflections, to shallower and apparently more irregular strata. In general, the GB reflection is covered by sediments of stratified character S, chaotic character C and transparent character D with varying thickness of up to ∼210 m (250 ms TWT) (Figure 5.9b, c, d). Their distribution is described in detail in the next paragraphs.

In the southern part of the study area, with water depths shallower than the truncation depth, the GB reflection is overlain by stratified sediments (Character S) (Figure 5.9b). Large incisions observed at the base of these sediments are up to 6 km wide and cut up to ∼210 m (250 ms TWT) deep into the pre-glacial sediments. These incisions are filled with stratified sediments of character S1 (Figure 5.3).

Towards the outer shelf, the acoustically stratified character S changes to a chaotic character C. This transition appears over a short distance on a seismic dip profile towards the Northwind Ridge (Figure 5.2a). Furthermore, the layer comprising of characters S and C thins towards the northeast and disappears where the GB reflection is cut at or close to the seafloor (Figure 5.2a, 5.9c). Further downslope, pre-glacial deposits are truncated and covered by a thin, laminated drape (Figure 5.2a, b; character T). Several areas of truncated pre-glacial sediments, indicated by character T (Figure 5.9f), as well as truncated stratified glacial sediments (Figure 5.2a), are observed in the study region in present day water depths of 150 − 750 m.

To the west, the transition between stratified glacial sediments S and chaotic sediments C takes place after a 20 km wide series of vertically-stacked incisions (Figure 5.4). The deepest buried channels eroded the pre-glacial strata, resulting in a sediment layer covering the GB that is up to ∼42 m (50 ms TWT) thicker than that of the surrounding areas. Further, many smaller incisions are found in the study area, cutting into packages of sediments with characters S and C (Figure 5.2a). These channels are up to 1 km wide and ∼50 m (60 ms TWT) deep (Figures 5.2a, 5.3, 5.4).

Acoustically transparent sediments (D) (Table 5.1) occur as a drape over the GB reflection in a larger area between Chukchi Rise and Northwind Ridge at depths of 280 − 750 m (375 ms TWT and 1000 ms TWT) (Figure 5.9d). The sediments reach a maximum thickness of ∼25 m (30 ms TWT) in a 20 km-wide wedge-like accumulation (Figure 5.5a). Several ridges with widths of 100 − 500 m are located on top of this wedge (Figures 5.5a, b, c). SBP data reveal the ridges to have maximum heights of 21 m (∼25 ms TWT). Multibeam data (Figure 5.5b) show an assemblage of ridges with slightly steeper southwestern flanks, orientated parallel to each other, at the seafloor. More ridges are observed in water depths between 400 m and 510 m (540 ms
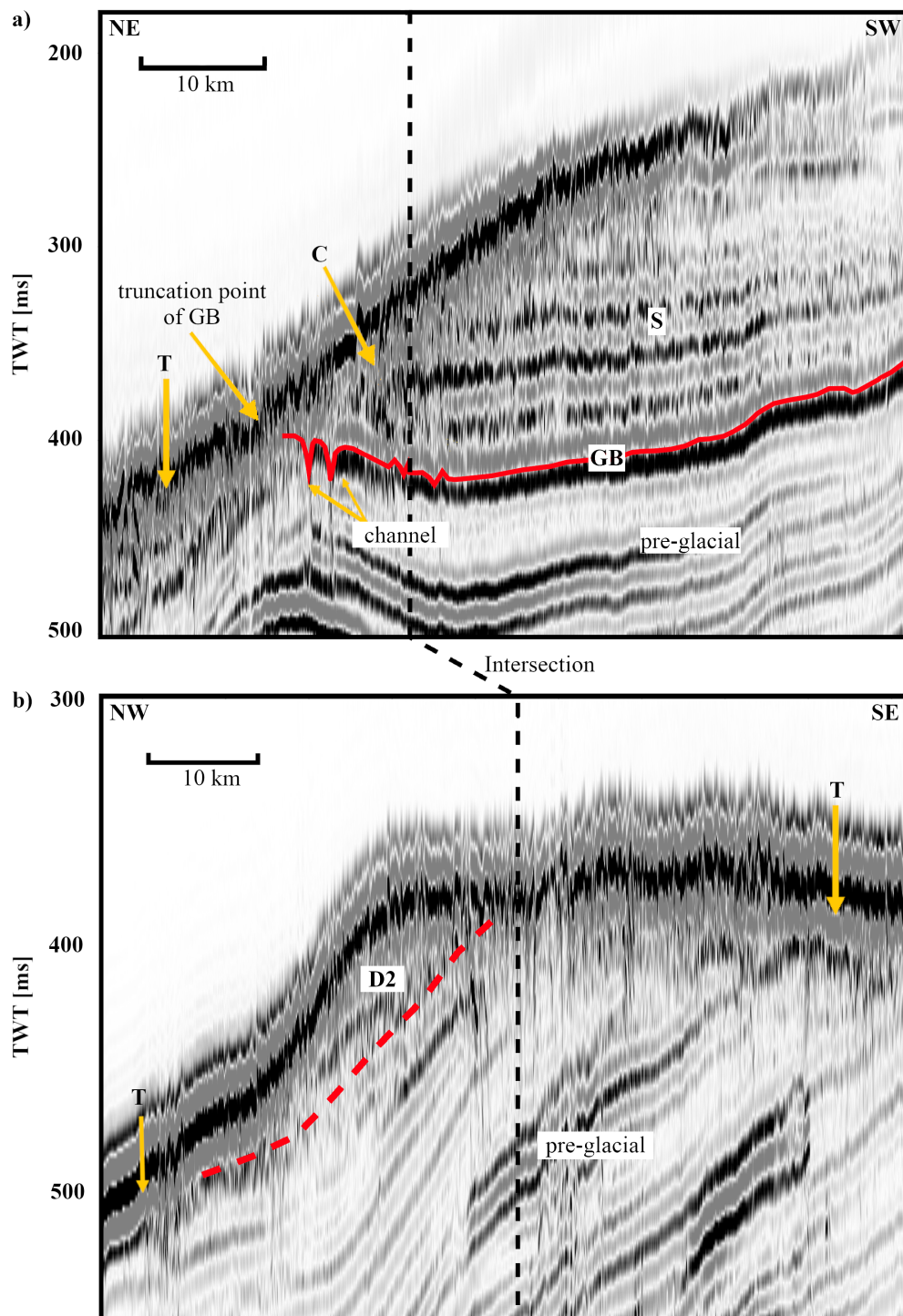
Figure 5.2. – Two seismic reflection profiles showing the truncated preglacial strata (Character T). Dashed vertical line indicates the intersection point of the two profiles. A) Stratified sediments (Character S) and chaotic sediments (Character C) over the glacial base reflection (GB); the truncation point of GB is close to the seafloor. B) Cross-profile of a wedge of sediments of character D2 between two areas with truncated pre-glacial strata (T). The stippled line indicates the base of the wedge. Location is shown in Figure 5.1
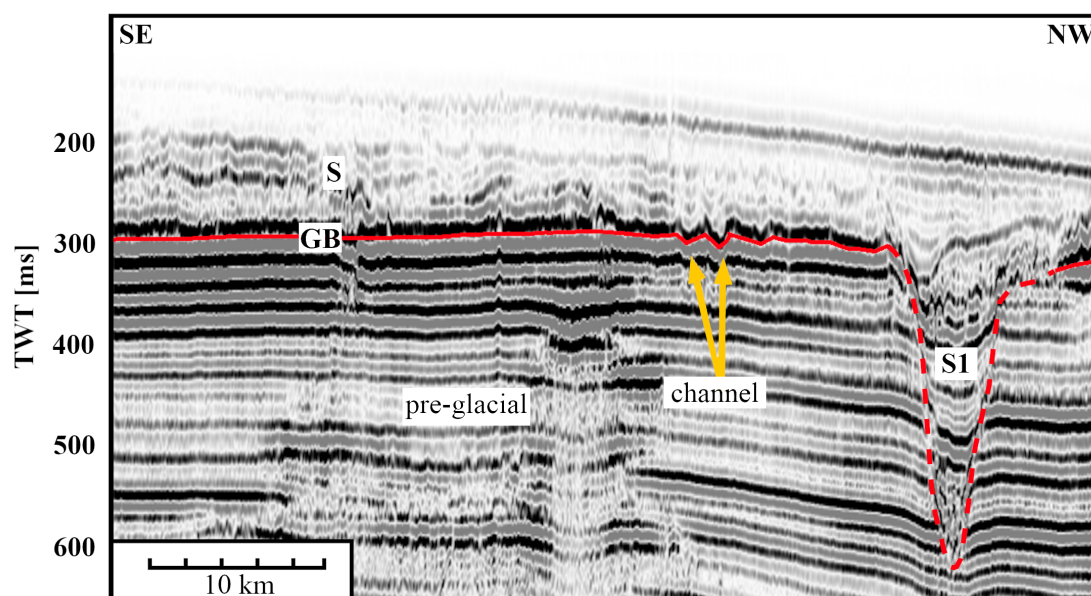
Figure 5.3. – Seismic reflection data of the Chukchi Shelf showing a large channel incised into pre-glacial strata and infilled with stratified sediments of character S1. Location is shown in Figure 5.1. Red line: glacial base reflection (GB). Dashed red line: boundary between channel fill and pre-glacial sediments.
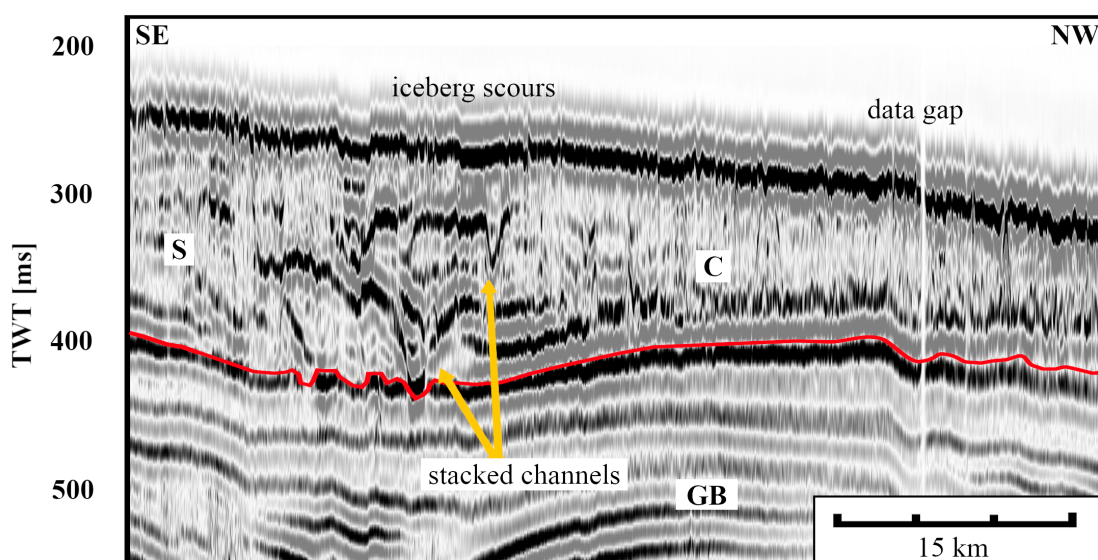
Figure 5.4. – Seismic reflection data showing vertically-stacked channels separating horizontal layers of chaotic and stratified sediments (Characters C and S). Location is shown in Figure 5.1. Red line: glacial base reflection (GB).

TWT and 680 ms TWT). The ridge crests trend 107° (ESE). In water depth of 335 m (550 ms TWT), character D and the top of the pre-glacial sediments are grooved by two sets of linear scours aligned approximately east-west (Figure 5.5a, b, d). Sediments of character D are buried by a layer of laminated reflections of ∼8 m (10 ms TWT) thickness (Figure 5.5c, d).
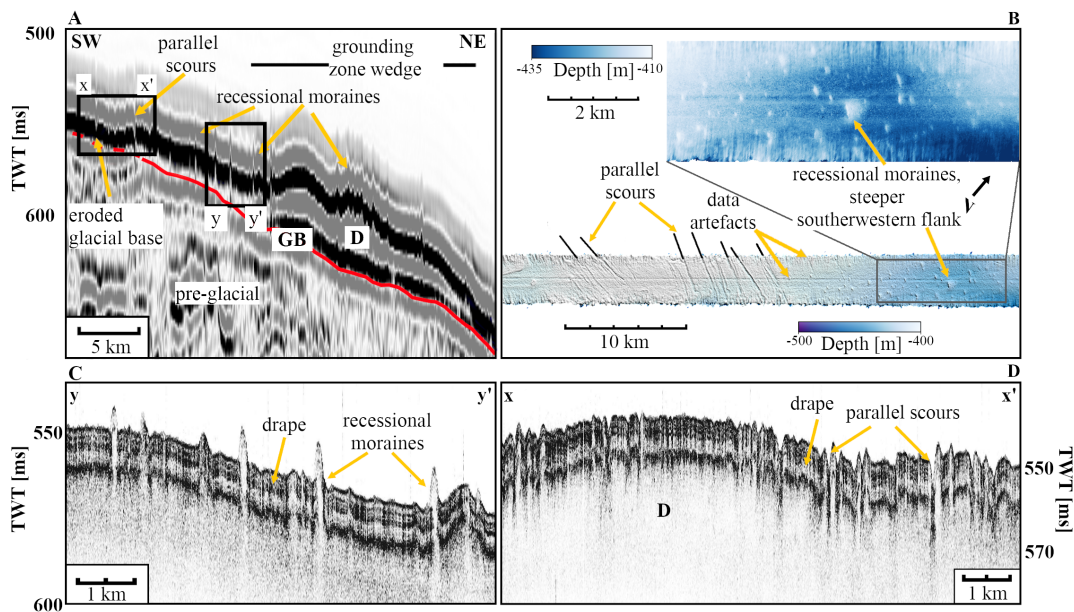
Figure 5.5. – Ridges, scours and GZW of and in transparent sediments (D) in the BBT. A) Seismic reflection data showing accumulation of sediments with character D above glacial base (GB). B) Multibeam bathymetric data showing the seafloor positions of the ridges and scours. C) SBP data showing parallel ridges topping sediments with character D. D) SBP data showing parallel scours in layer of sediment layers with character D. Location is shown in Figure 5.1.

5.4.2. Chukchi Rise

On the western side of the Chukchi Rise (Figure 5.1, approx. 170° W), where a strong GB reflection is absent, a layer with lobate-shaped acoustically stratified character D1 (Table 5.1) overlies truncated, stratified reflections in a basinward prograding wedge-like form (Figure 5.6). This package has a maximum thickness of ∼100 m (120 ms TWT) (Figure 5.9e). Below this layer, a cluster of incised channels is observed at the shelf break west of the Chukchi Rise (Figure 5.7). Spaced 1-3 km apart from each other, they reach widths of up to 1 km and depths of ∼65 m (75 ms TWT).

Sediments with a transparent acoustic character (D2, Table 5.1) appear in a large patch on the western side of the Chukchi Rise (Figure 5.8, #5 in Figure 5.10b). This patch has an asymmetric shape with a steeper flank at the shelf break and a shallower distal flank. Its thickness reaches up to ∼50 m (∼60 ms TWT). On the crossline, this accumulation extends for 39 km NE and SW (#5 in Figure 5.10b).
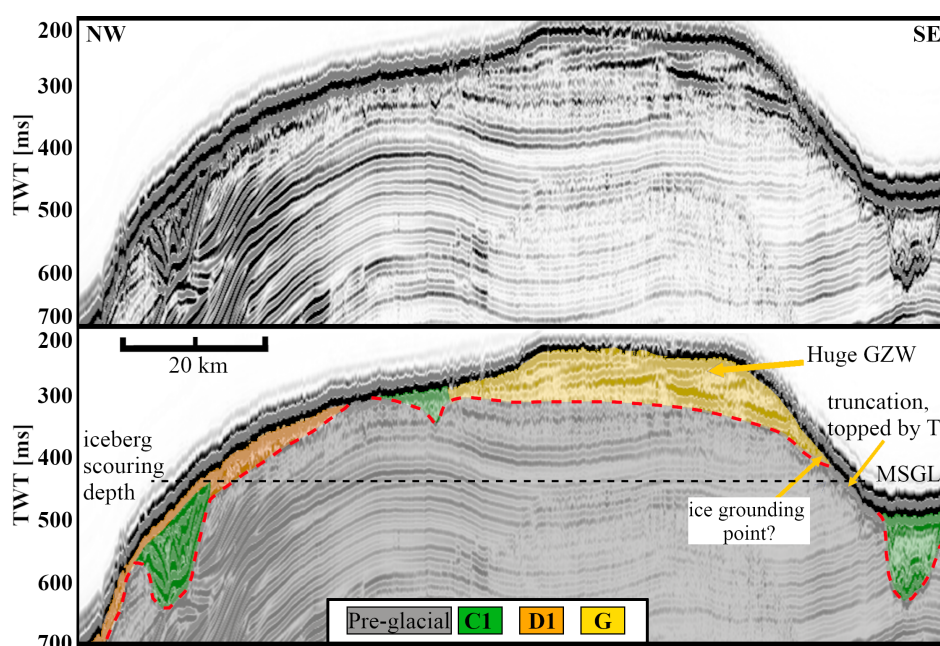
Figure 5.6. – Seismic reflection data from the Chukchi Rise. Top: Seismic profile of a line crossing the Chukchi Rise. Bottom: Interpreted seismic profile showing distribution of the sediments with characters C1, D1 and G on top of partly eroded pre-glacial strata. Dashed red line indicates the boundary between glacial and pre-glacial sediments. Dashed black line represents maximum water depth ~350 m for random orientated iceberg scours (Dove et al., 2014). Location is shown in Figure 5.1.
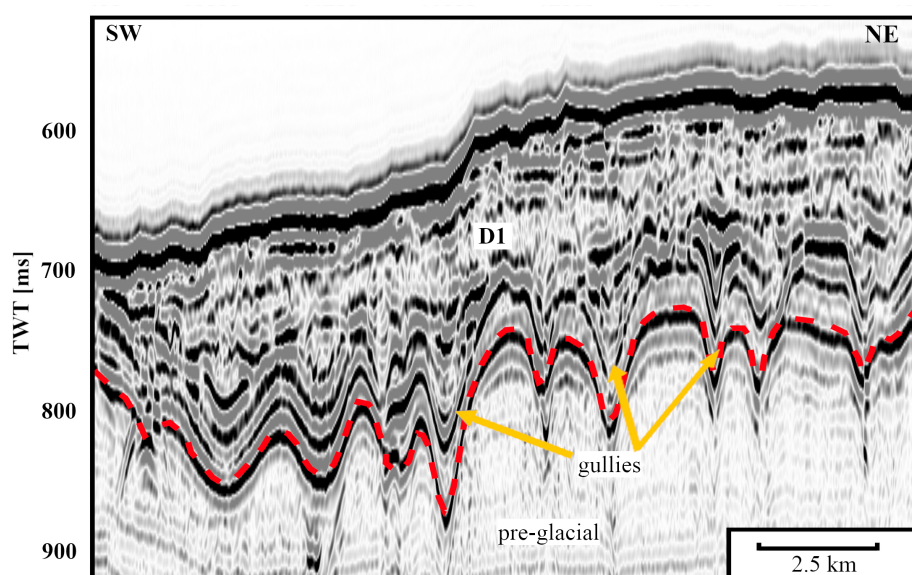
Figure 5.7. – Seismic reflection data showing several channels cutting into pre-glacial strata. Channels are filled with sediments of character D1. Dashed red line indicates the boundary between glacial and pre-glacial sediments. Location is shown in Figure 5.1.

Further to the east, a second accumulation of character D2 is observed at the transition between the Northwind Ridge and Northwind Basin (Figure 5.2b, #2 in Figure 5.10b). This accumulation displays a shallow southeastern side and a steeper northwestern flank closer to the basin, is around 15 km wide, and up to ∼70 m (80 ms TWT) high. To the southeast and northwest, seismic data show areas with truncated underlying reflections covered by a drape (T) (Figure 5.2b). Four smaller patches with a maximum height of ∼25 m (30 ms TWT) occur north and east of Chukchi Rise and on the Northwind Ridge (Figure 5.10b, #1 − 6).

On the Chukchi Rise, an up to ∼145 m (170 ms TWT) thick semi-transparent sedimentary wedge with dipping internal reflections (Character G) overlies stratified, partly truncated pre-glacial sediments (Figures 5.6, 5.8). The area covered by this wedge is 48 km wide and 75 km long (Figure 5.10a). Reflections within the wedge appear to dip eastward and westward. The wedge has a shorter, steeper western flank and a more gently dipping, longer eastern flank. Both flanks are marked by truncated horizontal stratified reflections covered with transparent sediments of character T (Figures 5.6, 5.8).

East and west of the Chukchi Rise, seismic data show three incisions, two with a width of 8 km and depth of ∼85 m (100 ms TWT), one with a width of ∼5 km and a depth of ∼42 m (50 ms TWT). All are filled with sediments showing a chaotic character C1. The channels are incised into the underlying pre-glacial strata (Figure 5.6).

Partly stratified to chaotic sediments (Character S2) are present north of Chukchi Rise in large incisions (Figure 5.8). The overall width of this area is ∼45 km. The incisions cut up to ∼380 m (400 ms TWT) into the underlying strata. While the character in the deepest incision has a more stratified pattern, in all other channels the sediments are less stratified and partly chaotic (Figure 5.8). The seafloor above the channels shows superimposed, low relief ridges (Figure 5.8).

Acoustically chaotic sediments (Character C2) occur on top of elevated pre-glacial strata on a bathymetric high, northeast of the incisions filled with sediments of character S2 (Figure 5.8). The maximum thickness of this layer is ∼100 m (∼120 ms TWT). It is lenticular, with a NE-SW extent of ∼20 km and a NW-SE extent of ∼15 km. Below it, the top pre-glacial strata show an irregular surface.
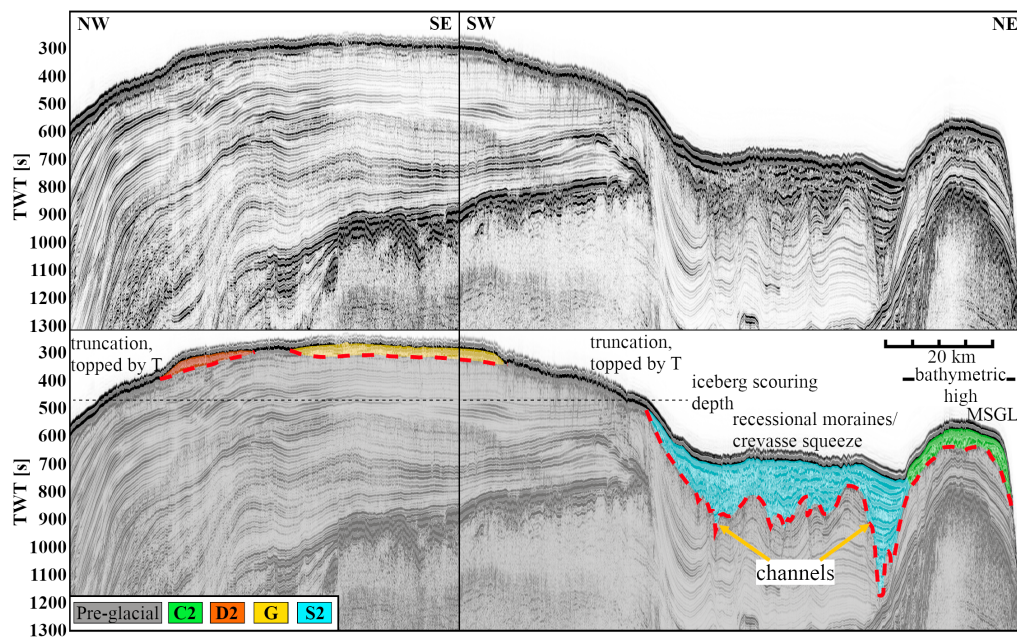
Figure 5.8. – Seismic reflection data from northwestern Chukchi Rise (Figure 5.1). Top: Seismic profile, Bottom: interpreted profile, showing the distributions of the seismic characters C2, D2, G and S2 on pre-glacial strata. Dashed red line indicates the boundary between glacial and pre-glacial sediments. Dashed black line indicates the maximum depth of random orientated iceberg scours at ∼350 m water depth (Dove et al., 2014). Location is shown in 5.1.
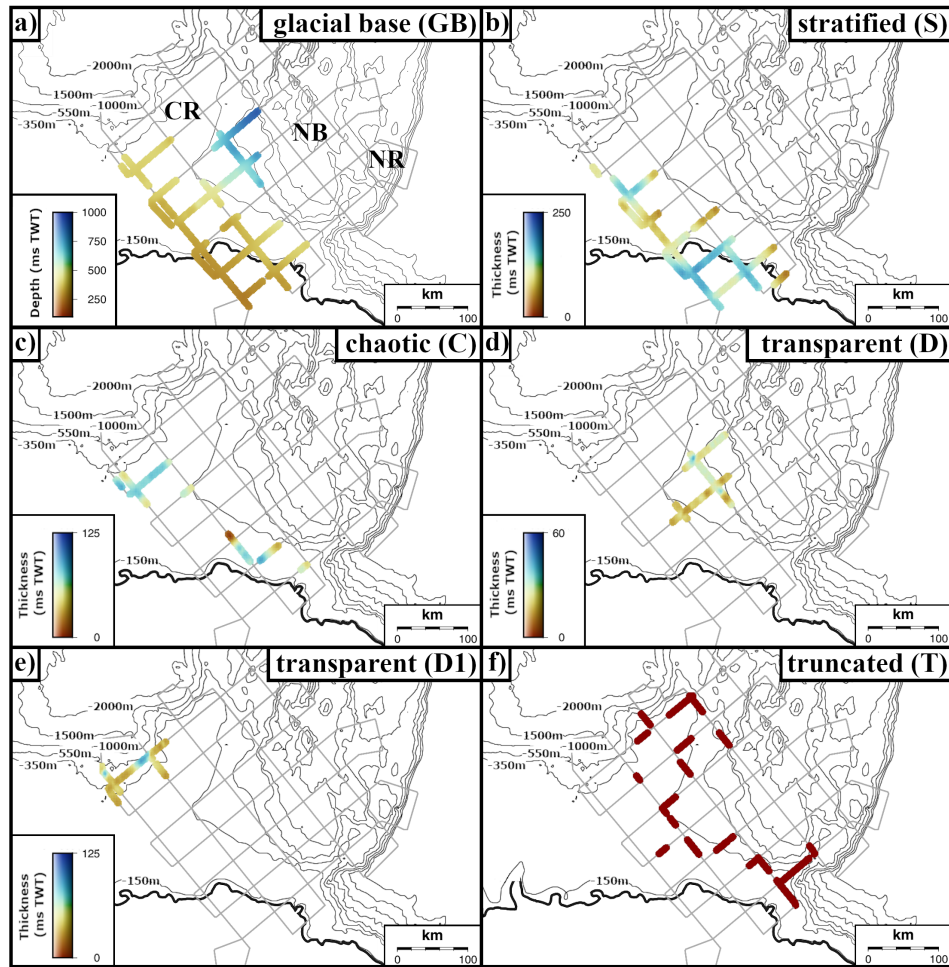
Figure 5.9. – Maps of the distribution and thickness of a) the glacial base GB, b) Character S, c) Character C, d) Character D, e) Character D1, and f) Character T. Light gray lines represent seismic profiles. Black line represents the 130 m contour line which is considered as shoreline during the last glacial maximum (P. U. Clark et al., 2009). Abbreviations: CR – Chukchi Rise, NB – Northwind Basin, NR – Northwind Ridge.

5.5. Interpretation and Discussion

Previous studies of multibeam and SBP data in our research area have focused entirely on seafloor structures which were formed by glacial processes (Dove et al., 2014; Jakobsson et al., 2005; Jakobsson et al., 2008; S. Kim et al., 2021; Polyak et al., 2007; Polyak et al., 2001). Fortunately, the seismic data allow a clear distinction between the glacial influenced and pre-glacial units in our research area. The up to 10 m deep gravity/piston cores provide vague information on the underlying glacial or non-glacial sediments (Park et al., 2017; Polyak et al., 2007). Therefore, we base our interpretation of glacially influenced sediments and landforms on comparisons to similar features imaged in other glaciated regions which have been better sampled (e.g., J. A. Dowdeswell et al., 2016; Kehew et al., 2012; Sættem et al., 1992).

5.5.1. Glacial landforms and bedforms

Glacial base reflection (GB)

We infer the GB reflection (Figure 5.2a, 5.3, 5.4, 5.5; GB) to mark the base of glacial erosion. The higher reflection amplitude compared to over- and underlying reflections indicates a change of the physical properties similar to an unconformity described in the Barents Sea (Bellwald et al., 2019; Sættem et al., 1992; Solheim et al., 1996). Here, this unconformity divides glacially over-compacted pre-glacial sedimentary rocks from unlithified, rapidly deposited glacial sediments (Bellwald et al., 2019; Sættem et al., 1992; Solheim et al., 1996). Its occurrence across the outer shelf (Figure 5.9a) and the strong impedance contrast to well stratified pre-glacial sediments suggests that the GB unconformity was formed at the base of an erosive ice sheet.

We favor the interpretation that the GB unconformity and sediments overlying it (Figures 5.2a, 5.3, 5.4) are products of several glacial advances and retreats as it is observed in the Barents Sea (e.g., Batchelor et al., 2013a; King, 1993; Sættem et al., 1992. The GB overlies basins filled with glacially redeposited sediments on the outer shelf east of the Chukchi Rise (Hegewald & Jokat, 2013b; Ilhan & Coakley, 2018). These filled basins indicate that a glacial advance preceded the formation of the GB. The truncation of the GB along the outer shelf, together with the underlying pre-glacial and overlying glacial sediments, indicates erosion by at least one later glacial event.

Stratified Sediments

By analogy to the Barents Sea (Sættem et al., 1992; Solheim et al., 1996), the up to 210 m thick stratified sediments (Character S) overlying the GB reflection are interpreted to be an alternation of glacial and interglacial sediments (Figures 5.2a,

5.3, 5.4). This interpretation is supported by analysis of shallow sediment cores on the Chukchi Shelf, which contain interglacial and glacial sediments (Polyak et al., 2007). The preserved stratification indicates that these areas were not strongly affected by subsequent glacial advances (Polyak et al., 2008).

Chaotic Sediments

The chaotic (character C) sediments covering GB (Figures 5.2, 5.4, 5.9c) were probably reworked after deposition by grounded ice of a subsequent glaciation. This is supported by the presence of reworked sediments in sediment cores from the ramp between the outer Chukchi Shelf and the Northwind Ridge (Polyak et al., 2007). Over this ramp to the Northwind Ridge (Figure 5.2a), the abrupt transition between sediments with characters S and C and their truncation at the seafloor indicates extensive reworking of stratified sediments and subsequent erosion of both units by grounded ice (Figures 5.4, 5.9c) (J. A. Dowdeswell et al., 2004; Ó Cofaigh et al., 2005).

Truncation of pre-glacial Sediments

The occurrence of character T sediments on top of pre-glacial strata (Figure 5.9f) is the result of the erosion and deposition of sediments by grounded ice, followed by hemipelagic sedimentation. In our survey area, this hemipelagic drape is found below a water depth of $\sim$350 m with varying thicknesses and postdates the most recent glacial grounding event(s) (Dove et al., 2014; S. Kim et al., 2021). In general, the erosion by grounded ice is present in water depths between 150 m (Figure 5.2a) and 750 m on the outer Chukchi Shelf and Borderland (Figure 5.9f) (Dove et al., 2014; Jakobsson et al., 2008; S. Kim et al., 2021; Polyak et al., 2007; Polyak et al., 2001).

(Semi-)transparent Sediments

A layer of acoustically transparent sediments (Character D) of up to 25 m thickness occurs east of the Chukchi Rise in water depths between 280 m and 750 m (Figure 5.9d). Due to its thickness and lack of internal reflections, we interpret this layer to consist of subglacial till. Till has been described as acoustically semi-transparent to transparent (Ó Cofaigh et al., 2005). Similar till layers occur in other formerly glaciated high-latitude regions (e.g., Batchelor et al., 2013b; J. A. Dowdeswell et al., 2016; Ó Cofaigh et al., 2005). Further, a wedge of transparent glacial till (Character D) within the BBT east of the Chukchi Rise is due to its shape interpreted as a GZW (Figures 5.5a, 5.10a) (Batchelor & J. A. Dowdeswell, 2015).

The set of ridges in the BBT (Figure 5.5a, b, d), which are $100 - 500$ m wide and

up to ∼20 m (25 ms TWT) high, is interpreted as hitherto unknown recessional moraines. Similar recessional moraines are found in bathymetric data in several areas in the Chukchi Region (Dove et al., 2014; Jakobsson et al., 2008; S. Kim et al., 2021; Polyak et al., 2001) and on other former glaciated margins (e.g., Burton et al., 2016; Ottesen & J. A. Dowdeswell, 2009; Winkelmann et al., 2010). These moraines are interpreted as the products of minor ice re-advances during a period of overall ice retreat (Ottesen & J. A. Dowdeswell, 2006). The steeper upslope flank representing the ice proximal side suggests a southward retreat, towards the Chukchi Shelf (Winkelmann et al., 2010). This is supported by the orientations of nearby MSGL (Dove et al., 2014).

Furthermore, the sets of east-west directed parallel grooves in the BBT cut into sediments of character D at the seabed (Figure 5.5a, b, d) are comparable to many MSGL in the Chukchi Region (Dove et al., 2014; Jakobsson et al., 2008; S. Kim et al., 2021; Polyak et al., 2001). MSGL are formed by deformation of soft sediments at the base of fast flowing ice sheets/streams (Spagnolo et al., 2014). Usually, these landforms appear as linear to curvilinear sediment ridges, each several tens of kilometers long and a few meters deep, which align with the direction of past ice flow (C. D. Clark, 1993; Spagnolo et al., 2014). Due to the limited data coverage, it is not possible to estimate the lengths of the grooves (Figure 5.5b), leaving open the possibility of a formation by the deep keels of large icebergs, as has been suggested for the Lomonosov Ridge between ∼85° N and ∼86° N (J. A. Dowdeswell et al., 2007; Kristoffersen et al., 2004).

Tunnel valleys

Large channels incising pre-glacial sediments and filled with various seismic characters (Character S1, S2, C1) (Figures 5.3, 5.6, 5.8) can be interpreted in different ways. These channels are comparable in size and geometry to channels found incised by as much as 50 m into Cretaceous strata on the southern inner Chukchi Shelf in modern water depths of up to 60 m (Hill & Driscoll, 2008; Hill et al., 2007). These channels have been interpreted as products of fluvial erosion by Alaskan rivers flowing across the shelf during sea level lowstands with periods of higher meltwater drainage during the late LGM (Hill & Driscoll, 2008; Hill et al., 2007). However, the channels on the outer shelf are located at water depths of up to 360 m (Figure 5.10a) which is below the level of regional lowstands during glacial times (P. U. Clark et al., 2009; Miller et al., 2020). The deep incision of these channels into pre-glacial sediments (Figure 5.3, 5.6, 5.8) is more consistent with the action of a subglacial drainage system, like those reported for other glaciated regions (e.g., Graham et al., 2016; Kehew et al., 2012; Stewart et al., 2013. Therefore, we interpret these chan-

nels as subglacial tunnel valleys formed by catastrophic outbursts from subglacial meltwater lakes or steady-state subglacial meltwater drainage (Huuse & Kristensen, 2016; Kehew et al., 2012). This interpretation is supported by the presence of overlying glacial landforms like MSGL (Figure 5.6) and as ice marginal crevasse squeeze/recessional moraines interpreted from superimposed, low relief ridges (Figure 5.8)(Dove et al., 2014). Multiple smaller tunnel valleys with widths of up to 1 km and depths of up to ∼50 m (60 ms TWT) can be observed in areas covered by stratified sediments of character S and C in the southwest of the research region (Figures 5.2a, 5.3, 5.4). The wide distribution of tunnel valleys suggests a widespread subglacial drainage system. The vertically-stacked configuration of tunnel valleys at the western transition to areas with sediments with a chaotic character C (Figure 5.4) indicates that this system was intermittently active during several glacial periods (Kehew et al., 2012; Walder & Fowler, 1994). The direction of meltwater flow cannot be determined from our widely spaced seismic profiles.

Gullies

The channels at the western shelf break (up 1 km and 65 m) filled with character D1 sediments (Figure 5.7, 5.10) can be interpreted as buried gullies as they are comparable to gullies at other high latitude shelf breaks occupied by paleo-ice streams (Gales et al., 2013,Batchelor et al., 2014 and references therein). The sediments (Character D1) filling the gullies (Figure 5.6) were previously interpreted as a GZW from the imaging of hummocky terrain in multibeam data and transparent glacial till in SBP data (Dove et al., 2014; S. Kim et al., 2021). Their burial by glacial sediments indicates development together with the first ice sheet advance to the paleo-shelf break by the release of sediment-laden meltwater (Engels et al., 2008; Gales et al., 2013; Ó Cofaigh et al., 2003; Polyak et al., 2001). Other gullies related to different glacial cycles are found in multibeam and SBP data along the western Chukchi Rise by S. Kim et al. (2021).

Grounding Zone Wedges

Grounding zone wedges (GZW) on the outer Chukchi Shelf are reported so far in multibeam and SBP data on the western flank of the Chukchi Rise (Dove et al., 2014; S. Kim et al., 2021). GZWs are the result of high sedimentation rates during long-lived still stands of the grounding zones of ice sheets, which produce wedge shaped bodies of seismically chaotic to transparent appearance (Batchelor & J. A. Dowdeswell, 2015; J. A. Dowdeswell & Fugelli, 2012; Ottesen & J. A. Dowdeswell, 2009). Truncations within the GZW are caused by modifications of the sediments during fluctuations of the grounding zone position (J. A. Dowdeswell & Fugelli, 2012). In this section, we discuss eight hitherto unknown GZWs found in our seis-

mic data (Figure 5.2b, 5.5, 5.6, 5.8, Numbers 1-8 in Figure 5.10).

Six asymmetric GZWs (Figure 5.10b; # 1-6) with a transparent character D2 topping pre-glacial strata (Figure 5.2b, 5.8) occur on the west-facing flanks of eroded bathymetric highs like the Northwind Ridge (Figure 5.10b). Such GZWs are known to build up behind topographic highs acting as pinning point for the grounding zone of an ice stream (Batchelor & J. A. Dowdeswell, 2015). Thus, we interpret GZWs #1-6 as remnants of the widespread grounding of westward moving ice from the Northwind Ridge to the Chukchi Rise.

Likewise, we interpret the layer of chaotic sediments with character C2 as a GZW (Figure 5.8, Figure 5.10b; #7), due to its internal structure, its thickness of ∼100 m (120 ms TWT) and its setting covering eroded pre-glacial strata on top of a bathymetric high northeast of the Chukchi Rise (Figure 5.8, 5.10b). Similar GZWs are also found on the Greenland Shelf on topographic highs that acted as pinning points for ice streams (J. A. Dowdeswell & Fugelli, 2012). The action of a paleo ice stream or ice shelf in this area is indicated by MSGL on the shallow slope towards the Northwind Basin (Dove et al., 2014), and crevasse squeeze/recessional moraines on its western side (Figure 5.8) (Dove et al., 2014).

A further GZW (GZW #8) is interpreted from a wedge of semi-transparent sediments of character G with internal dipping reflections, situated on the Chukchi Rise (Figures 5.6, 5.8; # 8 in Figure 5.10a). The interpretation is based on the wedge's asymmetry, with its steeper western and gentler eastern side, its dipping internal reflections, and the truncation of underlying reflections at its base (J. A. Dowdeswell & Fugelli, 2012). The westward dip of the internal reflections indicates the eastward glacial retreat (Figure 5.6). The dimensions of the Chukchi Rise GZW (48 km x 75 km, ∼145 m thick) (Figure 5.10a) are larger than most known high latitude GZWs, which usually are less than 15 km wide and only 50-100 m thick (Batchelor & J. A. Dowdeswell, 2015; J. A. Dowdeswell & Fugelli, 2012). Therefore, the GZW #8 might be the result of an amalgamation of multiple GZWs of successive ice sheets (Rüther et al., 2011), an unusually long-lived still stand of a single ice sheet-shelf system (Batchelor & J. A. Dowdeswell, 2015) or as a lateral GZW formed at the boundary to an ice free or slow-moving ice zone on the Chukchi Rise adjacent to an ice stream in the BBT (Batchelor & J. A. Dowdeswell, 2015; Batchelor et al., 2013b). However, without any age constraints and a denser seismic network, the GZW formation remains speculative.

5.5.2. Implications for glaciation history of the Chukchi margin

Grounded ice

Several observations described in the previous chapter indicate on East Siberian Shelf various morphological features, which indicate different glacial processes.

The GB unconformity identified over a large part of the study area (Figure 5.9a) suggests the existence of a grounded ice sheet at least on the outer Chukchi Shelf and the adjacent Chukchi Borderland. Considering the extensive overlying deposits increasing in thickness to 210 m southwards (Figures 5.3, 5.9b) leads us to assume that the GB unconformity was formed during the early or middle Quaternary. This inference is consistent with the interpretation of seismostratigraphic data from the Chukchi Rise (S. Kim et al., 2021) and the terrestrial evidence for the absence of expansive Late Quaternary glaciation in Beringia (Brigham-Grette, 2001; Brigham-Grette, 2013; Gualtieri et al., 2005). The resolution of the MCS data does not allow us to identify individual glacial events in sediments overlying the GB unconformity. Higher-resolution seismostratigraphic data from the Chukchi Rise indicate at least four glacial advances ranging in estimated age from the middle to late Pleistocene (S. Kim et al., 2021). The ice sheet(s) inferred from the marine data produced north-to northeastwards-flowing ice streams, which advanced and retreated through the bathymetric troughs on the eastern and western flanks of the Chukchi Rise (Figure 5.10a)(Dove et al., 2014; S. Kim et al., 2021). This is indicated by GZWs, drumlins, recessional moraines and MSGL formed in diamictons (Figure 5.5a, b, d). Truncations of pre-glacial strata observed in these areas (e.g., Figure 5.6) are similar to glacial erosion features in seismostratigraphic records from other formerly glaciated margins, including glacial trough edges (e.g., Bellec et al., 2016). The combined distribution of the glacial unconformity and geomorphic features indicative of the northwards flowing ice stream (Figure 5.10a) is consistent with a proposed East Siberian Ice Sheet (Niessen et al., 2013), or alternatively with an ice sheet centered on the Chukchi Shelf (Dove et al., 2014 and this study, S. Kim et al., 2021). However, the full extent of such an ice sheet cannot be resolved with the existing data, especially due to the lack of data from the Chukchi Shelf further south.

In addition to the local Chukchi Ice Sheet, glacial impacts could be related to grounded ice shelves transgressing from the Laurentide Ice Sheet across the outer Chukchi Shelf and Borderland. Those are indicated by the large eroded areas including the truncation of the GB reflection (Figure 5.9c, f) as well as multiple glacial bedforms like west-striking MSGL and moraines (Dove et al., 2014; Jakobsson et al., 2008; Polyak et al., 2001). Along with grounding zone wedges on the western flanks of local topographic highs down to water depths of 600 — 700 m (Figure
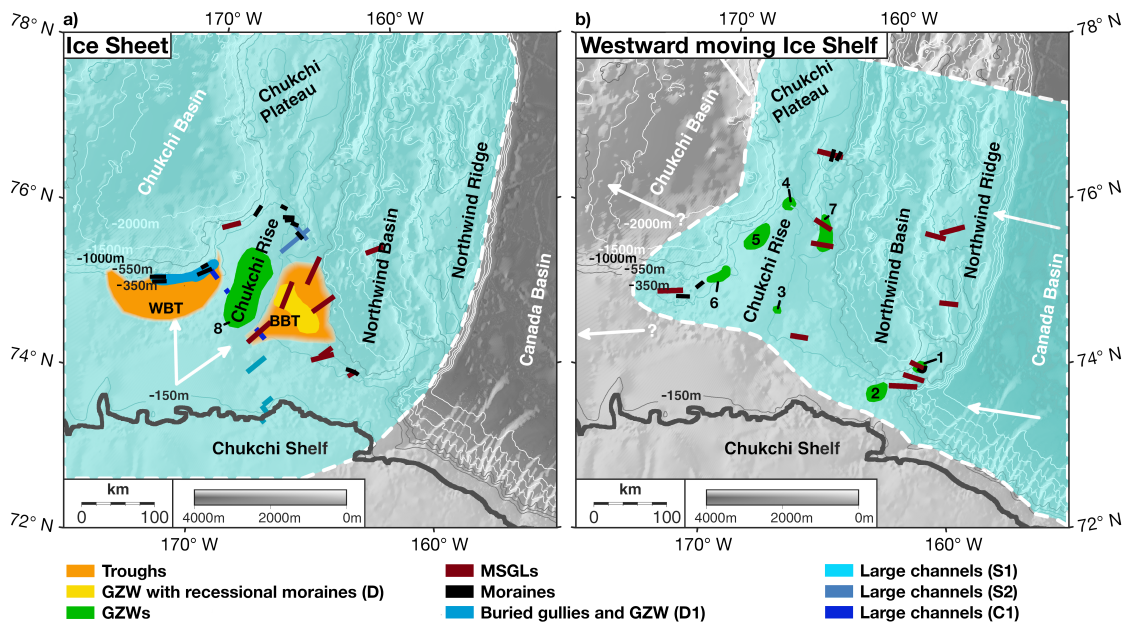
Figure 5.10. – Glacial features in the MGL1112 data (Dove et al., 2014, this study) consistent with: a) an ice sheet on the Chukchi Shelf, b) westward along slope advances of grounded ice shelves during succeeding glaciations. Numbers are GZWs (see text for deatils). Arrows indicate inferred ice movement direction. BBT Broad Bathymetric Trough, WBT Western Bathymetric Trough.

5.10b), westward to northwestward ice flow directions are indicated. Therefore, the ice shelves apparently must have originated from the Laurentide Ice Sheet. However, N-S trending MSGL in water depths of 360 - 380 m on the western flank of the Chukchi Rise associated with one of the last two grounding events in the western Chukchi Region, are difficult to reconcile with a westward moving ice shelf (S. Kim et al., 2021).

The last grounded ice shelf may have existed during the LGM along the entire Alaskan-Beaufort margin and across the Chukchi Borderland in present-day water depths between 150 – 450 m (Figure 5.10b). Evidence for erosion in water depths deeper than 150 m from our eastern study area (Figure 5.9f) and along the Alaskan Beaufort margin (Engels et al., 2008) along with the recovery of LGM (∼20 ka) dated sediments from the Chukchi Region support such an interpretation (Park et al., 2017; Polyak et al., 2007). Polyak et al. (2007) recovered diamicton from east-west striking MSGL in water depths of ∼450 m on the Northwind Ridge and Park et al. (2017) found glaciomarine sediments related to a nearby ice shelf in the bathymetric trough east of the Chukchi Rise. However, the preservation of MSGL in water depths of 580 m on the Northwind Ridge, which are dated to marine isotope stage 4/5 (71 – 123 kyr) (Polyak et al., 2007) as well as preserved NE-SW trending

MSGL on the Chukchi margin (Figure 5.10 and Dove et al., 2014; Jakobsson et al., 2014; S. Kim et al., 2021), preclude the existence of a thicker ice shelf during the LGM. This complies with the absence of large grounded ice masses on the Chukchi and East Siberian shelves and restricts the presence of grounded ice during the LGM to the outer shelf areas and the Chukchi Borderland.

Pan-Arctic ice?

Geoscientific data as sediment cores and acoustic data show extensive and widespread glacial erosion and bedforms on the Chukchi margin and the adjacent East Siberian and Beaufort margins in water depths shallower than 1200 m (Dove et al., 2014; Jakobsson et al., 2014; Jakobsson et al., 2008; S. Kim et al., 2021; Niessen et al., 2013; Polyak et al., 2007). Those glacial features rise the question if they were caused by local ice sheet-shelf systems or in part caused by a 1 km-thick pan-Arctic ice shelf (Grosswald & T. Hughes, 2002; Jakobsson et al., 2016b; Mercer, 1970). This ice shelf is suggested to have moved westward across the Chukchi Borderland (Jakobsson et al., 2016b). Bedforms as MSGL are reported in up to 1200 m water depth from multiple locations in and around the Chukchi Region (Dove et al., 2014; Jakobsson et al., 2014; Jakobsson et al., 2008; S. Kim et al., 2021; Niessen et al., 2013; Polyak et al., 2007). Based on their shelf to basinward orientation, these features are interpreted as remnants of a local ice sheet-shelf systems in the Chukchi Region (Dove et al., 2014; S. Kim et al., 2021; Polyak et al., 2001). In addition, our data show no evidence for extensive erosion below 750 m on the Chukchi margin (Figure 5.9) that can be expected from a moving pan-Arctic ice shelf. Erosion is only reported in a small area on the central Northwind Ridge to depths of 900 m, shallowing southwards to $550 - 750$ m and northwards to 620 m (Jakobsson et al., 2008). Other large-scale erosional features which would be comparable to the glacially flat-topped Lomonosov Ridge are not known to date in water depths below 750 m on the Northwind Ridge and Chukchi Plateau (Dove et al., 2014; Jakobsson et al., 2008). Beyond this, while our data set reveals glacio-morphological features supporting the existence of more localized ice sheets/shelves, they do not support a constantly 1 km-thick, westward moving pan-Arctic ice sheet/shelf system in the Chukchi Region. Shallower ice shelves moving westward across the Chukchi margin, however, seem likely to have existed during the Quaternary glaciations.

5.5.3. Conclusions

Regional MCS supported by SBP and bathymetric data collected by the R/V Marcus G. Langseth in 2011 allow a first view of the thickness and distribution of glacially modified sediments overlying eroded pre-glacial strata along the outer Chukchi Shelf and Chukchi Borderland region. Although the data coverage is sparse, we found a

variety of geomorphological features in the seismic data that are directly comparable to other glaciated continental shelves. Contrasting orientations of widespread MSGL and recessional moraines, as well as the widespread presence of GZWs, are consistent with multiple glacial cycles and ice sheet/shelf sources. However, in water depths shallower than 350 m, intense iceberg scouring has wiped out seafloor geomorphological features that might have been used for more precise reconstructions of ice sheet/shelf extents. Our main findings are:

1. A glacial unconformity is present over large parts of the Chukchi Shelf and within a bathymetric trough east of the Chukchi Rise. Along with north-south trending seafloor features, like MSGL and drumlins, it provides evidence for a grounded ice sheet-shelf system. Such a system developed likely during several glaciations. Recessional moraines as well as grounding zone wedges within bathymetric troughs east and west of the Chukchi Rise indicate a phase of still stand and minor re-advances during the southward retreat of an ice margin in this region.

2. The erosion of the glacial base reflection, reworked glacial/interglacial sediments and westward directed glacial bedforms indicate that a later erosional ice shelf advanced from the east, probably from the Laurentide Ice Sheet. The preservation of north/northwestward pointing seafloor features in greater water depths indicates that the ice shelf was thinner than previous ice advances from the Chukchi Shelf.

3. A huge, 48 km wide and 75 km long, grounding zone wedge with a thickness of up to ∼145 m on the Chukchi Rise may have formed over the course of several glacial cycles, during an unusually long stillstand of an ice stream/shelf of one glacial advance or as a lateral moraine adjacent to a trough.

4. Tunnel valleys with a width of up to 12 km and depths of up to 300 m, several smaller tunnel valleys distributed over the research area and gullies at the western shelf edge with a width of up to 1 km and a depth of up 65 m are imaged. All those suggest the existence of large subglacial drainage systems which directed large amounts of meltwater, partly during several glaciations.

Owing to few sediment core data, the complex erosion history, and sparse seismic data coverage, a reliable correlation of glacial morphological features to specific glacial cycles is not yet possible. Discussion about the extent and timing of ice sheets/shelves in the Chukchi Region, including during the LGM, continues.

Data Availability Statement

Acknowledgements

Funding

6. Seismic constraints for ice sheets along the northern margin of Beringia

Carsten Lehmann[1,2], Wilfried Jokat[1,2],

[1]Alfred-Wegener-Institute, Helmholtz Centre for Polar and Marine Research (AWI), Am Alten Hafen 26, 27568 Bremerhaven, Germany,

[2]University of Bremen, Geoscience Department, Klagenfurter Str. 4, 28359 Bremen.

Abstract

Beringia today is a partly submerged Arctic region bordered by the Lena River in East Siberia and the Mackenzie River in North America. Whilst emergent at times of eustatic sea-level fall, the northern Beringian Margin was affected by the repeated growth and decay of regional ice sheets. The size and dynamism of these ice sheets are a subject of some debate that can be addressed using geophysical data, which reveal widespread evidence for glacial processes on the continental shelves. We use published and reprocessed 2D multi-channel seismic reflection data from the northern margins of Beringia between 147° E to 149° W to investigate their glacially deposited sediments in detail. Deposition of up to 450 m of sediments caused the shelf break to migrate basinward by up to 13 km between 165° E and 161° W. On the Kucherov Terrace (175° E to 176° W) the data show evidence for erosion by grounded ice in water depths of 1200 m. Deposits in the Northwind Basin, between 165° W and 161° W, are separated by continuous reflections indicating at least $3-5$ glacial advances. However, the continental slopes of the western East Siberian Sea and the Beaufort Sea lack the thick glacial deposits found in the intervening region. Overall, the volume of glacial deposited sediments along the margins of Beringia are significantly smaller than the reported amounts along the Norwegian and Greenland margins. Therefore, we suggest a less dynamic and fewer number of glaciations of Beringia compared to other glaciated margins during the Quaternary.

6.1. Introduction

During Pleistocene sea-level lowstands controlled by continent-wide glaciations, a large portion of the up to 900 km wide shelf north of the Bering Strait between East Siberia and Alaska became emergent (Elias & Brigham-Grette, 2013). This area is part of a region named Beringia (Figure 6.1). Onshore geological investigations suggest that Beringia has not hosted large ice sheets like those on Greenland or the marine-based Kara-Barents ice sheet during the Quaternary (Brigham-Grette & Gualtieri, 2004; Elias & Brigham-Grette, 2013). Instead, a widespread mountain glaciation in East Siberia and Alaska was assumed from the presence of moraines and the lack of evidence for glacio-isostatic rebound along the coasts (Barr & C. D. Clark, 2012; Brigham-Grette & Gualtieri, 2004; Glushkova, 2011; Kaufman et al., 2011). Additionally, cored evidence for continuous deposition in lake El'gygytgyn over the last 2.8 Myrs (Figure 6.1) support models that no large ice sheets existed onshore East Siberia (Melles et al., 2012).

The offshore sedimentary record of its northern continental margin supports a contrasting scenario. Geophysical data from the northern margin of Beringia provide reliable information that the outer continental margins of the East Siberian and Chukchi Seas host widespread glacial seafloor features on the continental shelf (e.g., mega-scale glacial lineations, grounding zone wedges), and slope (glacial debris flows in water depths shallower than 1200 m) (Dove et al., 2014; Hegewald & Jokat, 2013b; S. Kim et al., 2021; Lehmann et al., 2022; Niessen et al., 2013). Further, glacial sediments raise evidence for larger glaciations prior to the Late Pleistocene are found on the New Siberian Islands and Wrangel Island (Gualtieri et al., 2005; Nikolskiy et al., 2017). The widespread presence and great variety of glacial features indicate the action of a regional marine-based ice sheet in the area of the Beringian continental margin (Dove et al., 2014; Niessen et al., 2013). Additionally, three bathymetric troughs likely eroded by ice streams (the DeLong Trough, the Western Bathymetric Trough and the Broad Bathymetric Trough (Figure 6.1, top panel 1 - 3) are found along the northern continental shelf of Beringia (Dove et al., 2014; S. Kim et al., 2021; O´Regan et al., 2017). However, the exact timing, geometries and dynamics of these ice sheets are at present unknown.

Grounded ice sheets have shaped the continental shelves and delivered large amounts of sediments to the continental slopes of most high latitude continental margins (Berger & Jokat, 2008; Dahlgren et al., 2005; Laberg et al., 2012; Nielsen et al., 2005). In seismic reflection data, glacial deposits on continental slopes appear as chaotic or opaque wedges separated by thinner acoustically stratified units (Laberg & Vorren, 1996; Ó Cofaigh et al., 2003). These patterns are the consequence of
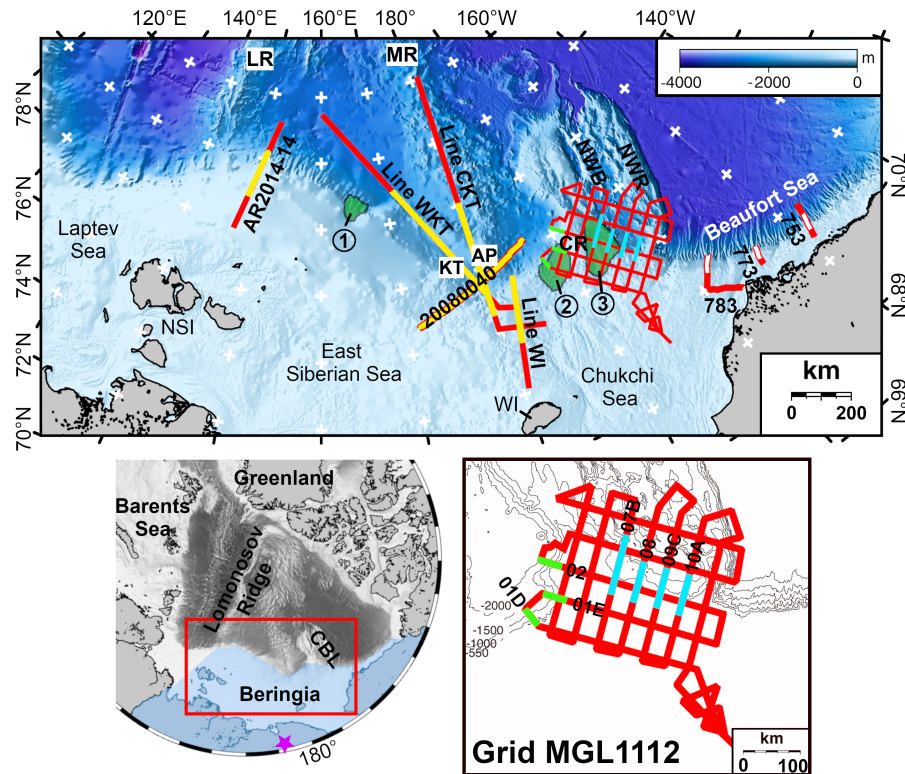
Figure 6.1. – Top panel: Overview of used seismic profiles. Bathymetric background map: IBCAO v4 (Jakobsson et al., 2020). Red lines: seismic profiles used in this study. Yellow lines: sections shown in figure 6.2 (East Siberian Sea), Light green lines: sections shown in figure 6.3 (Western Chukchi Rise), Light blue lines: sections used in figure 6.4 (Northwind Basin), White Lines: sections used in figure 6.5 (Beaufort Sea), Green areas: 1 – DeLong Trough, 2 – Western Bathymetric Trough, 3 – Broad Bathymetric Trough. Lower left panel: Overview Arctic Ocean and Beringia (transparent blue area). Purple Star: Lake El'gygytgyn. Lower right panel: Zoom of seismic profiles MGL1112. Abbreviations: AP – Arlis Plateau, CR – Chukchi Rise, CBL – Chukchi Borderland, KT- Kucherov Terrace, LR – Lomonosov Ridge, MR – Mendeleev Ridge, NWB – Northwind Basin, NWR – Northwind Ridge, NSI – New Siberian Islands, WI – Wrangel Island.

episodic delivery of unsorted glacially transported sediments, interspersed with interglacial periods of hemipelagic sedimentation (Ó Cofaigh et al., 2003). The volume of glacially transported sediments varies with different ice flow velocities along such margins (Dahlgren et al., 2002; J. Dowdeswell et al., 2002; Rydningen et al., 2015). The largest quantities of such sediments are delivered by fast flowing ice-streams to be deposited in trough mouth fans at the mouths of deep glacially scoured cross-shelf troughs (Batchelor & J. A. Dowdeswell, 2014; Vorren et al., 1989; Vorren & Laberg, 1997). In contrast, between ice streams the flow rate is one to two orders of magnitude slower leading to a relative dearth of glacially transported sediments on the continental slope (J. Dowdeswell et al., 2002). Glacially transported material forms prograding wedges that relocate shelf breaks towards the ocean. For example, the

continental margins of East Greenland and Scandinavia have prograded basinwards by up to 80 and 150 kilometers, respectively (Berger & Jokat, 2008; Rise et al., 2005; Vorren et al., 1998). Furthermore, Ó Cofaigh et al. (2003) stated that trough mouth fans require a wide continental shelf with abundant and erodible sediments and low gradient (<1°) continental slopes. However, along the northern rims of Beringia, wedges of chaotic strata overlying stratified, prograding sediment horizons have so far only been described at a few locations (Dove et al., 2014; Hegewald & Jokat, 2013a; S. Kim et al., 2021).

The objective of this paper is to review the accessible seismic data base to find evidence for: i) glacial sediments on the continental margin, and from this, ii) the existence and possible extent of former ice sheets and/or ice shelves along the continental margins from the Laptev Sea to the Beaufort Sea. For this, we use reprocessed 2D multi-channel seismic data from the outer Chukchi Shelf and Chukchi Borderland as well as published seismic reflection data (Niessen et al., 2013; Nikishin et al., 2017; Triezenberg et al., 2016) along the continental margin of Beringia to identify and describe glacial deposits. Afterwards, we compare these deposits with glacial deposits along the Norwegian and East Greenland margins.

6.2. Data and Methods

The R/V Marcus G. Langseth acquired a regional 2D seismic grid (Figure 6.1, in total 5300 km) across the Chukchi Shelf and Borderland (Coakley, 2011a; Coakley, 2011b; Ilhan & Coakley, 2018) in 2011. Details of this cruise can be found in Ilhan & Coakley (2018) and Lehmann et al. (2022). The multi-channel seismic data (MCS) were originally processed in 25 m bins by ION Geophysical (Ilhan & Coakley, 2018). We reprocessed the data with a 6.25 m binning to achieve better resolution of shallow and small-scale structures by using the closer hydrophone spacing. The reprocessing is described in detail in Lehmann et al. (2022).

In addition to the reprocessed profiles, we use the few previously-published seismic profiles that enable us to image the continental slopes from ~147° E in the East Siberian Sea to ~149° W in the Beaufort Sea (a distance of ~1800 km) (Figure 6.1). The profiles are of variable resolution; in some older ones, shallow acoustic sequences are difficult to interpret. We split the study area into four parts (East Siberian Margin, Chukchi Rise, Northwind Basin, Beaufort Sea; Figures 6.2 – 6.5). For the East Siberian Margin (Figure 6.2), we rely on seismic reflection data published by Nikishin et al. (2017) and Niessen et al. (2013). The reprocessed MCS profiles across the western Chukchi Rise and the Northwind Basin are shown in figure 6.3 and figure 6.4, respectively. Line drawings from the Beaufort Sea (Figure 6.5) are based on

published MCS data of the L-9-77-AR cruise (Triezenberg et al., 2016).

6.3. Results

We identified acoustically chaotic sequences and prograding wedges in all four sub-regions. These sediments are highlighted with light blue fill in Figures 6.2-6.5. Acoustically well-layered strata below the chaotic layers and wedges are filled in light gray in the figures. Individual reflectors highlighted with colored lines in the line drawings are adopted from the original interpretations.

6.3.1. East Siberian Margin (147° E − 175° W)

In the western East Siberian Sea sector (147° E to 165° E), no large-scale erosion is imaged on the continental shelf in the available MCS data (Figure 6.2a). In addition, the upper sedimentary units on the slope are well stratified and show no extensive shelf progradation consisting of chaotic sediments (Figure 6.2a). The slope angle is ∼0.8°.

Further east, from ∼170° E to ∼175° W, the shallow shelf of the East Siberian Sea hosts chaotic layered sediments with a maximum thickness of 150 m (200 ms TWT) (Figure 6.2 b, c, d). On profile WKT, a layer of chaotic sediments with a maximum thickness of ∼90 m (100 ms TWT) covers the shelf and slope in water depths less than 1200 m (Figure 6.2b). This sediment layer is on profile AWI-20080040 (Figure 6.2d) over the eastern Kucherov Terrace, in contrast, up to ∼325 m (380 ms TWT) thick. The development of this wedge shape relocated the shelf break outwards by ∼13 km towards the Kucherov Terrace (Figure 6.2d). A small terrace is present at a water depth of ∼650 m (Figure 6.2d) on profile AWI-20080040. On the western Kucherov Terrace in water depths below ∼1200 m (1600 ms TWT), the seafloor and the underlying reflections are flat and undisturbed (Figure 6.2b). However, at the northern and eastern flanks of the Kucherov Terraces, the MCS data image chaotic sediments in water depths of 1500 m (2 s TWT, figure 6.2c) and 2750 m (3 s TWT, figure 6.2d), respectively.

On profile WI (Figures 6.1, 6.2e), located between the Kucherov Terrace and the Chukchi Borderland, chaotic sediments have led to shelf progradation by ∼6 km. The slope angle is ∼1.5° (Figure 6.2e). The chaotic unit is up to ∼200 m (230 ms TWT) thick (Figure 6.2e). A terrace of ∼5 km width, with a rough seafloor, can be observed in water depths of ∼450 m (600 ms TWT) (Figure 6.2e).
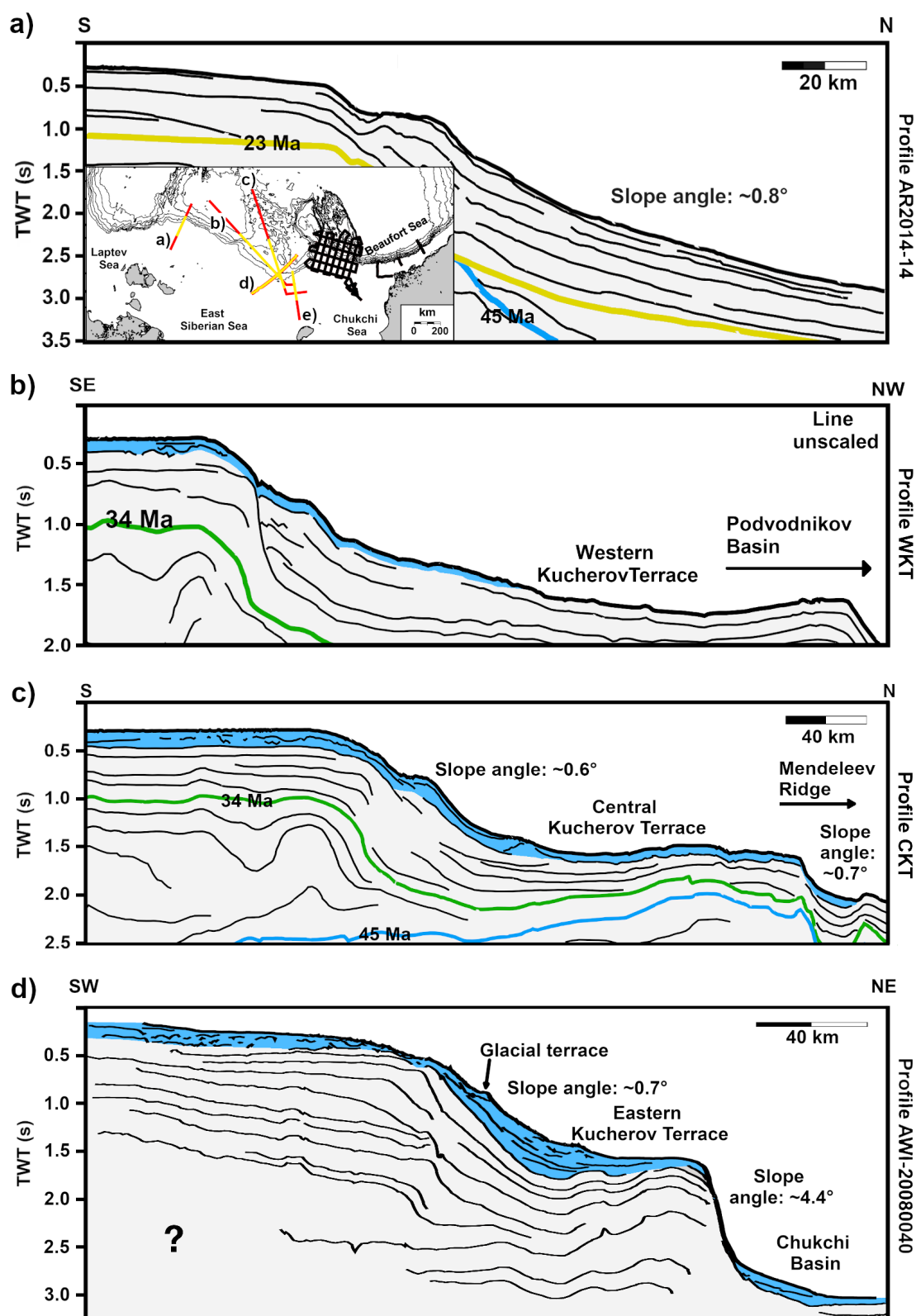
Figure 6.2. – Line drawings of seismic profiles in western East Siberian Sea. a) profile AR2014-14 just east of Lomonosov Ridge (Nikishin et al., 2017), b) across western Kucherov Terrace (Composite profile, unscaled, (Nikishin et al., 2017)), c) across the central and northern flank of the Kucherov Terrace (composite profile, Nikishin et al., 2017), d) eastern Kucherov Terrace (AWI20080040), e) from Wrangel island to Chukchi Basin (Nikishin et al., 2017)). Blue: glacial sediments, light gray: preglacial.
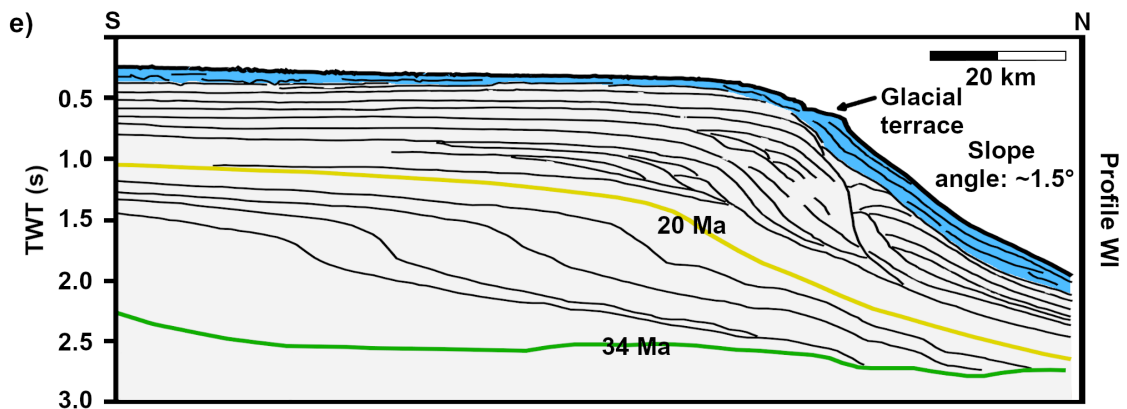
Figure 6.2 continued.

6.3.2. Western Chukchi Rise (175° W – 168° W)

Seismic profiles across the western flank of the Chukchi Rise show well layered strata to be truncated on the shelf, but to be covered by chaotic deposits and prograding chaotic sequences beyond the shelf break (Figure 6.3). The accumulation of chaotic seismic units on the slope has led to progradation of the shelf break by ∼6 km at 168° W (Figure 6.3a; profile 01D), ∼10 km on profile 01E at 170° W (Figure 6.3b; profile 01E) and ∼3 km on profile 02 at 172° W. The prograding wedge on profile 01D (Figure 6.3a) reaches a maximum thickness of ∼450 m (530 ms TWT). The thickness decreases eastward to ∼380 m (450 ms TWT) on profile 01E (Figure 6.3b) and just ∼140 m (160 ms TWT) on profile 02 (Figure 6.3c). Along with the decreasing thickness, the slope angle increases from west (∼1.7°, figure 6.3a) to east (∼3°, figure 6.3c).

6.3.3. Northwind Basin (165° W – 161° W)

Seismic data image basins on the outer Chukchi Shelf east of the Chukchi Rise. The basins are floored by preglacial strata and filled with chaotic sediments (Figure 6.4a, b). The basins are 32 km to 44 km wide (Figure 6.4a, b) and the thickness of their fill ranges between 425 m (500 ms TWT) and ∼220 m (250 ms TWT) on profile 07B and 08 (Figure 6.4a, b), respectively. The underlying well stratified sequences both up- and downslope of these basins are truncated and covered by chaotic sediments (Figure 6.4, zoom 6.4b).

The structure of the continental slope to the Northwind Basin changes from east to west. On profile 07B, no prograding chaotic sequences are observed beyond the shelf break to the Northwind Basin (Figure 6.4a). Instead, a thick wedge-shaped unit with chaotic seismic character is visible in the Northwind Basin (Figure 6.4a). The wedge extends for ∼62 km into the basin and onlaps an exposed basement high
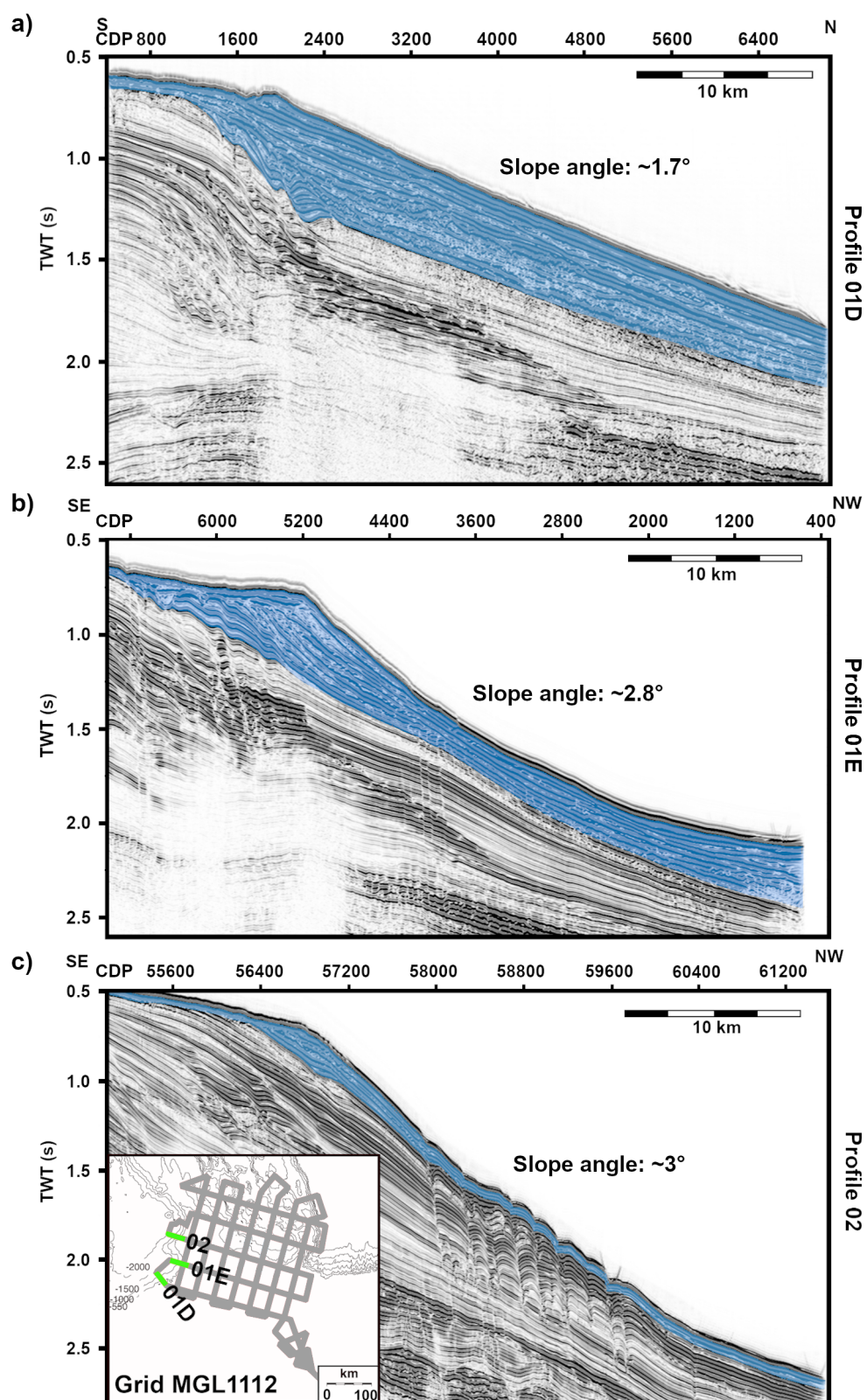
Figure 6.3. – Seismic profiles of the western flank of the Chukchi Rise with glacial deposited material in blue. Profiles A) 01D, b) 01E, c) 02 from southwest to northeast (see locations in inlet map).

at CDP 1600 (Figure 6.4a). The chaotic reflection character in this wedge is crossed by two relatively continuous reflections, dividing it into 3 different units (Figure 6.4a, zoom). The lowermost unit (blue fill in figure 6.4a, zoom) is wedge-shaped, and can be further subdivided by two semi-continuous reflections (white stippled lines). The wedge is thickest in the southwest, up to ~360 m (420 ms TWT), and thins towards the northeast to ~70 m (85 ms TWT). The continental slope on profile 07B has an angle of 11.5° (Figure 6.4a).

Similar to profile 07B (Figure 6.4a), prograding chaotic sequences are absent on the step-like slope to the Northwind Basin on profile 08 (Figure 6.4b). The upper slope is steep, with an angle of 8.1° (Figure 6.4b). A small basin ~300 m below the shelf break is filled with ~250 m (300 ms TWT) of chaotic sediments. Downslope of the small basin, the continental slope is covered by ~130 m (150 ms TWT) of chaotic deposits (Figure 6.4b).

The margin of the Northwind Basin is less steep in the east than in the west. Here, on the two eastern profiles 09C at ~162° W and 10 at ~161° W, prograding chaotic sequences have widened the shelf by 2 km and 1 km, respectively (Figure 6.4c, d). The continental margin of profile 9C (Figure 6.4c) is divided into two parts by a spike-like elevation of underlying stratified material that forms a step in the seafloor at CDP 6800 (Figure 6.4c). The maximum thicknesses of chaotic deposits of profile 09C are ~340 m (400 ms TWT) on the upper slope and ~280 m (330 ms TWT) on the lower slope (Figure 6.4c). On profile 10, chaotic sediments reach a maximum thickness of 255 m (300 ms TWT; profile 10), thinning basinward over a distance of 12.5 km to ~65 m (75 ms TWT) (Figure 6.4d). Slope angles on profile 09C are 1.5° on the upper part of the slope and ~0.4° further down. The slope angle on profile 10 is ~1.2° (Figure 6.4d).
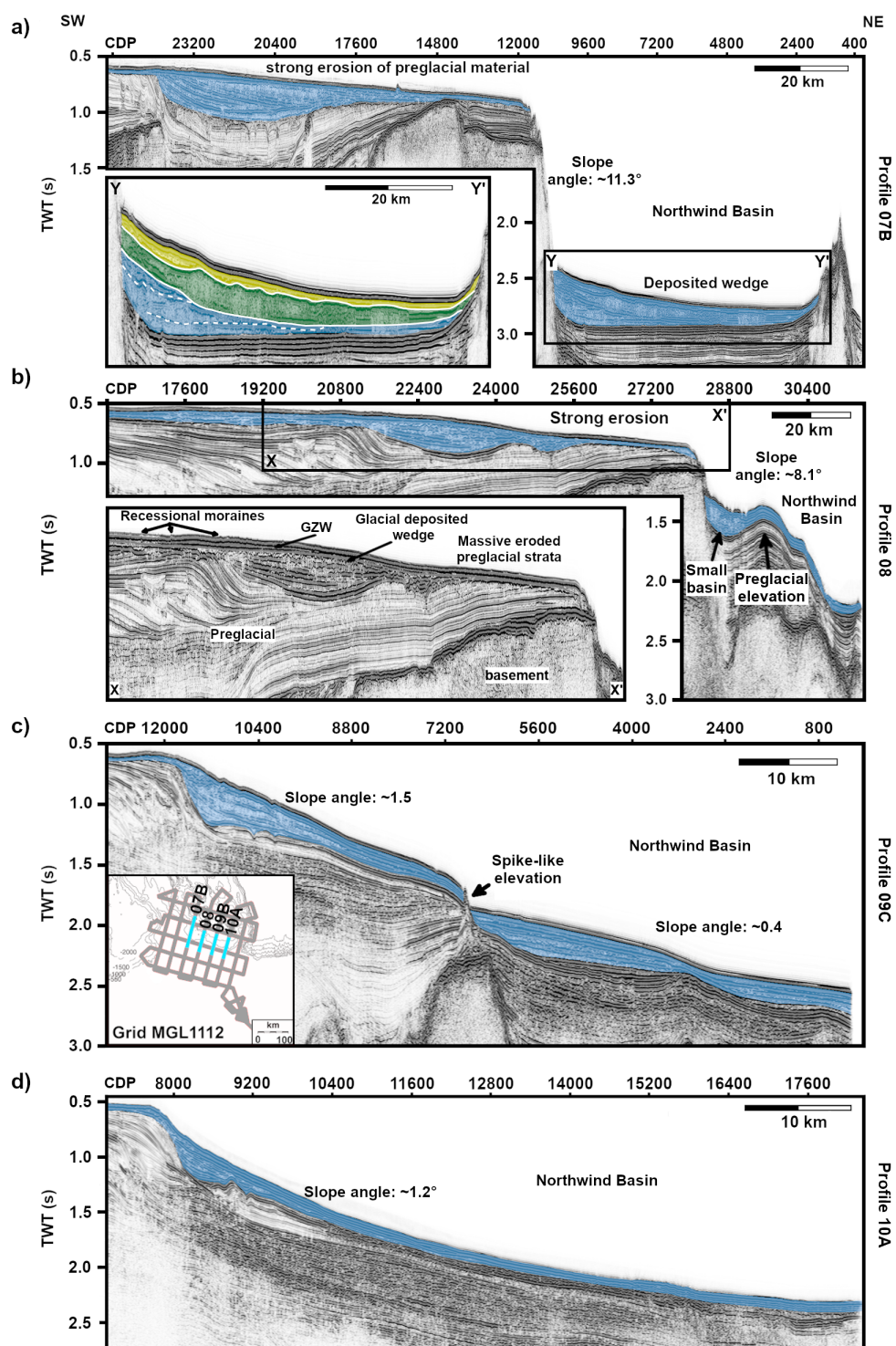
Figure 6.4. – Four seismic profiles with glacial material shaded in blue. Profiles a) 07, b) 08, c) 09 and d) 10 from west to east along the slope towards the Northwind Basin (see locations in inlet map). Zoom in a) shows sedimentary units: blue color: units 1 to 3, green: unit 4 and yellow: unit 5. Zoom in b) shows basins filled with glacial sediments and eroded preglacial sediments covered by glacial sediments and landforms (Lehmann et al., 2022).

6.3.4. Beaufort Margin (161° W – 149° W)

Typical prograding chaotic sequences of the kind described previously are absent along the Alaskan-Beaufort margin between 160° W and 149° W (Figure 6.5). Instead, well stratified reflections lie parallel to the dipping seafloor on the upper part of the slope close to the shelf break (Figure 6.5b). On profile 753, a ~200 m (250 ms TWT) thick disturbed sediment layer below a rough seafloor is present on the slope (Figure 6.5c).
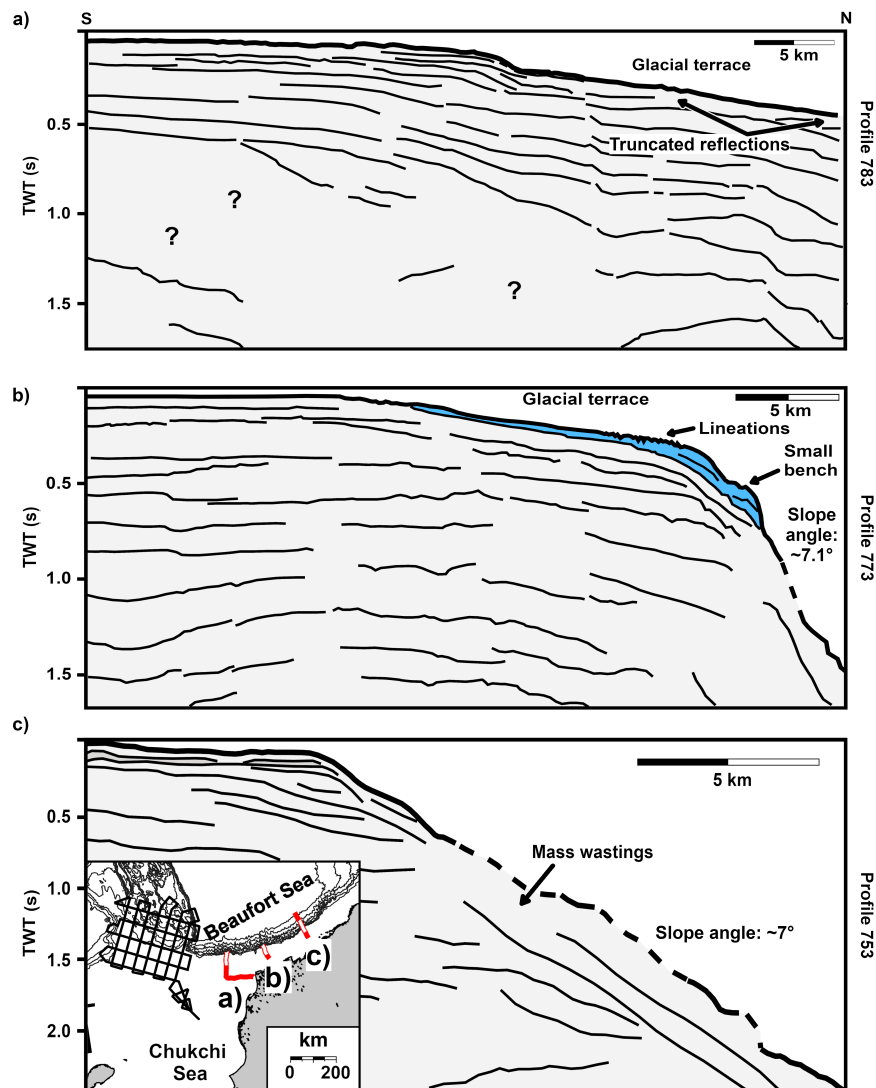
Figure 6.5. – Sketches of the Beaufort continental margin. A) profile 783 shows a glacial terrace, b) profile 773, glacial terrace is covered by a layer of transparent sediments (blue), c) profile 753 with a thick layer of mass-wastings (see locations in inlet map)

On the western profiles (Figure 6.5a, b), a planar terrace with slope angle lower to the wider slope is imaged which is absent from the eastern profile (753; figure

6.5c). This terrace is up to 35 km wide and located at a depth of 250 m to $\sim$500 m. Stratified reflections are partly truncated on this terrace (Figure 6.5a). A rough seafloor is present in water depths of 300 m (400 ms TWT) (Profile 773; figure 6.5b). Further, the terrace on this profile is covered by an acoustically transparent layer of 40 m thickness. This layer also forms a smaller 2.5 km wide bench on the slope beyond the shelf break (Figure 6.5b).

6.4. Discussion

During Quaternary times, almost all of the continental margins surrounding the northern North Atlantic, Baffin Bay, and the Arctic Ocean were strongly modified by processes related to the Northern Hemisphere glaciations (Batchelor et al., 2019 and references therein). Whilst it is in general well accepted that those parts of Beringia that are situated onshore today did not host major ice sheets during the Quaternary (Elias & Brigham-Grette, 2013; Glushkova, 2011; Kaufman et al., 2011), the of up to 900 km wide shelf regions have been suggested to have hosted a large ice sheet before the LGM (Dove et al., 2014; S. Kim et al., 2021; Lehmann et al., 2022; Niessen et al., 2013). To assess the significance of this so-called East Siberian Ice Sheet, we first discuss the available observations of its products from the Beringian margin. Afterwards, we compare those products with those of the better-known ice sheets of the northern hemisphere, using examples from East Greenland and Norway.

6.4.1. Glacial deposits at the Beringian Margin

Glacially reworked sediments and broad glacially scoured troughs are typical observations that provide information about the extent of glacial erosion from formerly glaciated shelf regions (e.g.,J. Dowdeswell et al., 2002; J. A. Dowdeswell et al., 2016; Laberg et al., 2012; Nielsen et al., 2005; Vorren et al., 1989). These sediments show a chaotic to transparent reflection pattern in a stratigraphic position above an erosive unconformity in acoustic data (Sættem et al., 1992). Along the Beringian margin glacially reworked sediments were recovered in piston cores on the Northwind Ridge (Dipre et al., 2018; Polyak et al., 2007) and on the slope of the Arlis Plateau (Joe et al., 2020). Therefore, we interpret the upper chaotic sequences and prograding sequences along the Beringian margin to be of glacial origin. Such sediments are imaged in seismic and sediment echosounder data covering not only the East Siberian Shelf (Figure 6.2b, c, d, e), but also wide areas of the outer Chukchi Shelf (Dove et al., 2014; S. Kim et al., 2021; Lehmann et al., 2022). Reworked glacial sediments are not imaged in seismic data at $\sim$147° E (Figure 6.2a) and further west (Nikishin et al., 2017; Weigelt et al., 2014). This is supported by geological investigations

which suggests that the Laptev Sea and western East Siberian continental shelf and margin (Figure 6.2a) remained free of large ice sheets throughout the Cenozoic northern hemisphere glaciations (Batchelor et al., 2019; Kleiber & Niessen, 1999; Romanovskii & Hubberten, 2001; Svendsen et al., 2004). Based on the location of the glacially eroded DeLong trough at ~165° E (Figure 6.6) (O´Regan et al., 2017) and glacial deposits on the New Siberian Islands (Nikolskiy et al., 2017), we assume that pre-LGM ice sheets developed northeast of the New Siberian Islands. The absence of extensive glacial deposits on profile 2014-14 (Figure 6.2a) limits the maximum ice sheets extension along the Beringian margin to the region east of this profile and west of the DeLong trough. This enables us to extend Niessen et al. (2013) estimate of the ice sheet limit slightly by ~70 km further to the Laptev Sea (Figure 6.6).

Further verification of the estimated extent of the ice sheet is difficult at present, for various reasons. Firstly, widespread and long-lived subaerial erosion of much of the shelf region (blue stipple in figure 6.6) during the LGM, which was accompanied by eustatic sea-level fall of 130 m (Miller et al., 2020). This erosion, along with the marine transgression(s) and post transgressive sediments, has likely removed much of the evidence of pre-LGM glaciations (Hill et al., 2007). Secondly, the existing geophysical database of the Beringian Shelf is sparse and focused on deeper sedimentary and tectonic structures, so that shallow reflections are not well imaged in seismic data. Furthermore, the remaining interpretable features, like erosional surfaces, moraines, and drainage channels that were probably incised by meltwater, are either undated or dated to the LGM (Hill & Driscoll, 2008; Hill & Driscoll, 2010; Jakobsson et al., 2017; Lehmann et al., 2022). Thirdly, iceberg scouring during the LGM has extensively eroded theargins of Beringia to present-day water depths of ~350 m (Figure 6.6, white hatched area), eliminating seafloor evidence for previous glaciations (Dove et al., 2014; Hill et al., 2007; Jakobsson et al., 2014; Polyak et al., 2007).

The thicknesses of glacial deposits vary along the continental slope between the De-Long Trough at 165° E in the East Siberian Sea and the Northwind Ridge at 161° W (Table 6.1). This variation can be interpreted in terms of variable ice flow velocities along the shelf edge causing fan and inter-fan areas (J. Dowdeswell et al., 2002). The limited available acoustic data of the trough mouth fan at the head of the De-Long trough suggest a glacial sediment thickness of at least 65 m (O´Regan et al., 2017).The thickest deposits occur on the eastern Kucherov Terrace at ~178° E as well as east and west of the Chukchi Rise between 170° W and 172° W and between 165° W and 163° W (Table 6.1) at the head of the suggested Western Bathymetric
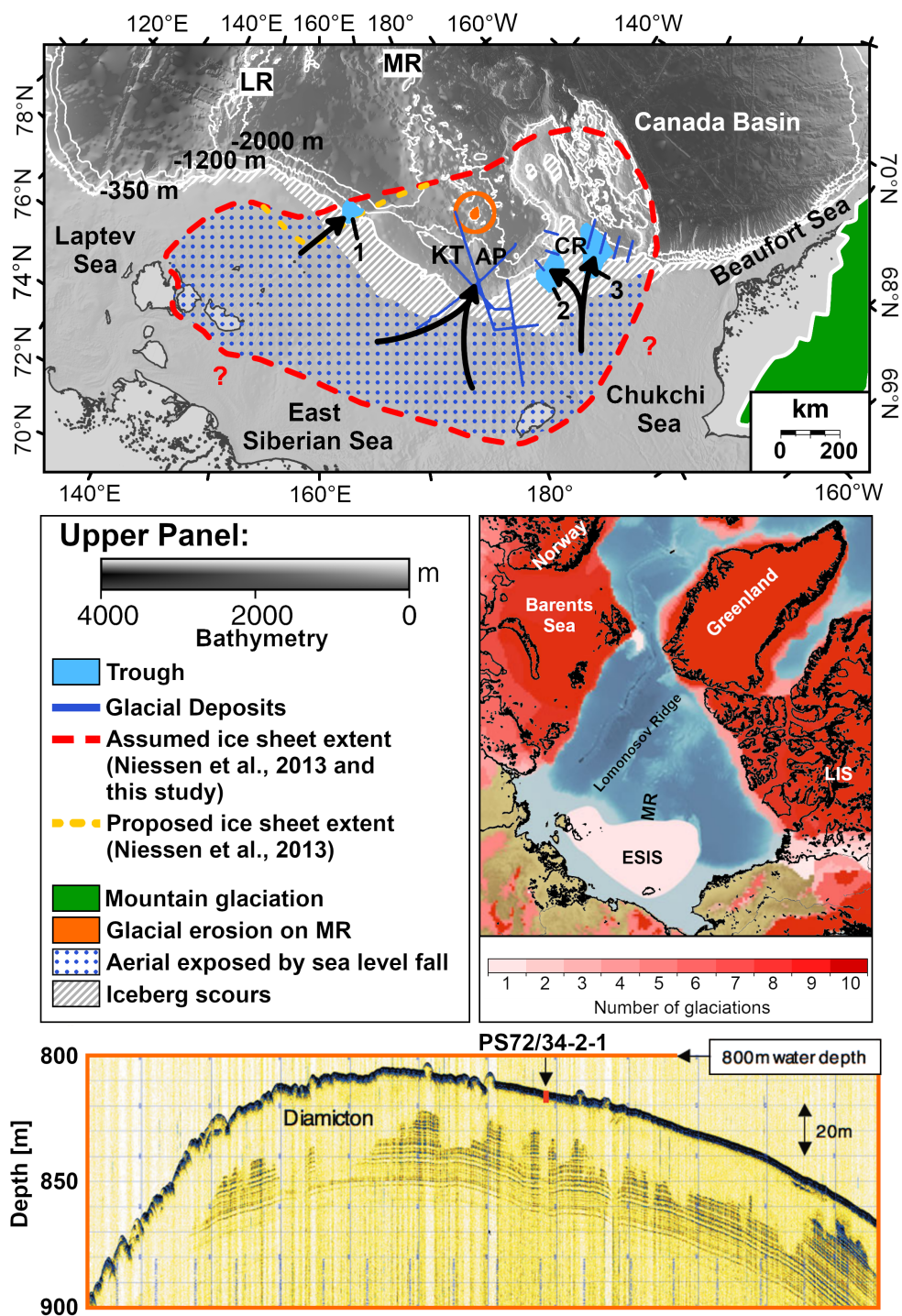
Figure 6.6. – Upper panel: suggested maximum ice sheet extent on the Beringian margin (Niessen et al., 2013). Bathymetric map from Jakobsson et al. (2020), 1) DeLong Trough, 2) Western Bathymetric Trough, 3) Broad Bathymetric Trough. Central right panel: maximum ice sheet extensions and number of regionally glaciations in the Northern Hemisphere regardless of time (modified from Batchelor et al., 2019), lower panel: sub-bottom profiler section showing glacial erosion and diamiton on the southern Mendeleev Ridge (modified from Stein et al., 2010). Abbreviations: ESIS – East Siberian Ice Sheet, LIS – Laurentide Ice Sheet, LR – Lomonosov Ridge, MR – Mendeleev Ridge

Trough and Broad Bathymetric Trough (Figure 6.6; upper panel) (Dove et al., 2014; S. Kim et al., 2021). As ice flow patterns are controlled by subglacial topography (Siegert & J. A. Dowdeswell, 1996; Winsborrow et al., 2010), it seems likely that the Chukchi Rise affected the routing of the ice streams that would have scoured these glacial troughs.

Sediments transported by ice streams are present in basins in the Broad Bathymetric Trough at the eastern flank of the Chukchi Rise (Figure 6.4a, b) and as a sedimentary wedge in the western Northwind Basin (Figure 6.4a). This wedge developed at the foot of the slope because the slope gradients of $\sim$11.5° and $\sim$8° were too steep to accumulate progradational strata between $\sim$165° W and $\sim$163° W (Figure 6.4 a, b) (Ó Cofaigh et al., 2003). This is comparable with an immature high gradient trough mouth fan with sigmoid slope with gradients $>$4° (Dahlgren et al., 2005; Rydningen et al., 2015). The sedimentary wedge is characterized by mainly chaotic reflections and subdivided by two continuous reflections into three main units, of which the lowermost unit may possibly be divisible by two further semi-continuous reflections (Figure 6.4a, zoom: yellow, green and blue areas). The continuous reflections are indications for the presence of hemipelagic sediments accumulated during interglacials (Ó Cofaigh et al., 2003) and so indicate a minimum of three and as many as five major ice streams advances through the Broad Bathymetric Trough. At least four glacial advances are assumed by seismostratigraphic studies of deposits at the head of the Western Bathymetric Trough (S. Kim et al., 2021). Diamictons on the western slope of the Kucherov Terrace also suggest at least five major glacial advances (Niessen et al., 2013). The suggested number of glacial advances supports a multi-cyclic glaciation history of the northern Beringian margin (Dove et al., 2014; S. Kim et al., 2021; Lehmann et al., 2022; Niessen et al., 2013).

The thickest glacial deposits occur between the shelf break and seafloor elevations formed by preglacial deposits on the central profiles 08 and 09C across the slope to the Northwind Basin (162° W – 163° W) (Figure 6.4b, c). Both seafloor elevations acted as barriers to glacial transportation, explaining the contrasting thicknesses of glacial material up- and downslope of the elevations (Figure 6.4b, c). Similar observations have been made along the East Greenland margin, where glacial deposits are thicker upslope of a basement high (1000 m) and thinner downslope of it (400 m) (Berger & Jokat, 2008).

Glacial erosion and sediments as imaged in figure 6.5 were interpreted along the Beaufort margin towards the Chukchi Borderland as the result of a margin parallel advancing ice shelf sourced from the Laurentide Ice Sheet (Engels et al., 2008;

Jakobsson et al., 2008; Polyak et al., 2007). Based on these interpretations and the absence of thick glacial deposits on the slope (Figure 6.5), it is possible that a ice sheet on the Beringian margin extended only as far as the Northwind Ridge. However, glacial debris from a more extensive ice sheet on the Chukchi Shelf could have bypassed the slope by turbidity currents into the deep Canada Basin facilitated by slope gradients in places exceeding 10° east of 161° W (Engels et al., 2008; Ó Cofaigh et al., 2003; Piper & Normark, 2009). This process is indicated by the abundance numerous canyons at the slope of the Beaufort margin (Engels et al., 2008). In addition, along the Beaufort margin at the base of the slope and in the adjacent Canada Basin (Figure 6.5c) the products of large mass wasting events are imaged (Dinter et al., 1990; Grantz et al., 1979). They affected more than 200 m of Upper Quaternary sedimentary cover and may have displaced glacially deposited material downslope (Dinter et al., 1990; Grantz et al., 1979). However, transparent sedimentary unit and erosion of preglacial sediments might also be the result of strong currents (Corlett & Pickart, 2017; Darby et al., 2009). Our database is not sufficient to investigate these possibilities for the Beaufort Sea in detail.

6.4.2. Comparisons to the Greenland and Norwegian continental shelves

Geophysical and sediment core data clearly shows that the northern margin of Beringia was glaciated at some time during the Quaternary (Dove et al., 2014; Jakobsson et al., 2014; S. Kim et al., 2021; Niessen et al., 2013; O´Regan et al., 2017; Polyak et al., 2007). However, the morphology shaped by glaciation in this region have yet to be compared to that of the better known glacially overprinted shelves from the East Greenland and Norwegian continental margins.

The ice sheets that affected the Norwegian and Greenland continental margins nucleated on the onshore mountain ranges with present-day elevations of up to 3700 m in Greenland and 2500 m in Norway. The mountain ranges of northern Alaska and East Siberia are similarly high, reaching 2750 m and 3000 m, respectively. However, geological and geomorphological studies onshore of East Siberia and Alaska excluded an extensive ice sheet in these regions during the Quaternary (Barr & C. D. Clark, 2012; Elias & Brigham-Grette, 2013; Glushkova, 2011; Kaufman et al., 2011). This is based partly on sedimentary deposits in Lake El'gygytgyn in East Siberia, which have been continuous since 2.8 Myr (Melles et al., 2012), and partly on moraines and glacial sediments, which show that the maximum extent of the glaciers was confined to the mountain ranges of East Siberia and Alaska (Barr & C. D. Clark, 2012; Glushkova, 2011; Kaufman et al., 2011; figure 6.6). All these studies show that an onshore source area is missing in Beringia to provide massive ice volume for the development of large-scale ice streams to the northern shelf areas, and in turn

Table 6.1. – Glacial sediments sequences found along the Beringian, Norwegian and East Greenland continental margins. The absence of propagation and slope angle measurements for profile WKT are related to the absence of a scale bar in the original figure. TMF: trough mouth fan.

Region	Profile	Basinward propagation [km]	Thickness glacial sediment [m]	Slope angle [°]	References
East Siberian Margin (147° E – 175° W)	AR2014-14	-	-	0.8	Figure 6.2a
	DeLong Trough	-	>65	1.2	O´Regan et al., 2017
	WKT	Not determinable	90	Not determinable	Figure 6.2b
	CKT	10	140	0.6	Figure 6.2c
	20080040	13	325	0.7 upper part, 4.4 lower part	Figure 6.2d
	WI	6	200	1.5	Figure 6.2e
Western Chukchi Rise (175° W – 168° W)	01D	6	450	1.7	Figure 6.3a
	01E	10	380	2.8	Figure 6.3b
	02	3	140	3	Figure 6.3c
Northwind Basin (165° W – 161° W)	07B	-	360	11.5	Figure 6.4a
	08	-	250	8.1	Figure 6.4b
	09C	2	340	1.5 upper part, 0.4 lower part	Figure 6.4c
	10A	1	255	1.2	Figure 6.4d
Beaufort Margin (161° W – 149° W)	783	Slope not displayed	-	Slope not displayed	Figure 6.5a
	773	-	-	7.1	Figure 6.5b
	753	-	-	7	Figure 6.5c
Norwegian Margin	Lofoten Margin	-	-	>10	Taylor et al., 2000
	Bear Island TMF	120	3500	0.8	Laberg & Vorren, 1996
Greenland Margin	Scoresby Sound TMF	45	2000	2.1	Vanneste et al., 1995

glacially eroded large-scale cross-shelf troughs.

As the onshore geology reports its absence, the today's outer shelf areas and continental margins of Beringia are left as a host for ice sheets. The northern Beringian Shelf is up to 900 km wide which exceeds the maximum 300 km and 250 km widths of the continental shelves of East Greenland and Norway (excluding the epicontinental Barents Sea), respectively (Arndt et al., 2015; Nielsen et al., 2005). Water depths across the Beringian Shelf range from <50 m on the inner shelf to present-day shelf breaks in water depths of 100 − 200 m in the Beaufort Sea to ∼300 − 750 m along the rest of the Beringian margin. The shelf break is deeper than its counterparts off East Greenland (142 m - 500 m) and Norway (50 m to 350 m south of 64° N, up to 400 m northwards) (Nielsen et al., 2005; Rise et al., 2005). Along the Norwegian and East Greenland margins, a number of deep glacial troughs are observed to cross the continental shelves with water depths as deep as 1000 m separated by shallow banks with water depths less than 100 m (Batchelor & J. A. Dowdeswell, 2014; Nielsen et al., 2005; Vorren et al., 1989). Some of these troughs are in part over-deepened on the inner shelf compared to the trough mouth (Batchelor & J. A. Dowdeswell, 2014; Nielsen et al., 2005). In contrast, only three troughs have been discovered along the northern Beringian margin (Dove et al., 2014; S. Kim et al., 2021; O´Regan et al., 2017). A maximum depth of 140 m is reported for the DeLong Trough northeast of the New Siberian Islands (O´Regan et al., 2017). The dimensions of the two glacial troughs on the flanks of the Chukchi Rise are not fully mapped and not precisely known, but are likely in a depth range of tens of meters. The major troughs of the East Greenland and Norwegian shelves are often associated with fjord systems at the coasts, and straits between islands of the Canadian Archipelago (Batchelor & J. A. Dowdeswell, 2014). These associations are not observed along the shores of Beringia (Figure 6.6). Trough depths are controlled by the intensity, duration and frequency of cross-shelf glaciations (Batchelor & J. A. Dowdeswell, 2014). Greenland and Norway have both experienced more than ten ice sheet advances during the Quaternary alone (central right panel figure6.6;Batchelor et al., 2019 and references therein). Owing to the lack of sediment cores, it is unknown how many shelf glaciations occurred on the Beringian Shelf during the lifetime of the East Siberian Ice Sheet. Imaging of diamictons separated by laminated hemipelagic sediments in the Northwind Basin (Figure 6.4a), at the flank of the Chukchi Rise (S. Kim et al., 2021) and in the vicinity of the Arlis Plateau (Niessen et al., 2013), indicate the occurrence of at least 3-5 major shelf glaciations. If this number is regionally applicable, it suggests that the less pronounced overdeepening of the Beringian troughs may be attributable to a relatively stable and/or short-lived ice sheet, or alternatively to an ice sheet with a relatively stable northern edge.

Tidewater glaciers and/or small ice caps calving into the adjacent ocean have existed since 44 Myrs in Greenland and and since ∼15-14 Myrs the northern Barents Sea (Knies & Gaina, 2008; Tripati & Darby, 2018). This is assumed from ice rafted detritus pulses in sediment cores drilled in and south of the Fram Strait (Knies & Gaina, 2008; Tripati & Darby, 2018). However, the onset of continental-scale glaciation of Greenland is reported at around 3.5 Ma (Jansen et al., 2000) while the glacially-induced progradation of the East Greenland continental shelf already started at around 15 Ma (Berger & Jokat, 2008). Along the Norwegian margin, ice sheets first reached the shelf break at 2.7 Ma (Jansen et al., 2000; Rise et al., 2005). According to the sedimentary record as observed in one sediment core retrieved in the Canada Basin, the oldest known glaciation of the Beringian margin is associated with MIS 12 (478-424 kyrs) (Dong et al., 2017). This considerably later than the onset of the Northern Hemisphere Glaciation.

If ice streams delivered large quantities of sediment to the continental margins, trough mouth fans formed (Batchelor & J. A. Dowdeswell, 2014; J. Dowdeswell et al., 2002; Ó Cofaigh et al., 2003; Vorren et al., 1998). The trough mouth fans of East Greenland and Norway locally prograded the shelves (Batchelor & J. A. Dowdeswell, 2014; Dahlgren et al., 2005; Vorren et al., 1998). This is partly evident from seawards-convex bathymetric contour segments (Batchelor & J. A. Dowdeswell, 2014). Examples of such fans can be observed off Scoresby Sound and Bear Island Trough, where the fan shows basinward prograding sequences of 45 km and 120 km, respectively. The sediments have accumulated to thicknesses of 2 km and 3.5 km, respectively (Laberg & Vorren, 1996; Vanneste et al., 1995; Vorren et al., 1998). Along the Beringian margin, in contrast, we found such propagating sequences only reach a maximum of 10 km for a maximum sediment thickness of 450 m at the head of the suggested Western Bathymetric Trough (Table 6.1) (S. Kim et al., 2021). These observations strongly support the hypothesis of a shorter-lived or less dynamic ice sheet or ice sheet edge.

Undoubtedly, glacial prograding sequences between the Northwind Ridge at ∼161° W and the DeLong Trough at ∼165° E record the sediment cross-shelf transport of an ice sheet on this part of the Beringian margin (Figure 6.6). As discussed before, the absence of voluminous glacially transported sediments suggests that the East Siberian Ice Sheet(s) did not reach the shelf edge west of 165° E (Figure 6.6; DeLong trough). However, further east it remains possible that an ice margin advanced at least to the western Beaufort Shelf. If this was the case, the ice sheet margin may have been slow-moving and, therefore, delivered relatively insignificant quantities of

sediment to the slope. Those were not deposited but instead transported further into the basin by turbidity flows down the steep continental slope. This would be a comparable scenario to that for the continental margin west of the Lofoten Islands, whose formerly glaciated shelf is located close to a steep continental slope with numerous canyons (Taylor et al., 2000). Here, the Eurasian Ice Sheet repeatedly reached the shelf edge but transported only small amounts of sediment to the slope, which were directly transported further into the deep sea (Taylor et al., 2000). A recent study reported that a grounded, westward flowing ice shelf in western Alaska caused isostatic depression during MIS 5 (130 – 70 ka) (Farquharson et al., 2018). However, it could also have been partly caused by a northeastward out-phase advance of an ice sheet, which might have existed at the same time, from a more westerly Beringian margin into the Beaufort Sea.

Our study reveals quite puzzling observations regarding the thickness variations of glacial deposits and the extent of ice sheets along the nearly 1800 km Beringian margin. Clearly, a denser network of acoustic and sediments core data is needed to better understand the more local variations visible in the sparse geophysical data. This study could be helpful in identifying specific areas for more focused geoscience research.

6.5. Conclusion

From our compilation of already published and new seismic data along the Beringian continental margin we conclude that:

1. The strongest impact of ice sheet(s) occurs along the continental margin of Beringia from the Northwind Ridge to the Kucherov Terrace, as indicated by the distribution and thickness of glacially deposited sediments. The adjacent Beaufort margin and the western East Siberian continental margin were either not glaciated during glacial cycles or experienced less intense cyclicity. More data, especially along the East Siberian margin, are necessary to more precisely constrain the ice sheet's geometry.

2. The largest depocenters for glacial sediments are located upslope of the eastern Kucherov Terrace, in the western Northwind Basin, and at the flank of the western Chukchi Plateau. This distribution reflects the locations of fast flowing ice and ice streams.

3. Erosion by grounded ice is only observed down to water depths of at maximum 1200 m on the western Kucherov Terrace.

4. The influence of ice sheets on Beringia is comparable to that on other glaciated margins in terms of the variety of products. However, in contrast to the Norwegian and Greenland margins, glacially products like troughs and prograding sequences are generally less developed in our research area. This indicates the action of an ice sheet, that was less dynamic and/or shorter-lived than its Greenland and Eurasian counterparts.

A more detailed ice sheet reconstruction and grounding history on the northern rim of Beringia must await the availability of a better geoscientific database and sediment core data to provide age control on it.

Acknowledgments

7. Evaluation of Methane Release Potential on the Chukchi Shelf with Seismic Data

Carsten Lehmann[1,2], Wilfried Jokat[1,2],

[1] Alfred-Wegener-Institute, Helmholtz Centre for Polar and Marine Research (AWI), Am Alten Hafen 26, 27568 Bremerhaven, Germany,

[2] University of Bremen, Geoscience Department, Klagenfurter Str. 4, 28359 Bremen.

7.1. Abstract

Methane released from shelf regions is considered to be an important contributor to climate change. Knowledge of the potential of specific regions and the amount of methane released is critical for estimating expected climate change. We are using multichannel seismic data from R/V Marcus G. Langseth cruise MGL1112 to image the subsurface and identify upwelling gas migration structures and permafrost on the outer Chukchi Shelf in the Arctic Ocean. To this end, we examine the upper 2500 ms TWT of sediments for distinct sedimentary structures and anomalous seismic velocities. The data show a wide distribution of direct hydrocarbon indicators throughout the study area. The geologic structures show upward gas migration from deeper sources. Nevertheless, no bottom simulating reflector is identified in the study area to indicate the base of a likely gas hydrate zone. Furthermore, no high seismic velocities or strong ground reflectors are observed as indicator for existing submarine permafrost in the investigated area of the outer Chukchi Shelf.

7.2. Introduction

Methane is a very powerful greenhouse gas, which is 25 times more climate relevant than carbon dioxide (Kerr, 2010). In the marine setting, methane can be dissolved in pore waters or exist as free gas if the saturation is exceeded (Fleischer et al., 2001). Further, large reservoirs of methane are stored in permafrost and gas hydrates in shelf regions surrounding the Arctic Oceans (Shakhova et al., 2010). The warming climate is deteriorating the permafrost cause methane to escape from its shallow reservoirs. When this methane is released into the atmosphere it will have a strong contribution to already ongoing global climate change (Kerr, 2010; Sarkar

et al., 2012).
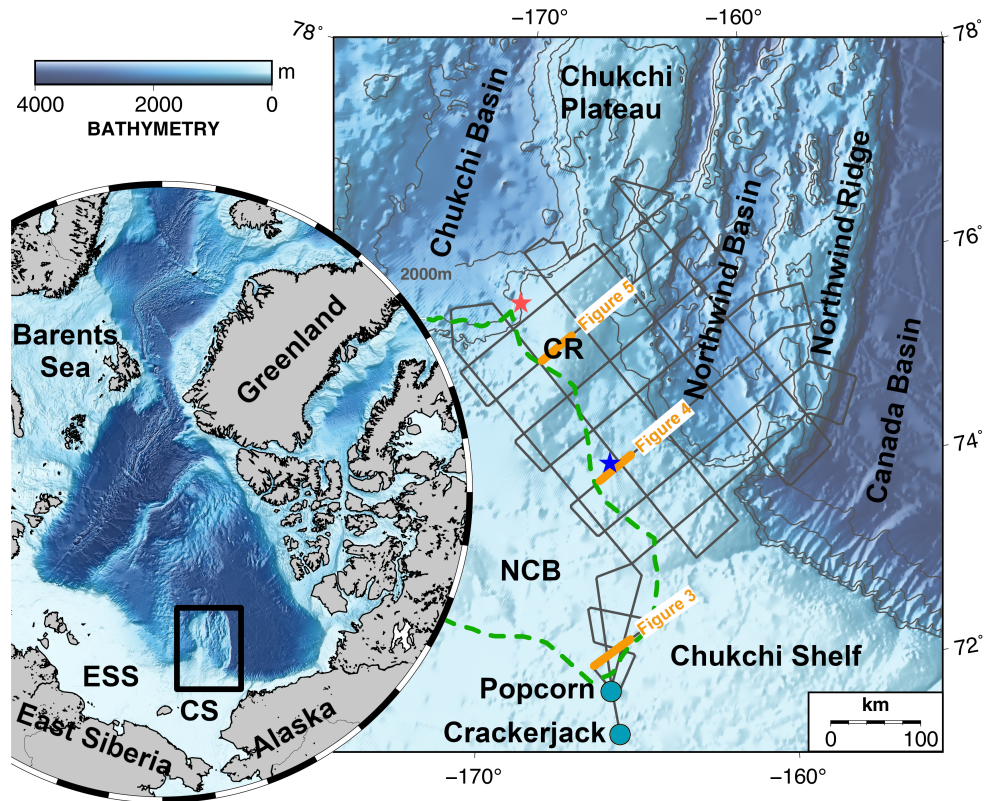
Figure 7.1. – Overview map of the study area and seismic lines acquired by R/V Marcus G. Langseth in 2011. Red star: Aaron mounds described in (J.-H. Kim et al., 2020; Y.-G. Kim et al., 2020). Blue star: Authigenic carbonate formations found at the seafloor in sediments in 200 m water depths (Kolesnik et al., 2014). Green dashed line: North Chukchi Basin, Orange points: Wells Popcorn and Crackerjack (Sherwood et al., 2002). Abbreviations: CR – Chukchi Rise, CS – Chukchi Shelf, ESS – East Siberian Shelf, NCB – North Chukchi Basin.

The up to 900 km wide East Siberian and Chukchi shelves are the largest shelf regions in the Arctic Ocean (Jakobsson, 2002). Previous studies already provided evidence for a high release of methane in the East Siberia and Chukchi seas (Li et al., 2017; Matveeva et al., 2015; Shakhova et al., 2010). For the southern, shallow Chukchi Shelf shallow gas-saturated Cretaceous-Quaternary sediments are reported for many areas (Bogoyavlenskiy & Kishankov, 2020; Hill et al., 2007; Matveeva et al., 2015). For the southwestern slope of the Chukchi Rise, evidence for existence of gas seepage is given by gas hydrate mounds and a bottom simulating reflector in water depths of more than 550 m (Choi et al., 2022; Kang et al., 2021; J.-H. Kim et al., 2020; Y.-G. Kim et al., 2020). The analyses of gas hydrates and pore water showed that the gas is methane with thermogenic sources at depths of >1 km below the seafloor (J.-H. Kim et al., 2020). Hereby, faults must act as a pathway

for fluid/gas migration (Y.-G. Kim et al., 2020; Nanda, 2021; Roberts et al., 2006).

Seismic reflection data have been used for decades not only to explore hydrocarbon reservoirs, but also to detect permafrost and shallow gas hydrate layers (Andreassen et al., 1995; Johansen et al., 2003; Nanda, 2021). Fluid migration beneath the seafloor manifests itself in a variety of seismically detectable features such as vertical fluid conduits, chimneys, pipes, bright spots, and acoustic blanking (Cartwright et al., 2007; Løseth et al., 2009). These features are referred to as direct hydrocarbon indicators (Cartwright et al., 2007; Løseth et al., 2009). Bright spots appear as high-amplitude reflections with polarity reversal and a velocity drop under a bright spot due to a change in acoustic impedance (e.g. gas content/gas-water filled sediment contrast) (Løseth et al., 2009; Nanda, 2021). Acoustic blanking shows reduced acoustic amplitude reflections due to lower sediment density caused by the presence of gas (Løseth et al., 2009) or superimposed enhanced reflections due to acoustic impedance contrast with surrounding sediment (Davis, 1992). Fluid/gas migration imaged by seismic reflection data results in vertical to subvertical chimney or pipe-like structures with circular or elliptical footprints that exhibit discontinuous or chaotic reflections and seismic blanking (Løseth et al., 2011; Robinson et al., 2021). Hereafter, these structures are referred to as chimneys and pipes. Finally, seismic data can also be used to detect submarine permafrost and gas hydrates in the polar regions (Andreassen et al., 1995; Johansen et al., 2003; Rekant et al., 2015). Permafrost shows high acoustic interval velocities >3500 m/s in seismic reflection data (Johansen et al., 2003; Rekant et al., 2015). Gas hydrates form under specific temperature and pressure conditions from a mixture of water and methane in shallow sediments or on the seafloor (Andreassen et al., 1995). In seismic data, they are usually detected as bottom simulating reflection (Andreassen et al., 1995).

The objective of this study is to describe i) direct hydrocarbon indicators (DIH), ii) structures indicative of fluid/gas migration through sedimentary layers, and iii) the presence of permafrost on the outer Chukchi shelf. Thus, we analyzed the first 2500 ms TWT in a 2D seismic reflection dataset acquired during a cruise of the RV Marcus G. Langseth in 2011. By comparing our results with other areas in the adjacent to the Arctic Ocean, we improve the current understanding of the distribution of permafrost and gas hydrate, as well as possible fluid/gas migration pathways across the Chukchi Margin.

7.3. Geological setting of the Chukchi Shelf

The study area is located on the outer Chukchi Shelf and the southern Chukchi Borderland in the Arctic Ocean (Figure 7.1). The Chukchi Shelf is an up to 900 km

wide continental shelf north of the Bering Strait. Its water depths vary from $<50\,m$ to $450 - 750\,m$ at the shelf break to $>2500\,m$ in the Chukchi Basin, the Northwind Basin, and the Canada Basin.

A thick sediment layer covers the Chukchi Shelf and reaches thicknesses of up to $18\,km$ in basins like the North Chukchi Basin (Artyushkov, 2010; Ilhan & Coakley, 2018; Petrov et al., 2016). The oldest sediments might have an age of Late Devonian (?) (Sherwood et al., 2002). Here, we focus mainly on the Cenozoic sediments.

Due to the absence of drill cores, little is known about the Cenozoic sediments on the outer Chukchi Shelf (Freiman et al., 2019). However, those sediments are composed of clinoform complexes prograding into the Arctic Basin above a Mid-Brookian unconformity (Freiman et al., 2019; Hegewald & Jokat, 2013b; Ilhan & Coakley, 2018). These clinoforms can be subdivided into the upper Brookian megasequence (66 Myrs - 23 Myrs) and sediments deposited since the Miocene. The clinoforms suggest a sediment transport direction from SSE to NNW in the Cenozoic (Houseknecht & Bird, 2011). Their likely source areas are the Chukotka and Brooks Range orogens (Houseknecht & Bird, 2011; Ilhan & Coakley, 2018). The upper Brookian Megasequence is in general $6.5\,km$ thick with a maximum thicknesses of up to $8.5\,km$ in the southern part of the Chukchi Shelf (Ilhan & Coakley, 2018). Miocene to present sediments have a thickness of $2.5\,km$ on the outer shelf (Hegewald & Jokat, 2013b; Ilhan & Coakley, 2018). Several deep-seated vertical faults affect the entire sediment column down to the Lower Cretaceous Unconformity at the southwestern slope of the Chukchi Plateau (Hegewald & Jokat, 2013a; Ilhan & Coakley, 2018). These Cenozoic sequences are considered to be a promising source rock for hydrocarbons making the Chukchi Shelf to one of the largest hydrocarbon reservoirs of North America (Craddock & Houseknecht, 2016; Homza et al., 2019a) with possible gas/fluid leakages at the seafloor. The migration of methane to the seafloor is documented by the analysis of gas hydrates (J.-H. Kim et al., 2020; Y.-G. Kim et al., 2020) and methane-derived authigenic carbonates (Kolesnik et al., 2014). The isotopic signatures of gas hydrates at the ARAON Mounds at the Chukchi Margin (Figure 7.1) imply their thermogenic origin in deep-seated sediments ($>1\,km$) (J.-H. Kim et al., 2020). Further, the accumulation of free gas at the western Chukchi Rise below a gas hydrate layer is indicated by the presence of a bottom simulating reflector and velocity changes (Choi et al., 2022). However, migration pathways on the outer Chukchi Shelf north of 73°N to the Chukchi Margin could not yet be investigated due to the sparse seismic data coverage.

During the Quaternary, the outer Chukchi Shelf and Borderland were subject to

widespread glaciation and eustatic sea-level fluctuations with retreats of up to 120 m (Dove et al., 2014; Jakobsson et al., 2008; Lehmann et al., 2022; Polyak et al., 2007). The ice grounding events created various glacial bedforms including mega scale glacial lineations, grounding zone wedges, tunnel valleys, and a regional glacial unconformity in water depths shallower than 900 m (Dove et al., 2014; S. Kim et al., 2021; Lehmann et al., 2022) as well as extensive iceberg scours in water depths shallower than 350 m (Dove et al., 2014; Hill et al., 2007). Further, eustatic sea-level lowering is thought to have favored the development of widespread permafrost, possibly still present in relics, on the Chukchi Margin (Matveeva et al., 2015).

7.4. Methods

In September and October 2011, a scientific cruise to investigate the tectonic evolution and seismic stratigraphy was conducted across the Chukchi Shelf and Chukchi Borderland. During this cruise sub-bottom profiler data and a regional grid of 5,300 km of 2D multi-channel seismic (MCS) profiles were acquired by R/V Marcus G. Langseth (Figure 7.1) (Coakley, 2011a; Coakley, 2011b).

The tuned airgun array, with a total volume of 1,830 cubic inches ($\sim$30 l) for generating seismic energy, consisted of ten bolt guns. This setup produced seismic signals with a frequency spectrum between 5 Hz and 125 Hz. The seismic source was towed at 6 m and the streamer at 9 m water depth. The distance-defined shot interval was set at 37.5 m. However, a distance-defined shot interval could not be achieved due to differential GPS losses in parts of the survey network. Therefore, seismic energy on the profiles in these areas had to be released in a time-controlled manner every 12.8 s to achieve a shot interval of approximately 37.5 m. Seismic data were recorded by 468 hydrophones (5850 m SentinelTM streamer) with a spacing of 12.5 m. The recording time was 10 s with a sampling rate of 2 ms.

To investigate the tectonic evolution of the Chukchi boundary, ION Geophysical processed the MCS data with 25 m bins (Ilhan & Coakley, 2018). The seismic profiles were reprocessed with a common depth point interval of 6.25 m, resulting in a maximum fold of 78 (see Lehmann et al. (2022) for more details). In shallow areas with water depths <100 m, the distance of $\sim$200 m between the source and the first channel combined with the low CDP fold resulted in negative interference between the direct wave and seafloor reflection, leading to suppression or attenuation of seafloor and shallow reflections. The upper 2500 ms TWT of the seismic data was used for our analysis.

Knudsen Chirp 3260 echosounder with a source frequency range of 2 to 6 kHz was

used as sub-bottom profiler (SBP). The maximum penetration depth of SBP ranges
between 10 to 100 m.

7.5. Results and Interpretation

Structures associated with the appearance and migration of fluids/gas are widely
distributed and at various stratigraphic levels in the research area (Figure 7.2).
Here, we show and interpret examples from three profiles located in the southern
(Figure 7.3), the central (Figure 7.4) and the northern part of our seismic network
(Figure 7.5).
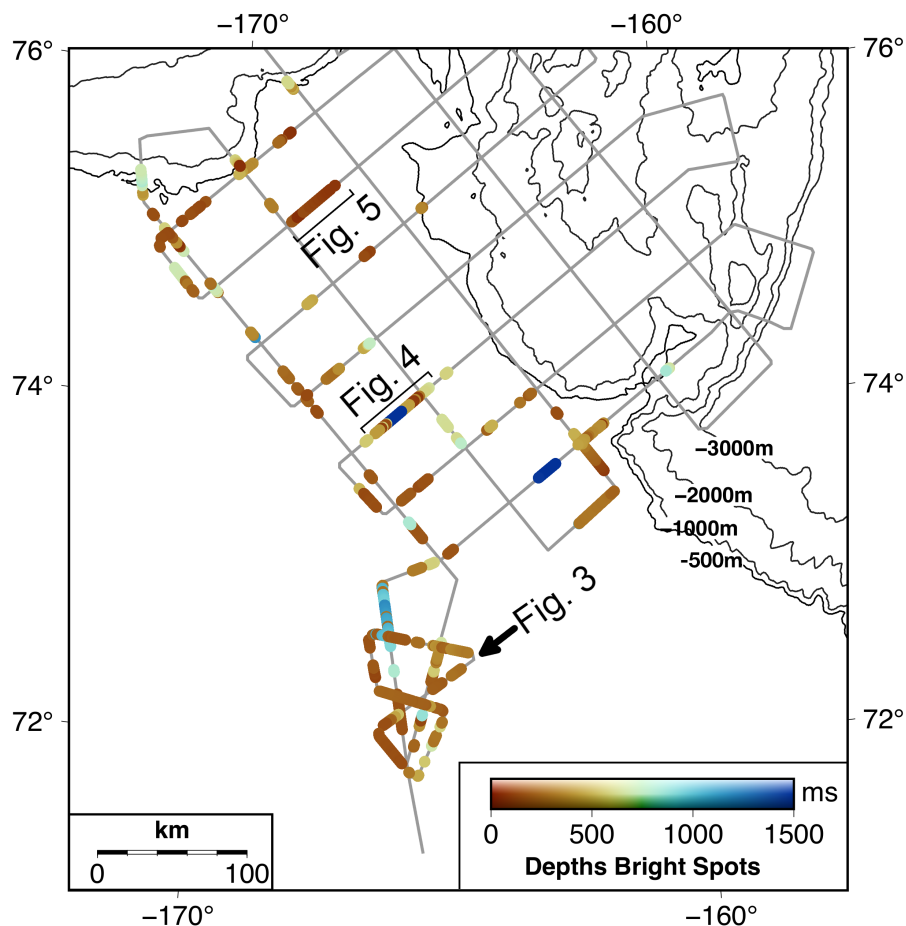
Figure 7.2. – Location and depths of bright spots distributed over the study area and the
locations of seismic profiles used in figures 7.3 - 7.5.

Figure 7.3 shows profile 16 on the southern research area on the Chukchi Shelf.
Cenozoic sediments are well layered above the angular mid-Brookian unconformity.
Shallow sediments show high amplitude reflections down to 400 ms TWT. Here, high-

amplitude zones alternate vertically with low-amplitude reflection zones. These may indicate the presence and horizontal migration of accumulated gas in the sediments (Løseth et al., 2009). Exceptional strong amplitudes occur at $300 - 500$ ms TWT between CDPs $13000 - 11000$ (approx. 12.5 km), while reflections below 500 ms TWT are distorted and chaotic (Figure 7.3). We interpret these structures as migration pathways for gas (Løseth et al., 2009). However, the data also image vertical zones of acoustic blanking and reflections (Figure 7.3). Prominent reduction in seismic energy occurs between CDP 8250 and 10250 below 1250 ms TWT as a "ghost-shaped" feature. This acoustic blanking has sharp margins, indicating that it is likely not lithology-related. Therefore, we interpret the acoustic blanking to be caused by pore fluids (gas) migration and/or the absorption of acoustic energy in gas-charged sediments (Robinson et al., 2021). At CDP 8500, upward-bending reflections extend from the ghost-shaped feature along a fault. We interpret this as upward migration of fluids from the ghost-shaped structure through sediments (Løseth et al., 2009). Several more vertical gas migration pathways ending at different TWT can be observed on this profile (Figure 7.3). However, neither the seismic data nor the sediment echosounder data can clarify whether these faults extend to the seafloor.

The sediment echosounder data show an uneven to rough and irregular seafloor with U- to V-shaped depressions (Figure 7.3b, c). Due to the shallow water depth of less than 50 m and the deep-sea setting of the multibeam system, the swath width is not wide enough to provide a complete image of these features. Therefore, it is difficult to decide whether the depressions are formed by icebergs or whether they are caused by gas seepage (Brown et al., 2017). Below the seafloor, sediment echosounder data show a strong reflection 5 ms below the seafloor. Such an unconformity is visible over the whole Chukchi Shelf and represents the Quaternary unconformity (Houseknecht et al., 2016) or the most recent transgressive surface (Hill et al., 2007). Several filled depressions are visible below the unconformity (Figure 7.3c). We interpret these depressions as typical Chukchi Shelf channels of either subglacial or subaerial origin (Dove et al., 2014; Hill et al., 2007; Lehmann et al., 2022).

On profile 09F in the central part of our seismic grid (Figure 7.4), the seafloor amplitude is partly weak southeastward of CDP 8000 at depths shallower than 250 ms TWT. This is the result of the interfering signals of the seafloor reflection and the direct wave. At depths greater than 1000 ms TWT, several stacked high-amplitude features started to evolve directly beneath and at the glacial unconformity on the Chukchi Shelf (Figure 7.4). Some of these high amplitude reflections (e.g., between CDPs 2250 and 3500 at 400 ms TWT in Figure 7.4) show polarity changes and can be interpreted as bright spots indicating the presence of gas (Løseth et al., 2009;
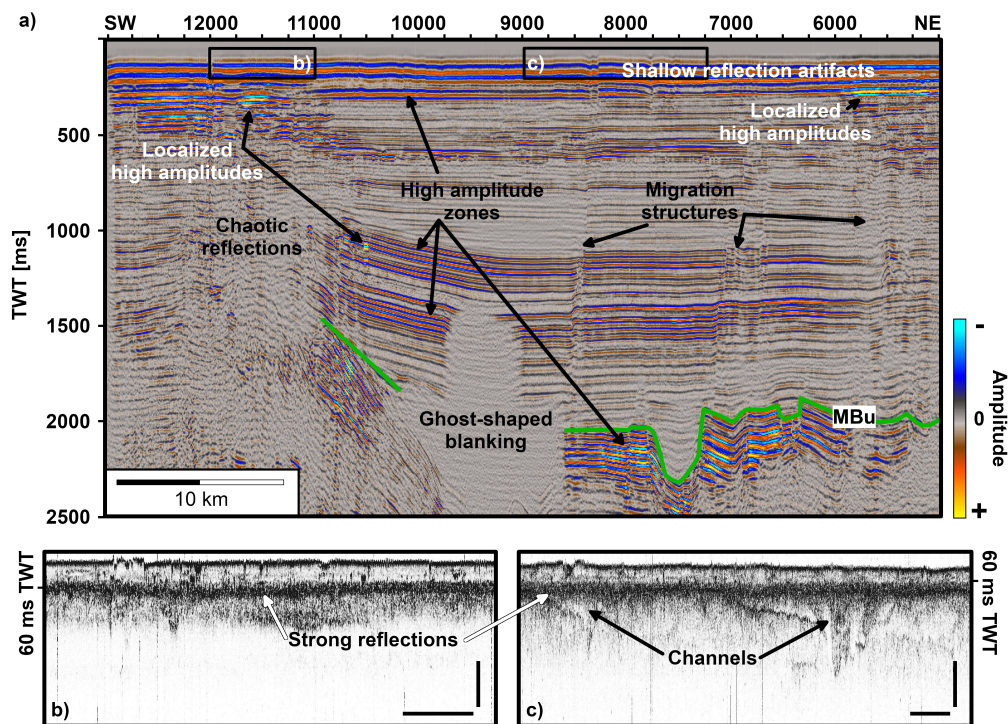
Figure 7.3. – a) Seismic profile 16 showing gas migration and accumulations on a profile 16 in the southern study area (see Figure 7.1 and 7.2); for figures 7.3-7.5 the same color code is used: high positive amplitudes are displayed in yellow and the low negative amplitude in blue, b) and c) Echsosounder data showing uneven to rough and irregular seafloor. Prominent is a strong reflection and a shallow penetration depth. The seismic data in figures 7.3-7.5 are plotted without Automated Gain Control (AGC) to make the blankening areas visible. Horizontal bars in b) and c): 1000 m, vertical bars: 10 ms. MBu – Mid-Brookian unconformity (Ilhan & Coakley, 2018)

Nanda, 2021). The high amplitude reflections and bright spots surround two structures with chaotic, damped, and downward bending reflections (Figure 7.4). The downward curvature is referred to as push down or the "sag" effect. This is due to a reduced acoustic velocity caused by the presence of gas (Løseth et al., 2009; Nanda, 2021). Both structures are interpreted as chimneys. They indicate an upward gas/fluid migration from deeper reservoirs (Løseth et al., 2009). The chimneys originate from a layer with attenuated reflections more than 2000 ms TWT deep (Figure 7.4). Based on the damped amplitudes, we interpret this layer as possible fluid/gas charged (Løseth et al., 2009; Nanda, 2021). The amplitude of the seafloor reflection increases from SW to NE (Figure 7.4). This seems to be due not only to the less interfering signals from the direct wave and the seafloor, but also to the migration of gas to the seafloor. High amplitudes occur primarily at depths between 500 ms TWT and 1000 ms TWT between the chimney structures at CPDs 2500 and 7500 (Figure 7.4). This further suggests lateral migration of fluids through the sediments (Løseth et al., 2009). Seismic interval velocities imaged at CDP 4500

gradually increase from 1730 m/s close to the seafloor to 3730 m/s at around 2000 ms TWT depth (Figure 7.4). These velocities were also reported in other parts of the research area (Choi et al., 2022; Hegewald & Jokat, 2013b).
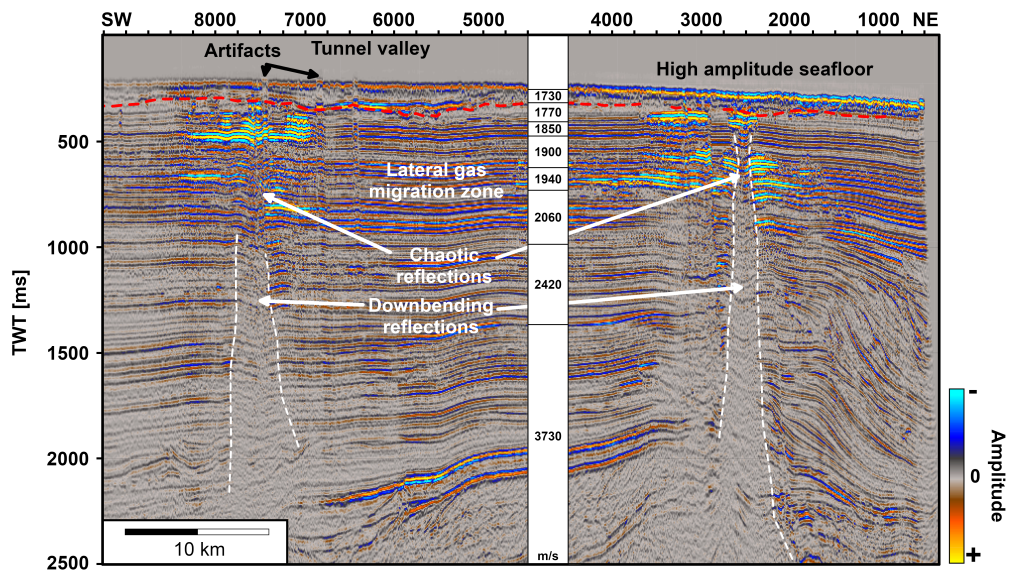
Figure 7.4. – Seismic profile 09F showing gas migration in the central research area. Vertical migration from a deeper layers appears through two pipe structures and gas accumulates below the glacial base (red stippled line according to Lehmann et al. (2022)). Lateral gas migration occurs between the pipes. The column in the center of the figure shows the seismic interval velocities in m/s. MBU (MBu − Mid-Brookian unconformity) is located below the seismic section shown.

In the northern research area along profile 06 (Figure 7.5), a high amplitude zone up to 36 km wide is imaged in a depth range of 300 - 600 ms TWT (Figure 7.5; CDP 12750-18500). Below this broad high amplitude zone, almost all reflections above the basement are strongly attenuated (Figure 7.5). The large bright spots have an inverse polarity compared to the surrounding reflections (Figure 7.5). This indicates the presence of accumulated gas (e.g., Nanda, 2021). Below the shallow bright spot at CDP 14000, the reflections are scattered and bend downward indicating the migration of gas through a chimney (Figure 7.5). Below CDP 19000 (Figure 7.5) another 10 km wide high amplitude area/bright spot is observed at approx. 600 ms TWT feeding a more localized gas migration (Løseth et al., 2011; Robinson et al., 2021).
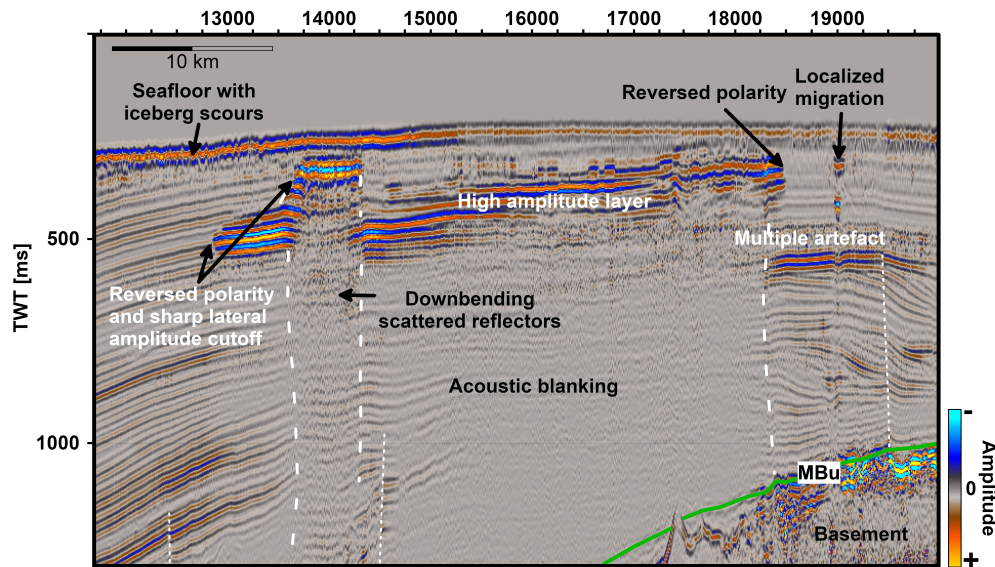
Figure 7.5. – Seismic profile 06 on the Chukchi Rise showing shallow gas accumulations and migration pathways. The data show several large shallow bright spots and acoustic blanking below them. MBu – Mid-Brookian unconformity (Ilhan & Coakley, 2018).

7.6. Discussion

7.6.1. Migration and leakage

The identified bright spots (high amplitudes with phase reversal, Figures 7.4 – 7.5) are a strong indicator for the presence of gas (Løseth et al., 2009; Nanda, 2021). Migration of thermogenic methane from greater depths (>1000 m below the seafloor) has previously been suggested for the Chukchi Shelf through authigenic carbonate formations and gas mounds (Figure 7.1) (J.-H. Kim et al., 2020; Y.-G. Kim et al., 2020; Kolesnik et al., 2014). Our MCS data show the widespread occurrence of vertical migration structures (chimneys and pipes) in the upper 2500 ms TWT of the research area (Figures 7.3 – 7.5). The chimneys and bright spots along faults connect higher amplitude layers at different stratigraphic levels in the Cenozoic sediments (Figures 7.3-7.5). Deep faults that serve as migration paths are reported near the shelf edge of the Chukchi continental margin (J.-H. Kim et al., 2020; Hegewald & Jokat, 2013b; Ilhan & Coakley, 2018). Such faults extend in places to a depth of about 3000 ms TWT below the seafloor (Hegewald & Jokat, 2013b; Ilhan & Coakley, 2018). In addition, clinoform complexes on the Chukchi Shelf are thought to favor gas migrations (Bird & Houseknecht, 2011). These migration structures are commonly observed in hydrocarbon rich regions around the world (e.g., Løseth et al., 2009; Nanda, 2021; Robinson et al., 2021; Waage et al., 2019).

The lateral migration of gas is indicated by high amplitude zones vertically stacked

with low amplitude zones at different depths on the shelf area (Figures 7.3 – 7.5). In other hydrocarbon-rich areas, it is a well constrained pattern where over-pressurized fluids accumulate in permeable rocks beneath a seal rock (Løseth et al., 2009). Increasing pressure of the still rising gas causes hydrofracturing at the weakest point of the seal. After the seals breach the upward migration continues to shallower levels (Løseth et al., 2009). Therefore, the migration pathways need to be located directly above the source rocks (Løseth et al., 2009). However, such lateral extended higher amplitudes especially below unconformities like the mid-Brookian unconformity might be associated with a change in impedance like higher rock densities.

Accumulations of gas in shallow sediments (<600 ms TWT) are indicated by bright spots (Figures 7.3 – 7.5). The largest accumulation occurs on the outer shelf areas in the western part of the Chukchi Rise (Figure 7.5). The accumulations are comparable to gas pockets distributed across the southern Chukchi Shelf (Bird & Houseknecht, 2011; Bogoyavlenskiy & Kishankov, 2020; Hill et al., 2007). The shallower gas accumulations on the Chukchi shelf could be caused by former ice sheets and associated glacial deposits or permafrost. Submarine permafrost would be evident in the shallow seismic data with sound velocities up to 3500 m/s (Homza et al., 2019a). Such high sound velocities in shallow sediments are not observed in the study area, indicating the absence of permafrost (Figure 7.4). This interpretation is supported by the fact that no other study has found evidence of the presence of permafrost on the Chukchi Shelf (Homza et al., 2019a). However, it is likely that permafrost, which served as a seal for upward migrating gas, formed over large areas of the aerially exposed Chukchi shelf during the Quaternary sea level lowstands (Homza et al., 2019a).

Another reason for shallow gas accumulations could be ice sheets that formed on the outer Chukchi shelf during Quaternary ice ages (Dove et al., 2014; S. Kim et al., 2021; Lehmann et al., 2022; Niessen et al., 2013). It is likely that thermogenic methane migrated upward from deeper layers and accumulated as gas hydrates that were stable under the given pressure and temperature conditions beneath such ice sheets (Nickel et al., 2012). Gas hydrates are are reported at the western flank of the Chukchi Rise and in the Beaufort Sea (Collett et al., 2011; Phrampus et al., 2014; Choi et al., 2022). However, unlike the Beaufort Sea and the flank of the Chukchi Rise, our data of the shelf area show no hints for the gas hydrates stability zone marked by a bottom simulating reflector (BSR) (Figures 7.3 – 7.5). This observation could indicate (a) that gas hydrates do not occur everywhere on the Chukchi Shelf, (b) that they are not underlain by a BSR, or (c) that gas hydrate concentrations are low in the shallow sediments, or (d) gas hydrates are confined to a very thin area and

no BSR is reflected in our data due to small variations in interval velocities. Similar observations are reported for the BSR in the Beaufort Sea (Andreassen et al., 1995).

It is also likely that with the disappearance of the ice sheet on the Chukchi Shelf during deglacialization, pressure conditions changed and led to the decomposition of the hydrate layer (Nickel et al., 2012). We assume that the decomposed gas began its migration through the glacial unconformity and glacial sediments and began to seep out at the seafloor several 10 ka to 100 ka. Such a scenario is suggested by the accumulation of gas below the glacial unconformity and it is also considered for the formation of the Aaron Mounds at the flank of the Chukchi Rise. Here, gas migrated through glacial sediments and formed the authigenic carbonate structures on the seafloor (J.-H. Kim et al., 2020; Y.-G. Kim et al., 2020; Kolesnik et al., 2014). A similar migration process is reported in the Barents Sea (Waage et al., 2019). However, we are not able to interpret small-scale migration structures in the shallowest sediments based on our seismic data. This is common because of the limited seismic band-width, interference of reflections and presence of noise affecting the estimation of true polarity and signal strength (Nickel et al., 2012). Further, the shallow penetration depth of sediment echosounder together with a small swath width of the bathymetric data limit the possible detection of seafloor features by migration of gas to the seafloor (Nickel et al., 2012). Nevertheless, at the Norwegian and Svalbard margins where gas/fluid migration is described without distinctive migration paths above a glacially eroded upper regional unconformity (Waage et al., 2019). Additionally, gas migration processes can also be facilitated or reactivated by isostatic rebound by ice sheet growth and decay causing pressure and temperature changes even in deeper sedimentary strata (Kjemperud & Fjeldskaar, 1992).

The previously discussed chimneys and fault structures suggest the migration of gas to the seafloor, raising the question of gas leakage on the Chukchi Shelf (Figures 7.3 - 7.5). It is important to study the leakage of methane gas or its degradation products into the water column to determine the methane contribution of the Arctic shelf area to the global budget. Leakage systems often manifest as pockmarks, craters, elevations on the seafloor or a change in the seafloor reflectivity (J.-H. Kim et al., 2020; Løseth et al., 2011; Roberts et al., 2006). On the flank of the Chukchi Rise, the Aaron Mounds are yet the only described gas seepage features (Y.-G. Kim et al., 2020). However, a seafloor reflectivity with high amplitude and no phase reversals over large areas as observed on profile 09F (Figure 7.4) is suggested to indicate a slow delivery of gas to the seafloor, the occurrence of authigenic carbonate mounds and the existence of gas hydrates in the subsurface (Roberts et al., 2006). This is supported by dredged authigenic carbonate in water depths of 200 m close to this

profile (Kolesnik et al., 2014). Other features associated with seepage have not yet been discovered (Figure 7.3b, c). This is partly due to insufficient coverage by geoscientific data, and partly due to the fact that the seafloor in water depths of less than 350 m is densely scoured by icebergs, which may have superimposed or even destroyed seafloor features in the past (Dove et al., 2014). Nevertheless, the leakage of methane is likely suggested by methane supersaturated shallow and bottom water layers on the Chukchi Shelf and on the adjacent East Siberian and Beaufort shelves (Li et al., 2017; Phrampus et al., 2014; Shakhova et al., 2005; Shakhova et al., 2010).

7.6.2. Source rocks

The Chukchi Shelf is considered to host large hydrocarbon reservoirs south of 72° N (e.g., Bird & Houseknecht, 2011; Homza et al., 2019a). The sediments from the late-Devonian to the Cenozoic are reported as oil-prone source rocks while sedimentary formations in the Cenozoic are reported to have an excellent reservoir potential in the southern research area (Homza et al., 2019a; Sherwood et al., 2002). Our seismic data imaged gas migration and accumulations distributed over the entire outer Chukchi Shelf (Figure 7.2). Most migration paths in the data seem to emanate in sedimentary formations at depths of more than 1000 m (>1000 ms TWT) below the seafloor (Figures 7.3 – 7.4). However, since the only deeper wells (Figure 7.1) are located in the southern research area, little is known about the sediment compositions on the outer shelf areas north of 72° N to interpret possible source rocks. Nevertheless, the generation of hydrocarbons is assumed as still ongoing after the late Eocene for the Beaufort Sea (Houseknecht & Bird, 2011). We assume the same for the Chukchi Sea.

7.7. Conclusion

The outer Chukchi Shelf is one of the least explored shelf regions in the Arctic Ocean. Therefore, the studied seismic data represent the first indication for regional gas migrations and gas seepage of the outer Chukchi Shelf and the southern Chukchi Borderland region:

- The seismic data show several anomalous zones and features with high amplitude. These alternate with lower amplitude sequences, suggesting lateral migration and accumulation of gas at different stratigraphic levels.

- Gas chimneys and bright spots along faults indicate upward migration of deep thermogenic gas. The widespread distribution of such features suggests widespread gas migration across the outer shelf region.

- Shallow gas accumulations, seafloor faulting, and high seafloor amplitude indi-

cate the release of gas at least to the seafloor. This is confirmed by authigenic carbonate formations and marine mounds in the study area.

- Seismic interval velocities representative for sediments reveals the absence of widespread permafrost on the outer Chukchi Shelf.

For a more comprehensive and detailed study of the outer Chukchi region a denser network of geoscientific data is required to better map the geometries and spatial distribution of migration pathways and leakage-related (seismic) anomalies. This will help to better assess the potential of the Chukchi Shelf to contribute to climate change.

8. Conclusion

In this study, I examined sedimentary structures, particularly seafloor features and erosion by grounded ice on the outer 75 km of the Chukchi Shelf and Chukchi Borderland, and along the Beringian margin, with respect to the history of a probable former Beringian Ice Sheet. I also studied the gas migration and seepage, and the occurrence of permafrost. The data provide for the first time a detailed insight into the sedimentary structures shallower than 2500 ms TWT. The following section summarizes the results of three publications, presented in Chapters 5, 6 and 7, according to the main questions in Section 1.2.

Which glacial landforms can be identified in geophysical data?
MCS data show a variety of glacial landforms as numerous grounding zone wedges and recessional moraines as well as large meltwater discharge systems. A GZW with a width of 48 km x 75 km and a height of 145 m on the Chukchi Rise is even one of the largest found GZWs to date. Further, the found meltwater discharge systems is widely distributed over the Chukchi Shelf and Borderland.

How are glacial sediments and landforms distributed along the Chukchi Margin?
Examination of the sediments using seismic data shows that the sediments have been eroded and reworked by grounded ice masses throughout the study area in water depths of less than 750 m. South of 73° N, the glacially influenced sediments are up to 210 m thick and cover a glacial unconformity. This unconformity separates glacial and preglacial sediments and is comparable to glacial unconformities at other formerly glaciated margins such as the upper regional unconformity in the Barents Sea.

Do the data reveal any evidence for an ice sheet in the Chukchi region?
The identified glacial landforms and their distribution paint an ambivalent picture of the glacial history of the Chukchi Shelf. A glacial unconformity together with glacial troughs, recessional moraines, and other north-south trending features indicate an advancing and retreating ice sheet on the East Siberian and Chukchi shelves prior to the Early Quaternary. In contrast, shelfbreak-parallel mega scale glacial lineations and GZWs on the western flanks of bathymetric seafloor elevations, together with a pronounced erosion, provide evidence for a westward advancing ice shelf during

the later Quaternary, for which the plateaus of the Chukchi Borderland acted as pinning points.

Were glacial sediments deposited along the Beringian Margin?
Can lateral thickness variations of glacially transported sediments be determined to investigate the dynamics of the ice sheet?
Can these results be used to further constrain the extent of a former Beringian Ice Sheet?
Along the Beringian Margin, I interpreted the chaotically deposited sediments as glacially transported sediments. Several depositional centers of glacial deposits up to 450 m thick are mapped between the De Long Trough (165° E) and the Northwind Ridge (161° W). Within the depositional centers, evidence for three to five glacial advances across the northern Beringian Margin are preserved. In addition, the changing thickness of glacial deposits along the margin provide evidence for varying flow rates of the Beringian Ice Sheet. The absence of seismically imageable glacial deposits along the East Siberian Margin west of 165° E and the Beaufort Margin east of 161° W constrains the extent of the Beringian Ice Sheets between the DeLong Trough and the Northwind Ridge.

Can the changes on the continental shelf caused by a Beringian Ice Sheet be compared to the continental margins of Norway and Greenland in terms of the duration and dynamics of glaciation(s)?
The glacial features of the seafloor formed by ice sheets along the Beringian Margin are comparable to those found along the margins of East Greenland and Norway. However, along the Norwegian and East Greenland margins, glacial sediments deposited by ice streams in bathymetric troughs are 2000 m and 3500 m thick, respectively. Deposits along the Beringian Margin reach only 450 m in thickness, suggesting a shorter glaciation history and/or less dynamic ice sheet margins compared to the Norwegian and East Greenland margins.

Do seismic data show the (upward) migration structures of gas on the outer Chukchi Shelf?
Are the reported gas hydrates and migrations limited to the known locations or do more spots exist?
MCS data from the Chukchi Margin show a variety of sedimentary structures indicative of gas migration and accumulation, such as bright spots and gas chimneys. The migration pathways emanate at different depths, i.e., upward migration does not appear to be restricted to a particular depth or reflector. Rather, seismic and sediment echosounder data demonstrate that the gas migrates widely distributed

across the outer Chukchi Shelf directly to the seafloor.

Do our seismic data show large permafrost structures that could release large amounts of methane into the atmosphere through thawing?
Permafrost shows distinct structures in seismic data and has a high acoustic velocity. I did not find such evidence for permafrost in the seismic data set of MGL1112.

9. Outlook

Key interest areas

Large parts of the study area in the Chukchi region and along the Beringian continental margin, especially the Russian shelf areas, have not yet been covered systematically by hydroacoustic measurements due to remoteness, difficult geopolitical situation, and year-round sea ice cover. Consequently, the complete distribution of submarine glacial landforms remains unknown. For an even more complete reconstruction of the extent of the ice sheets that once covered the northern Beringian Shelf, more mapping is needed to create better numerical models of Earth's history and climate and to better predict the future climate change. Therefore, I suggest focus areas for different research questions:

Seismic data from this study may show the existence of a steep trough-mouth fan (TMF) in an area northwest of 163° W (see Chapter 6). Steep TMFs are rare on formerly glaciated shelf margins because sediments delivered by ice sheets reduce the dip angle of the continental slope over a long period of time (Rydningen et al., 2015; Rydningen et al., 2016). Steep TMFs are suggested to represent an initial immature phase of TMF development (Rydningen et al., 2015; Rydningen et al., 2016), which may indicate only a short-lived advance of the ice sheet(s) from the Chukchi Shelf into the Northwind Basin. The slope to Northwind Basin between Chukchi Rise and Northwind Ridge is imaged by only four seismic profiles (area I in figure 9.1). Consequently, it is important to study the slopes from the Chukchi Shelf and Chukchi Rise to the Northwind Basin with more closely spaced hydroacoustic profiles. The results would improve not only our understanding of processes in the early stages of TMF formation, but also our understanding of ice sheet dynamics at the Beringian Margin. In addition, the results of the slope studies will help constrain the estimate of former ice sheet extents on the Beringian Margin by providing a more detailed picture of the decreasing glacial sediment cover observed east of ~162° W in this study.

The sparse bathymetric data coverage outer Chukchi region already shows a widespread existence of glacial landscapes (this study, Dove et al., 2014; Jakobsson et al., 2014; Jakobsson et al., 2008; S. Kim et al., 2021; Polyak et al., 2007; Polyak et al.,
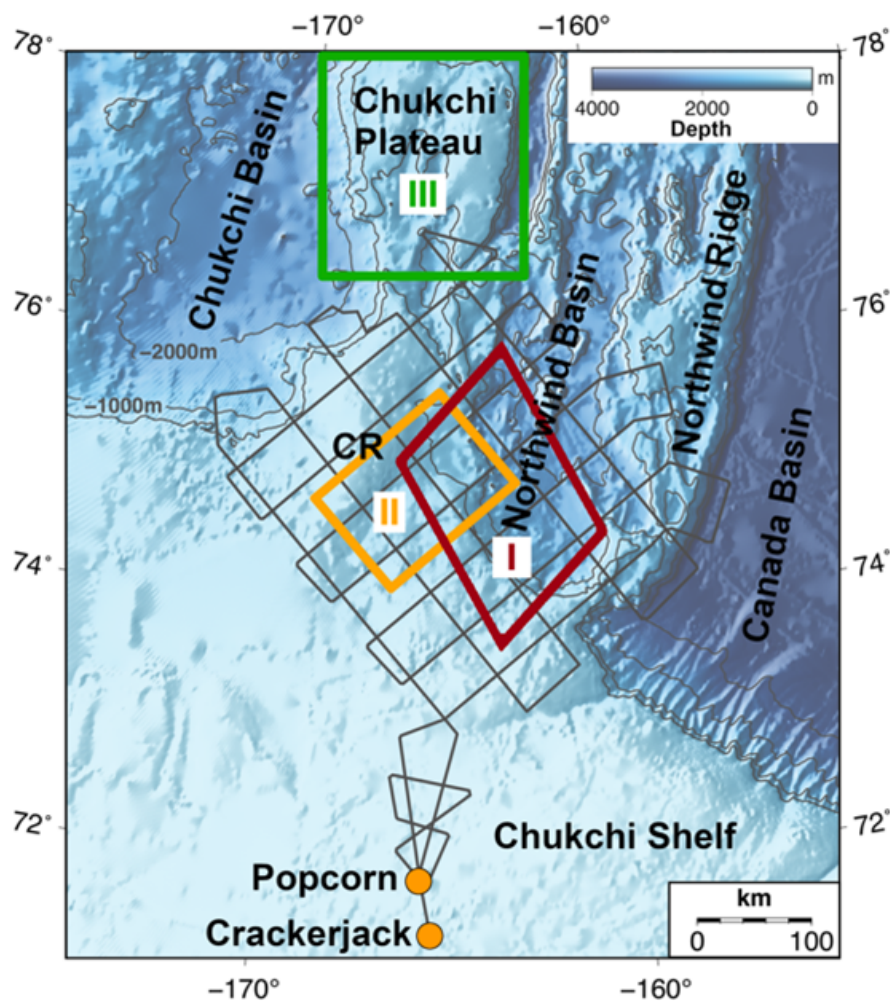
Figure 9.1. – Areas of interest for further investigations of the glacial history of the Chukchi Margin.

2001). The first contiguous area covered by bathymetric and echosounder data was acquired in the Western Bathymetric Trough area on the western Chukchi Rise (S. Kim et al., 2021). The evaluation of these data provided a tremendous improvement in the understanding of ice mass dynamics and history in this region (S. Kim et al., 2021). The Broad Bathymetric Trough (area II in Figure 9.1) and the Chukchi Plateau (area III in Figure 9.1) have been sparsely covered with hydroacoustic data. However, a higher density of hydroacoustic data could provide a better picture of the direction of ice flows, the extent of ice sheets, or the history of successive ice advances.

Existing seismic data

Acquiring new hydroacoustic data, especially seismic data, is costly and time consuming. By using existing seismic data sets, both can be minimized. However,

existing seismic data, particularly south of 73° N, focuses on hydrocarbon explo-
ration and deeper sedimentary structures, resulting in poorly resolved shallow sed-
imentary structures. Reprocessing of the multichannel seismic data set from cruise
MGL1112 for this work has shown that it is possible to improve data resolution for
shallow structures, providing important pieces of the puzzle for the glacial history of
the Chukchi region. Reprocessing and reinterpretation of key profiles from existing
datasets can, consequently, provide further advancement for the evaluation of our
knowledge about former ice sheet extents.

Age constraints

The Chukchi Shelf is covered by sediments up to 18 km thick. The seismic network of
cruise MGL1112 extended to 76.6°N. However, the northernmost deepest wells are
the Popcorn and Crackerjack wells (Figure 9.1) at 71.9°N and 71.4°N, respectively
(Sherwood et al., 2002). Ilhan & Coakley (2018) and Hegewald & Jokat (2013b)
made initial attempts to link seismic stratigraphy to these wells. Both authors were
able to estimate an upper Miocene reflector in the sedimentary deposits. This re-
flector lies several kilometers below the seafloor in places, leading to a lack of sound
age interpretations of sediment deposition and erosional processes over the past 5.3
million years. Therefore, it is of great interest to initiate a drilling campaign on the
outer Chukchi Shelf, the Borderland, and the deep-sea basins surrounding them.
This is necessary not only for a better estimation of the timing of the ice sheets on
the Beringian Margin, but also for the paleoclimatic, tectonic, and sedimentation
history of the Arctic Ocean.
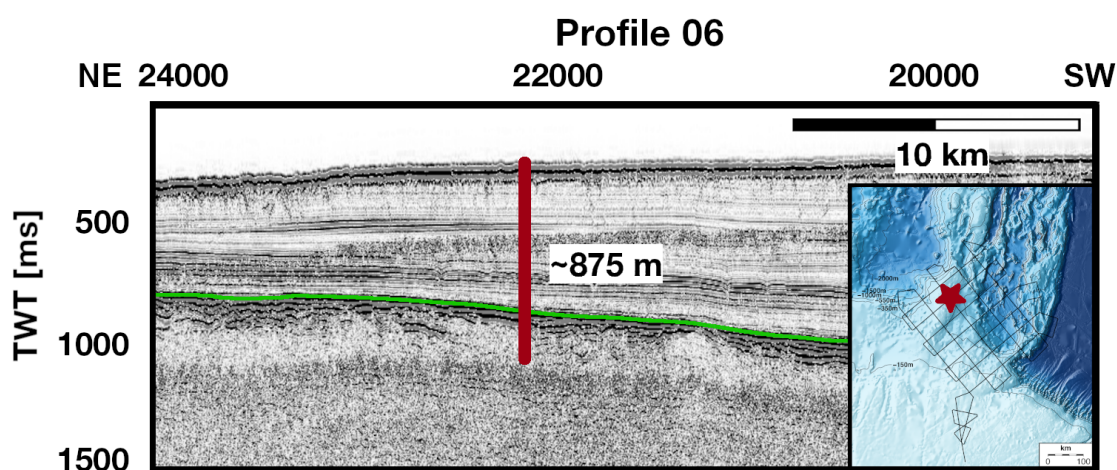
Figure 9.2. – Possible location for drilling on the Chukchi Rise. Green line: Mid-Brookian
unconformity.

One possible drilling site is shown in Figure 9.2. It is located directly on the intersec-

tion of profiles 06 and 02 on the Chukchi Rise. As can be seen, the reflections, which are like the 66-myrs-old Mid-Brookian unconformity (green line in figure 9.2; Ilhan & Coakley (2018)) traceable over large parts of the Chukchi Shelf, are horizontally layered. At this point it would not only be possible to close an age gap of several million years, but also to drill into the acoustic foundation. From these layers, which appear to be the continental crust, it is possible to draw conclusions about the formation of the Chukchi Borderland. However, some of the upper sediments have been eroded by grounded ice masses, and it is likely that several thousand years of history are still missing after the drilling. The drilling depths of 875 m is estimated with a velocity of 2000 m/s.

10. Bibliography

Andreassen, K., Hart, P. & Grantz, A. (1995). "Seismic studies of a bottom simulating reflection related to gas hydrate beneath the continental margin of the Beaufort Sea". In: *Journal of Geophysical Research: Solid Earth* 100.B7, pp. 12659–12673. ISSN: 0148-0227. DOI: 10.1029/95JB0096.

Arndt, J. E., Jokat, W., Dorschel, B., Myklebust, R., Dowdeswell, J. A. & Evans, J. (2015). "A new bathymetry of the Northeast Greenland continental shelf: Constraints on glacial and other processes". In: *Geochemistry, Geophysics, Geosystems* 16.10, pp. 3733–3753. DOI: 10.1002/2015GC005931.

Artyushkov, E. V. (2010). "The superdeep North Chukchi Basin: formation by eclogitization of continental lower crust, with petroleum potential implications". In: *Russian Geology and Geophysics* 51.1, pp. 48–57. ISSN: 1068-7971. DOI: 10.1016/j.rgg.2009.12.004.

Barr, I. D. & Clark, C. D. (2012). "Late Quaternary glaciations in Far NE Russia; combining moraines, topography and chronology to assess regional and global glaciation synchrony". In: *Quaternary Science Reviews* 53, pp. 72–87. ISSN: 0277-3791. DOI: 10.1016/j.quascirev.2012.08.004.

Batchelor, C. & Dowdeswell, J. A. (2014). "The physiography of High Arctic cross-shelf troughs". In: *Quaternary Science Reviews* 92, pp. 68–96. ISSN: 0277-3791. DOI: 10.1016/j.quascirev.2013.05.025.

Batchelor, C. & Dowdeswell, J. A. (2015). "Ice-sheet grounding-zone wedges (GZWs) on high-latitude continental margins". In: *Marine Geology* 363, pp. 65–92. ISSN: 0025-3227. DOI: 10.1016/j.margeo.2015.02.001.

Batchelor, C., Dowdeswell, J. A. & Pietras, J. T. (2013a). "Seismic stratigraphy, sedimentary architecture and palaeo-glaciology of the Mackenzie Trough: evidence for two Quaternary ice advances and limited fan development on the western Canadian Beaufort Sea margin". In: *Quaternary Science Reviews* 65, pp. 73–87. ISSN: 0277-3791. DOI: 10.1016/j.quascirev.2013.01.021.

Batchelor, C., Dowdeswell, J. A. & Pietras, J. T. (2014). "Evidence for multiple Quaternary ice advances and fan development from the Amundsen Gulf cross-shelf trough and slope, Canadian Beaufort Sea margin". In: *Marine and Petroleum Geology* 52, pp. 125–143. ISSN: 0264-8172. DOI: 10.1016/j.marpetgeo.2013.11.005.

Batchelor, C., Dowdeswell, J. A. & Pietras, J. (2013b). "Variable history of Quaternary ice-sheet advance across the Beaufort Sea Margin, Arctic Ocean". In: *Geology* 41.2, pp. 131–134. ISSN: 0091-7613. DOI: 10.1130/G33669.1.

Batchelor, C., Margold, M., Krapp, M., Murton, D., Dalton, A. S., Gibbard, P., Stokes, C. R., Murton, J. & Manica, A. (2019). "The configuration of Northern Hemisphere ice sheets through the Quaternary". In: *Nature Communications* 10.1, p. 3713. ISSN: 2041-1723 (Electronic) 2041-1723 (Linking). DOI: 10.1038/s41467-019-11601-2.

Bellec, V. K., Plassen, L., Rise, L. & Dowdeswell, J. A. (2016). "Malangsdjupet: a cross-shelf trough on the North Norwegian margin". In: *Geological Society, London, Memoirs* 46.1, pp. 169–170. ISSN: 0435-4052 2041-4722. DOI: 10.1144/m46.30.

Bellwald, B., Planke, S., Lebedeva-Ivanova, N., Piasecka, E. D. & Andreassen, K. (2019). "High-resolution landform assemblage along a buried glacio-erosive surface in the SW Barents Sea revealed by P-Cable 3D seismic data". In: *Geomorphology* 332, pp. 33–50. ISSN: 0169-555X. DOI: 10.1016/j.geomorph.2019.01.019.

Berger, D. & Jokat, W. (2008). "A seismic study along the East Greenland margin from 72°N to 77°N". In: *Geophysical Journal International* 174.2, pp. 733–748. ISSN: 0956-540X. DOI: 10.1111/j.1365-246X.2008.03794.x.

Bird, K. J. & Houseknecht, D. W. (2011). "Geology and petroleum potential of the Arctic Alaska petroleum province". In: *Geological Society, London, Memoirs* 35.1, pp. 485–499. ISSN: 0435-4052.

Bogoyavlenskiy, V. & Kishankov, A. (2020). "Dangerous gas-saturated objects in the World Ocean: the Chukchi Sea (Russia and the USA)". In: *Arctic: Ecology and Economy* 2(38), pp. 45–58. ISSN: 22234594 22234594. DOI: 10.25283/2223-4594-2020-2-45-58.

Brigham-Grette, J. (2001). "New perspectives on Beringian Quaternary paleogeography, stratigraphy, and glacial history". In: *Quaternary Science Reviews* 20.1-3, pp. 15–24. ISSN: 0277-3791. DOI: 10.1016/S0277-3791(00)00134-7.

Brigham-Grette, J. (2013). "Palaeoclimate: A fresh look at Arctic ice sheets". In: *Nature Geoscience* 6.10, pp. 807–808. ISSN: 1752-0908. DOI: 10.1038/ngeo1960.

Brigham-Grette, J. & Gualtieri, L. (2004). "Response to Grosswald and Hughes (2004), Brigham-Grette et al.(2003)."Chlorine-36 and 14 C Chronology support a limited last glacial maximum across central Chukotka, northeastern Siberia, and no Beringian ice Sheet," and Gualtieri et al.(2003),"Pleistocene raised marine deposits on Wrangel Island, northeastern Siberia: implications for Arctic ice sheet history"". In: *Quaternary Research* 62.2, pp. 227–232. ISSN: 0033-5894. DOI: 10.1016/j.yqres.2004.05.002.

Brown, C. S., Newton, A. M. W., Huuse, M. & Buckley, F. (2017). "Iceberg scours, pits, and pockmarks in the North Falkland Basin". In: *Marine Geology* 386, pp. 140–152. ISSN: 0025-3227. DOI: 10.1016/j.margeo.2017.03.001.

Brumley, K., Miller, E. L., Konstantinou, A., Grove, M., Meisling, K. E. & Mayer, L. A. (2015). "First bedrock samples dredged from submarine outcrops in

the Chukchi Borderland, Arctic Ocean". In: *Geosphere* 11.1, pp. 76–92. ISSN: 1553-040X. DOI: 10.1130/ges01044.1.

Burton, D. J., Dowdeswell, J. A., Hogan, K. A. & Noormets, R. (2016). "Little Ice Age terminal and retreat moraines in Kollerfjorden, NW Spitsbergen". In: *Geological Society, London, Memoirs* 46.1, pp. 71–72. ISSN: 0435-4052 2041-4722. DOI: 10.1144/m46.35.

Cartwright, J., Huuse, M. & Aplin, A. (2007). "Seal bypass systems". In: *AAPG Bulletin* 91.8, pp. 1141–1166. ISSN: 0149-1423. DOI: 10.1306/04090705181.

Choi, Y., Kang, S.-G., Jin, Y. K., Hong, J. K., Shin, S.-R., Kim, S. & Choi, Y. (2022). "Estimation of the gas hydrate saturation from multichannel seismic data on the western continental margin of the Chukchi Rise in the Arctic Ocean". In: *Frontiers in Earth Science* 10. ISSN: 2296-6463. DOI: 10.3389/feart.2022.1025110.

Clark, C. D. (1993). "Mega-scale glacial lineations and cross-cutting ice-flow landforms". In: *Earth Surface Processes and Landforms* 18.1, pp. 1–29. ISSN: 0197-9337. DOI: 10.1002/esp.3290180102.

Clark, P. U., Dyke, A. S., Shakun, J. D., Carlson, A. E., Clark, J., Wohlfarth, B., Mitrovica, J. X., Hostetler, S. W. & Mccabe, A. M. (2009). "The Last Glacial Maximum". In: *Science* 325.5941, pp. 710–714. ISSN: 1095-9203 (Electronic) 0036-8075 (Linking). DOI: 10.1126/science.1172873.

Coakley, B. (2011a). Dataset. DOI: 10.7284/903767.

Coakley, B. (2011b). *Summary Report MGL1112*. Report.

Colleoni, F., Kirchner, N., Niessen, F., Quiquet, A. & Liakka, J. (2016). "An East Siberian ice shelf during the Late Pleistocene glaciations: Numerical reconstructions". In: *Quaternary Science Reviews* 147, pp. 148–163. ISSN: 0277-3791. DOI: 10.1016/j.quascirev.2015.12.023.

Collett, T. S., Lee, M. W., Agena, W. F., Miller, J. J., Lewis, K. A., Zyrianova, M. V., Boswell, R. & Inks, T. L. (2011). "Permafrost-associated natural gas hydrate occurrences on the Alaska North Slope". In: *Marine and Petroleum Geology* 28.2, pp. 279–294. ISSN: 0264-8172. DOI: 10.1016/j.marpetgeo.2009.12.001.

Corlett, W. B. & Pickart, R. S. (2017). "The Chukchi slope current". In: *Progress in Oceanography* 153, pp. 50–65. ISSN: 0079-6611. DOI: 10.1016/j.pocean.2017.04.005.

Craddock, W. H. & Houseknecht, D. W. (2016). "Cretaceous–Cenozoic burial and exhumation history of the Chukchi shelf, offshore Arctic Alaska". In: *AAPG Bulletin* 100.1, pp. 63–100. ISSN: 0149-1423. DOI: 10.1306/09291515010.

Dahlgren, K. I. T., Vorren, T. O. & Laberg, J. S. (2002). "The role of grounding-line sediment supply in ice-sheet advances and growth on continental shelves: an example from the mid-Norwegian sector of the Fennoscandian ice sheet during the Saalian and Weichselian". In: *Quaternary International* 95, pp. 25–33. ISSN: 1040-6182. DOI: 10.1016/S1040-6182(02)00024-1.

Dahlgren, K. I. T., Vorren, T. O., Stoker, M. S., Nielsen, T., Nygård, A. & Petter Sejrup, H. (2005). "Late Cenozoic prograding wedges on the NW European continental margin: their formation and relationship to tectonics and climate". In: *Marine and Petroleum Geology* 22.9, pp. 1089–1110. ISSN: 0264-8172. DOI: `10.1016/j.marpetgeo.2004.12.008`.

Darby, D., Ortiz, J., Polyak, L., Lund, S., Jakobsson, M. & Woodgate, R. A. (2009). "The role of currents and sea ice in both slowly deposited central Arctic and rapidly deposited Chukchi-Alaskan margin sediments". In: *Global and Planetary Change* 68.1-2, pp. 56–70. ISSN: 0921-8181. DOI: `10.1016/j.gloplacha.2009.02.007`.

Davis, A. M. (1992). "Shallow gas: an overview". In: *Continental Shelf Research* 12.10, pp. 1077–1079. ISSN: 0278-4343. DOI: `10.1016/0278-4343(92)90069-V`.

Dinter, D. A., Carter, L. D., Brigham-Grette, J., Grantz, A., Johnson, L. & Sweeney, J. F. (1990). "Late Cenozoic geologic evolution of the Alaskan North Slope and adjacent continental shelves". In: *The Arctic Ocean Region*. Vol. L. Geological Society of America. Chap. 25, pp. 459–490. ISBN: 9780813754635. DOI: `10.1130/dnag-gna-l.459`.

Dipre, G. R., Polyak, L., Kuznetsov, A. B., Oti, E. A., Ortiz, J. D., Brachfeld, S. A., Xuan, C., Lazar, K. B. & Cook, A. E. (2018). "Plio-Pleistocene sedimentary record from the Northwind Ridge: new insights into paleoclimatic evolution of the western Arctic Ocean for the last 5 Ma". In: *arktos* 4.1, p. 24. ISSN: 2364-9461. DOI: `10.1007/s41063-018-0054-y`.

Dong, L., Liu, Y., Shi, X., Polyak, L., Huang, Y., Fang, X., Liu, J., Zou, J., Wang, K., Sun, F. & Wang, X. (2017). "Sedimentary record from the Canada Basin, Arctic Ocean: implications for late to middle Pleistocene glacial history". In: *Clim. Past* 13.5, pp. 511–531. ISSN: 1814-9332. DOI: `10.5194/cp-13-511-2017`.

Dove, D., Polyak, L. & Coakley, B. (2014). "Widespread, multi-source glacial erosion on the Chukchi margin, Arctic Ocean". In: *Quaternary Science Reviews* 92, pp. 112–122. ISSN: 0277-3791. DOI: `10.1016/j.quascirev.2013.07.016`.

Dowdeswell, J. A. & Fugelli, E. (2012). "The seismic architecture and geometry of grounding-zone wedges formed at the marine margins of past ice sheets". In: *Bulletin* 124.11-12, pp. 1750–1761. ISSN: 1943-2674. DOI: `10.1130/B30628.1`.

Dowdeswell, J., Cofaigh, C. Ó., Taylor, J., Kenyon, N., Mienert, J. & Wilken, M. (2002). "On the architecture of high-latitude continental margins: the influence of ice-sheet and sea-ice processes in the Polar North Atlantic". In: *Geological Society, London, Special Publications* 203.1, pp. 33–54. ISSN: 0305-8719. DOI: `10.1144/GSL.SP.2002.203.01.03`.

Dowdeswell, J. A., Canals, M., Jakobsson, M., Todd, B. J., Dowdeswell, E. K. & Hogan, K. (2016). *Atlas of submarine glacial landforms: modern, Quaternary and ancient*. Geological Society of London, p. 618. ISBN: 1786202689. DOI: `10.1144/M46`.

Dowdeswell, J. A., Cofaigh, C. Ó. & Pudsey, C. J. (2004). "Thickness and extent of the subglacial till layer beneath an Antarctic paleo–ice stream". In: *Geology* 32.1, pp. 13–16. ISSN: 0091-7613. DOI: 10.1130/g19864.1.

Dowdeswell, J. A., Ottesen, D., Rise, L. & Craig, J. (2007). "Identification and preservation of landforms diagnostic of past ice-sheet activity on continental shelves from three-dimensional seismic evidence". In: *Geology* 35.4, pp. 359–362. ISSN: 0091-7613. DOI: 10.1130/g23200a.1.

Elias, S. & Brigham-Grette, J. (2013). "Late Pleistocene Glacial Events in Beringia". In: *Encyclopedia of Quaternary Science* 2, pp. 191–201. DOI: 10.1016/B978-0-444-53643-3.00116-3.

Engels, J. L., Edwards, M. H., Polyak, L. & Johnson, P. D. (2008). "Seafloor evidence for ice shelf flow across the Alaska–Beaufort margin of the Arctic Ocean". In: *Earth Surface Processes and Landforms* 33.7, pp. 1047–1063. ISSN: 0197-9337. DOI: 10.1002/esp.1601.

Farquharson, L., Mann, D., Rittenour, T., Groves, P., Grosse, G. & Jones, B. (2018). "Alaskan marine transgressions record out-of-phase Arctic Ocean glaciation during the last interglacial". In: *Geology* 46.9, pp. 783–786. ISSN: 0091-7613. DOI: 10.1130/g40345.1.

Fleischer, P., Orsi, T., Richardson, M. & Anderson, A. (2001). "Distribution of free gas in marine sediments: a global overview". In: *Geo-Marine Letters* 21.2, pp. 103–122. ISSN: 1432-1157. DOI: 10.1007/s003670100072.

Freiman, S., Nikishin, A. & Petrov, E. (2019). "Cenozoic Clinoform Complexes and the Geological History of the North Chukchi Basin (Chuckchi Sea, Arctic)". In: *Moscow University Geology Bulletin* 74.5, pp. 441–449. ISSN: 0145-8752 1934-8436. DOI: 10.3103/S0145875219050053.

Gales, J. A., Forwick, M., Laberg, J. S., Vorren, T. O., Larter, R. D., Graham, A. G. C., Baeten, N. J. & Amundsen, H. B. (2013). "Arctic and Antarctic submarine gullies—A comparison of high latitude continental margins". In: *Geomorphology* 201, pp. 449–461. ISSN: 0169-555X. DOI: 10.1016/j.geomorph.2013.07.018.

Gebhardt, C., Jokat, W., Niessen, F., J, M., Geissler, W. H. & Schenke, H. W. (2011). "Ice sheet grounding and iceberg plow marks on the northern and central Yermak Plateau revealed by geophysical data". In: *Quaternary Science Reviews* 30.13-14, pp. 1726–1738. ISSN: 0277-3791. DOI: 10.1016/j.quascirev.2011.03.016.

Glushkova, O. Y. (2011). "Chapter 63 - Late Pleistocene Glaciations in North-East Asia". In: *Developments in Quaternary Sciences*. Ed. by J. Ehlers, P. L. Gibbard & P. D. Hughes. Vol. 15. Developments in Quaternary Sciences. Elsevier, pp. 865–875. ISBN: 1571-0866. DOI: 10.1016/B978-0-444-53447-7.00063-5.

Graham, A. G. C., Jakobsson, M., Nitsche, F. O., Larter, R. D., Anderson, J. B., Hillenbrand, C.-D., Gohl, K., Klages, J. P., Smith, J. A. & Jenkins, A. (2016). "Submarine glacial-landform distribution across the West Antarctic margin,

from grounding line to slope: the Pine Island–Thwaites ice-stream system". In: *Geological Society, London, Memoirs* 46.1, pp. 493–500. ISSN: 0435-4052 2041-4722. DOI: `10.1144/m46.173`.

Grantz, A., Eittreim, S. L. & Whitney, O. T. (1979). *Geology and physiography of the continental margin north of Alaska and implications for the origin of the Canada Basin*. Report 79-288. DOI: `10.3133/ofr79288`.

Grantz, A., Hart, P. E. & Childers, V. A. (2011). "Chapter 50 Geology and tectonic development of the Amerasia and Canada Basins, Arctic Ocean". In: *Geological Society, London, Memoirs* 35, pp. 771–799. DOI: `10.1144/M35.50`.

Grosswald, M. G. (1998). "Late-Weichselian ice sheets in Arctic and Pacific Siberia". In: *Quaternary International* 45-46, pp. 3–18. ISSN: 1040-6182. DOI: `10.1016/S1040-6182(97)00002-5`.

Grosswald, M. G. & Hughes, T. (2002). "The Russian component of an Arctic Ice Sheet during the LGM". In: *Quaternary Science Reviews* 21.1-3, pp. 121–146. ISSN: 02773791. DOI: `10.1016/S0277-3791(01)00078-6`.

Grosswald, M. G. & Hughes, T. J. (1995). "Paleoglaciology's grand unsolved problem". In: *Journal of Glaciology* 41.138, pp. 313–332. ISSN: 0022-1430. DOI: `10.3189/S0022143000016208`.

Gualtieri, L., Vartanyan, S., Brigham-Grette, J. & Anderson, P. (2003). "Pleistocene raised marine deposits on Wrangel Island, northeast Siberia and implications for the presence of an East Siberian ice sheet". In: *Quaternary Research* 59.3, pp. 399–410. ISSN: 0033-5894. DOI: `10.1016/S0033-5894(03)00057-7`.

Gualtieri, L., Vartanyan, S. L., Brigham-Grette, J. & Anderson, P. M. (2005). "Evidence for an ice-free Wrangel Island, northeast Siberia during the Last Glacial Maximum". In: *Boreas* 34.3, pp. 264–273. ISSN: 0300-9483. DOI: `10.1111/j.1502-3885.2005.tb01100.x`.

Hall, J. K., Grantz, A., Johnson, L. & Sweeney, J. F. (1990). "Chukchi Borderland". In: *The Arctic Ocean Region*. Vol. L. Geological Society of America. Chap. 19, pp. 337–350. ISBN: 9780813754635. DOI: `10.1130/dnag-gna-l.337`.

Hampson, D. (1986). "Inverse velocity stacking for multiple elimination". In: *SEG Technical Program Expanded Abstracts 1986*, pp. 422–424. DOI: `10.1190/1.1893060`.

Hegewald, A. (2012). "The Chukchi Region - Tectonic and Seminentary Evolution". Thesis.

Hegewald, A. & Jokat, W. (2013a). "Relative sea level variations in the Chukchi region - Arctic Ocean - since the late Eocene". In: *Geophysical Research Letters* 40.5, pp. 803–807. ISSN: 0094-8276. DOI: `10.1002/grl.50182`.

Hegewald, A. & Jokat, W. (2013b). "Tectonic and sedimentary structures in the northern Chukchi region, Arctic Ocean". In: *Journal of Geophysical Research: Solid Earth* 118.7, pp. 3285–3296. ISSN: 2169-9313. DOI: `10.1002/jgrb.50282`.

Heiser, P. A. (1997). "Extent, timing, and paleogeographic significance of multiple Pleistocene glaciations in the Bering Strait region". Thesis.

Hill, J. & Driscoll, N. (2008). "Paleodrainage on the Chukchi shelf reveals sea level history and meltwater discharge". In: *Marine Geology* 254.3-4, pp. 129–151. ISSN: 0025-3227. DOI: 10.1016/j.margeo.2008.05.018.

Hill, J. & Driscoll, N. (2010). "Iceberg discharge to the Chukchi shelf during the Younger Dryas". In: *Quaternary Research - QUATERNARY RES* 74.1, pp. 57–62. ISSN: 0033-5894. DOI: 10.1016/j.yqres.2010.03.008.

Hill, J., Driscoll, N., Brigham-Grette, J., Donnelly, J., Gayes, P. & Keigwin, L. (2007). "New evidence for high discharge to the Chukchi shelf since the Last Glacial Maximum". In: *Quaternary Research* 68.2, pp. 271–279. ISSN: 0033-5894. DOI: 10.1016/j.yqres.2007.04.004.

Homza, T. X., Bergman, S. C. & Memoirs, A. (2019a). "Geologic Interpretation of Chukchi Sea Petroleum Province". In: *AAPG Bulletin*.

Homza, T. X. & Bergman, S. C. (2019). *A Geologic Interpretation of the Chukchi Sea Petroleum Province: Offshore Alaska, USA*. The American Association of Petroleum Geologists. ISBN: 9780891814276. DOI: 10.1306/aapg119.

Homza, T. X., Bergman, S. C., Homza, T. X. & Bergman, S. C. (2019b). "Introduction and Objectives". In: *A Geologic Interpretation of the Chukchi Sea Petroleum Province: Offshore Alaska, USA*. Vol. 119. The American Association of Petroleum Geologists, p. 0. ISBN: 9780891814276. DOI: 10.1306/13662196m1223819.

Hopkins, D. M. (1959). "Cenozoic History of the Bering Land Bridge". In: *Science* 129.3362, pp. 1519–1528. ISSN: 00368075, 10959203. DOI: 10.1126/science.129.3362.1519.

Houseknecht, D. W. & Bird, K. J. (2011). "Geology and petroleum potential of the rifted margins of the Canada Basin". In: *Geological Society, London, Memoirs* 35.1, pp. 509–526. ISSN: 0435-4052. DOI: 10.1144/M35.34.

Houseknecht, D. W., Craddock, W. H. & Lease, R. O. (2016). *Upper Cretaceous and Lower Jurassic strata in shallow cores on the Chukchi Shelf, Arctic Alaska*. Report 1814C. DOI: 10.3133/pp1814C.

Hughes, T., Denton, G. H. & Grosswald, M. G. (1977). "Was there a late-Würm Arctic Ice Sheet?" In: *Nature* 266.5603, pp. 596–602. ISSN: 1476-4687. DOI: 10.1038/266596a0.

Hunkins, K., Herron, T., Kutschale, H. & Peter, G. (1962). "Geophysical studies of the Chukchi Cap, Arctic Ocean". In: *Journal of Geophysical Research (1896-1977)* 67.1, pp. 235–247. ISSN: 0148-0227. DOI: 10.1029/JZ067i001p00235.

Hutchinson, D., Jackson, H. R., Houseknecht, D. W., Li, Q., Shimeld, J. W., Mosher, D. C., Chian, D., Saltus, R. & Oakey, G. N. (2017). "Significance of northeast-trending features in Canada Basin, Arctic Ocean". In: *Geochemistry, Geophysics, Geosystems* 18.11, pp. 4156–4178. DOI: 10.1002/2017GC007099.

Huuse, M. & Kristensen, T. B. (2016). "Pleistocene tunnel valleys in the North Sea Basin". In: *Geological Society, London, Memoirs* 46.1, pp. 207–208. ISSN: 0435-4052 2041-4722. DOI: 10.1144/m46.129.

Ilhan, I. & Coakley, B. (2018). "Meso–Cenozoic evolution of the southwestern Chukchi Borderland, Arctic Ocean". In: *Marine and Petroleum Geology* 95, pp. 100–109. ISSN: 0264-8172. DOI: 10.1016/j.marpetgeo.2018.04.014.

IPCC (2018). *Global warming of 1.5°C. An IPCC Special Report on the impacts of global warming of 1.5°C above pre-industrial levels and related global greenhouse gas emission pathways, in the context of strengthening the global response to the threat of climate change, sustainable development, and efforts to eradicate poverty.* Report. DOI: 10.1017/9781009157940.

IPCC (2021). *Climate Change 2021: The Physical Science Basis. Contribution of Working Group I to the Sixth Assessment Report of the Intergovernmental Panel on Climate Change.* Report. DOI: 10.1017/9781009157896.

Jakobsson, M. (2016). "Submarine glacial landform distribution in the central Arctic Ocean shelf–slope–basin system". In: *Geological Society, London, Memoirs* 46.1, pp. 469–476. ISSN: 0435-4052 2041-4722. DOI: 10.1144/m46.179.

Jakobsson, M., Gyllencreutz, R., Mayer, L. A., Dowdeswell, J. A., Canals, M., Todd, B. J., Dowdeswell, E. K., Hogan, K. A. & Larter, R. D. (2016a). "Mapping submarine glacial landforms using acoustic methods". In: *Geological Society, London, Memoirs* 46.1, pp. 17–40. DOI: 10.1144/m46.182.

Jakobsson, M., Pearce, C., Cronin, T. M., Backman, J., Anderson, L. G., Barrientos, N., Björk, G., Coxall, H., De Boer, A., Mayer, L. A., Mörth, C. M., Nilsson, J., Rattray, J. E., Stranne, C., Semiletov, I. & O'regan, M. (2017). "Post-glacial flooding of the Bering Land Bridge dated to 11 cal ka BP based on new geophysical and sediment records". In: *Clim. Past* 13.8, pp. 991–1005. ISSN: 1814-9332. DOI: 10.5194/cp-13-991-2017.

Jakobsson, M. (2002). "Hypsometry and volume of the Arctic Ocean and its constituent seas". In: *Geochemistry Geophysics Geosystems - GEOCHEM GEOPHYS GEOSYST* 3. DOI: 10.1029/2001GC000302.

Jakobsson, M., Andreassen, K., Bjarnadóttir, L. R., Dove, D., Dowdeswell, J. A., England, J. H., Funder, S., Hogan, K., Ingólfsson, Ó., Jennings, A., Krog Larsen, N., Kirchner, N., Landvik, J. Y., Mayer, L., Mikkelsen, N., Möller, P., Niessen, F., Nilsson, J., O'regan, M., Polyak, L., Nørgaard-Pedersen, N. & Stein, R. (2014). "Arctic Ocean glacial history". In: *Quaternary Science Reviews* 92, pp. 40–67. ISSN: 0277-3791. DOI: 10.1016/j.quascirev.2013.07.033.

Jakobsson, M., Gardner, J., Vogt, P., Mayer, L., Armstrong, A., Backman, J., Brennan, R., Calder, B., Hall, J. & Kraft, B. (2005). "Multibeam bathymetric and sediment profiler evidence for ice grounding on the Chukchi Borderland, Arctic

Ocean". In: *Quaternary Research* 63.2, pp. 150–160. ISSN: 0033-5894. DOI: 10.1016/j.yqres.2004.12.004.

Jakobsson, M., Mayer, L., Coakley, B., Dowdeswell, J. A., Forbes, S., Fridman, B., Hodnesdal, H., Noormets, R., Pedersen, R. & Rebesco, M. (2012). "The international bathymetric chart of the Arctic Ocean (IBCAO) version 3.0". In: *Geophysical Research Letters* 39.12. ISSN: 0094-8276. DOI: 10.1029/2012GL052219.

Jakobsson, M., Mayer, L. A., Bringensparr, C., Castro, C. F., Mohammad, R., Johnson, P., Ketter, T., Accettella, D., Amblas, D., An, L., Arndt, J. E., Canals, M., Casamor, J. L., Chauché, N., Coakley, B., Danielson, S., Demarte, M., Dickson, M.-L., Dorschel, B., Dowdeswell, J. A., Dreutter, S., Fremand, A. C., Gallant, D., Hall, J. K., Hehemann, L., Hodnesdal, H., Hong, J., Ivaldi, R., Kane, E., Klaucke, I., Krawczyk, D. W., Kristoffersen, Y., Kuipers, B. R., Millan, R., Masetti, G., Morlighem, M., Noormets, R., Prescott, M. M., Rebesco, M., Rignot, E., Semiletov, I., Tate, A. J., Travaglini, P., Velicogna, I., Weatherall, P., Weinrebe, W., Willis, J. K., Wood, M., Zarayskaya, Y., Zhang, T., Zimmermann, M. & Zinglersen, K. B. (2020). "The International Bathymetric Chart of the Arctic Ocean Version 4.0". In: *Scientific Data* 7.1, p. 176. ISSN: 2052-4463. DOI: 10.1038/s41597-020-0520-9.

Jakobsson, M., Nilsson, J., Anderson, L., Backman, J., Björk, G., Cronin, T. M., Kirchner, N., Koshurnikov, A., Mayer, L., Noormets, R., O'regan, M., Stranne, C., Ananiev, R., Barrientos Macho, N., Cherniykh, D., Coxall, H., Eriksson, B., Flodén, T., Gemery, L., Gustafsson, Ö., Jerram, K., Johansson, C., Khortov, A., Mohammad, R. & Semiletov, I. (2016b). "Evidence for an ice shelf covering the central Arctic Ocean during the penultimate glaciation". In: *Nature Communications* 7.1, p. 10365. ISSN: 2041-1723. DOI: 10.1038/ncomms10365.

Jakobsson, M., Polyak, L., Edwards, M., Kleman, J. & Coakley, B. (2008). "Glacial geomorphology of the Central Arctic Ocean: the Chukchi Borderland and the Lomonosov Ridge". In: *Earth Surface Processes and Landforms* 33.4, pp. 526–545. ISSN: 0197-9337. DOI: 10.1002/esp.1667.

Jansen, E., Fronval, T., Rack, F. & Channell, J. E. T. (2000). "Pliocene-Pleistocene ice rafting history and cyclicity in the Nordic Seas during the last 3.5 Myr". In: *Paleoceanography* 15.6, pp. 709–721. ISSN: 0883-8305. DOI: 10.1029/1999PA000435.

Joe, Y. J., Polyak, L., Schreck, M., Niessen, F., Yoon, S. H., Kong, G. S. & Nam, S.-I. (2020). "Late Quaternary depositional and glacial history of the Arliss Plateau off the East Siberian margin in the western Arctic Ocean". In: *Quaternary Science Reviews* 228, p. 106099. ISSN: 0277-3791. DOI: 10.1016/j.quascirev.2019.106099.

Johansen, T. A., Digranes, P., Van Schaack, M. & Lønne, I. (2003). "On seismic mapping and modeling of near-surface sediments in polar areas". In: *Geophysics* 68.2, pp. 566–573. ISSN: 0016-8033. DOI: 10.1190/1.1567226.

Johnson, G. L., Grantz, A., Weber, J. R., Grantz, A., Johnson, L. & Sweeney, J. F. (1990). "Bathymetry and physiography". In: *The Arctic Ocean Region*. Vol. L. Geological Society of America, p. 0. ISBN: 9780813754635. DOI: 10.1130/dnag-gna-l.63.

Jokat, W., Weigelt, E., Kristoffersen, Y., Rasmussen, T. & Schöne, T. (1995). "New insights into the evolution of the Lomonosov Ridge and the Eurasian Basin". In: *Geophysical Journal International* 122.2, pp. 378–392. ISSN: 0956-540x. DOI: 10.1111/j.1365-246X.1995.tb00532.x.

Kang, S.-G., Jang, U., Kim, S., Choi, Y., Kim, Y.-G., Hong, J. K. & Jin, Y. K. (2021). "Exploration of the gas hydrates on the southwestern continental slope of the Chukchi Plateau in the Arctic Ocean". In: *Journal of the Korean Society of Mineral and Energy Resources Engineers* 58.5, pp. 418–432. DOI: 10.32390/ksmer.2021.58.5.418.

Kaufman, D. S., Young, N. E., Briner, J. P. & Manley, W. F. (2011). "Chapter 33 - Alaska Palaeo-Glacier Atlas (Version 2)". In: *Developments in Quaternary Sciences*. Ed. by J. Ehlers, P. L. Gibbard & P. D. Hughes. Vol. 15. Developments in Quaternary Sciences. Elsevier, pp. 427–445. ISBN: 1571-0866. DOI: 10.1016/B978-0-444-53447-7.00033-7.

Kehew, A. E., Piotrowski, J. A. & Jørgensen, F. (2012). "Tunnel valleys: Concepts and controversies — A review". In: *Earth-Science Reviews* 113.1, pp. 33–58. ISSN: 0012-8252. DOI: 10.1016/j.earscirev.2012.02.002.

Kerr, R. A. (2010). "'Arctic Armageddon' Needs More Science, Less Hype". In: *Science* 329.5992, pp. 620–621. ISSN: 1095-9203 (Electronic) 0036-8075 (Linking). DOI: 10.1126/science.329.5992.620.

Kim, J.-H., Hachikubo, A., Kida, M., Minami, H., Lee, D.-H., Jin, Y. K., Ryu, J.-S., Lee, Y. M., Hur, J., Park, M.-H., Kim, Y.-G., Kang, M.-H., Park, S., Chen, M., Kang, S.-G. & Kim, S. (2020). "Upwarding gas source and postgenetic processes in the shallow sediments from the ARAON Mounds, Chukchi Sea". In: *Journal of Natural Gas Science and Engineering* 76, p. 103223. ISSN: 1875-5100. DOI: 10.1016/j.jngse.2020.103223.

Kim, S., Polyak, L., Joe, Y. J., Niessen, F., Kim, H. J., Choi, Y., Kang, S.-G., Hong, J. K., Nam, S.-I. & Jin, Y. K. (2021). "Seismostratigraphic and geomorphic evidence for the glacial history of the northwestern Chukchi margin, Arctic Ocean". In: *Journal of Geophysical Research: Earth Surface* n/a.n/a, e2020JF006030. ISSN: 2169-9003. DOI: 10.1029/2020JF006030.

Kim, Y.-G., Kim, S., Lee, D.-H., Lee, Y. M., Kim, H. J., Kang, S.-G. & Jin, Y. K. (2020). "Occurrence of active gas hydrate mounds in the southwestern slope of the Chukchi Plateau, Arctic Ocean". In: *International Union of Geological Sciences* 43.2, pp. 811–823. ISSN: 0705-3797 2586-1298. DOI: 10.18814/epiiugs/2020/020053.

King, L. H. (1993). "Till in the marine environment". In: *Journal of Quaternary Science* 8.4, pp. 347–358. ISSN: 0267-8179. DOI: 10.1002/jqs.3390080406.

Kjemperud, A. & Fjeldskaar, W. (1992). "Pleistocene glacial isostasy — implications for petroleum geology". In: *Structural and Tectonic Modelling and its Application to Petroleum Geology*. Ed. by R. M. Larsen, H. Brekke, B. T. Larsen & E. Talleraas. Vol. 1. Amsterdam: Elsevier, pp. 187–195. ISBN: 09288937. DOI: `10.1016/B978-0-444-88607-1.50017-6`.

Kleiber, H. P. & Niessen, F. (1999). "Late Pleistocene Paleoriver Channels on the Laptev Sea Shelf - Implications from Sub-Bottom Profiling". In: *Land-Ocean Systems in the Siberian Arctic: Dynamics and History*. Ed. by H. Kassens, H. A. Bauch, I. A. Dmitrenko, H. Eicken, H.-W. Hubberten, M. Melles, J. Thiede & L. A. Timokhov. Berlin, Heidelberg: Springer Berlin Heidelberg. Chap. Chapter 49, pp. 657–665. ISBN: 978-3-642-60134-7. DOI: `10.1007/978-3-642-60134-7_49`.

Knies, J. & Gaina, C. (2008). "Middle Miocene ice sheet expansion in the Arctic: Views from the Barents Sea". In: *Geochemistry, Geophysics, Geosystems* 9.2. ISSN: 1525-2027. DOI: `10.1029/2007GC001824`.

Kolesnik, O. N., Kolesnik, A. N. & Pokrovskii, B. G. (2014). "A find of an authigenic methane-derived carbonate in the Chukchi Sea". In: *Doklady Earth Sciences* 458.1, pp. 1168–1170. ISSN: 1028-334X. DOI: `10.1134/S1028334X1409030X`.

Kristoffersen, Y., Coakley, B., Jokat, W., Edwards, M., Brekke, H. & Gjengedal, J. (2004). "Seabed erosion on the Lomonosov Ridge, central Arctic Ocean: A tale of deep draft icebergs in the Eurasia Basin and the influence of Atlantic water inflow on iceberg motion?" In: *Paleoceanography* 19.3. ISSN: 0883-8305. DOI: `10.1029/2003pa000985`.

Kristoffersen, Y., Grantz, A., Johnson, L. & Sweeney, J. F. (1990). "Eurasia Basin". In: *The Arctic Ocean Region*. Vol. L. Geological Society of America. Chap. 21, pp. 365–378. ISBN: 9780813754635. DOI: `10.1130/dnag-gna-l.365`.

Kristoffersen, Y., Spencer, A. M., Embry, A. F., Gautier, D. L., Stoupakova, A. V. & Sørensen, K. (2011). "Geophysical exploration of the Arctic Ocean: the physical environment, survey techniques and brief summary of knowledge". In: *Arctic Petroleum Geology*. Vol. 35. Geological Society of London, pp. 685–702. ISBN: 9781862393288. DOI: `10.1144/m35.45`.

Laberg, J. S. & Vorren, T. O. (1996). "The Middle and Late Pleistocence evolution and the Bear Island Trough Mouth Fan". In: *Global and Planetary Change* 12.1, pp. 309–330. ISSN: 0921-8181. DOI: `10.1016/0921-8181(95)00026-7`.

Laberg, J. S., Andreassen, K. & Vorren, T. O. (2012). "Late Cenozoic erosion of the high-latitude southwestern Barents Sea shelf revisited". In: *GSA Bulletin* 124.1-2, pp. 77–88. ISSN: 0016-7606. DOI: `10.1130/b30340.1`.

Lawver, L. A., Scotese, C. R., Grantz, A., Johnson, L. & Sweeney, J. F. (1990). "A review of tectonic models for the evolution of the Canada Basin". In: *The Arctic Ocean Region*. Vol. L. Geological Society of America. Chap. 31, pp. 593–618. ISBN: 9780813754635. DOI: `10.1130/dnag-gna-l.593`.

Lehmann, C., Jokat, W. & Coakley, B. (2022). "Glacial sediments on the outer Chukchi Shelf and Chukchi Borderland in seismic reflection data". In: *Marine Geophysical Research* 43.3, p. 33. ISSN: 1573-0581. DOI: 10.1007/s11001-022-09497-7.

Li, Y., Zhan, L., Zhang, J., Chen, L., Chen, J. & Zhuang, Y. (2017). "A significant methane source over the Chukchi Sea shelf and its sources". In: *Continental Shelf Research* 148, pp. 150–158. ISSN: 0278-4343. DOI: 10.1016/j.csr.2017.08.019.

Løseth, H., Gading, M. & Wensaas, L. (2009). "Hydrocarbon leakage interpreted on seismic data". In: *Marine and Petroleum Geology* 26.7, pp. 1304–1319. ISSN: 0264-8172. DOI: 10.1016/j.marpetgeo.2008.09.008.

Løseth, H., Wensaas, L., Arntsen, B., Hanken, N.-M., Basire, C. & Graue, K. (2011). "1000 m long gas blow-out pipes". In: *Marine and Petroleum Geology* 28.5, pp. 1047–1060. ISSN: 02648172. DOI: 10.1016/j.marpetgeo.2010.10.001.

Lurton, X. (2010). *An introduction to underwater acoustics: principles and applications.* Vol. 2. Springer Praxis Books. Heidelberg: Springer. ISBN: 978-3-540-78480-7 978-3-662-49969-6.

Matveeva, T., Savvichev, A. S., Semenova, A., Logvina, E., Kolesnik, A. N. & Bosin, A. A. (2015). "Source, Origin, and Spatial Distribution of Shallow Sediment Methane in the Chukchi Sea". In: *Oceanography* 28.3, pp. 202–217. ISSN: 10428275, 2377617X. DOI: 10.5670/oceanog.2015.66.

Melles, M., Brigham-Grette, J., Minyuk, P. S., Nowaczyk, N. R., Wennrich, V., Deconto, R. M., Anderson, P. M., Andreev, A. A., Coletti, A., Cook, T. L., Haltia-Hovi, E., Kukkonen, M., Lozhkin, A. V., Rosén, P., Tarasov, P., Vogel, H. & Wagner, B. (2012). "2.8 Million Years of Arctic Climate Change from Lake El'gygytgyn, NE Russia". In: *Science* 337.6092, pp. 315–320. ISSN: 1095-9203 (Electronic) 0036-8075 (Linking). DOI: 10.1126/science.1222135.

Mercer, J. H. (1970). "A former ice sheet in the Arctic Ocean?" In: *Palaeogeography, Palaeoclimatology, Palaeoecology* 8.1, pp. 19–27. ISSN: 0031-0182. DOI: 10.1016/0031-0182(70)90076-3.

Miller, K. G., Browning, J. V., Schmelz, W. J., Kopp, R. E., Mountain, G. S. & Wright, J. D. (2020). "Cenozoic sea-level and cryospheric evolution from deep-sea geochemical and continental margin records". In: *Science Advances* 6.20, eaaz1346. ISSN: 2375-2548 (Electronic) 2375-2548 (Linking). DOI: 10.1126/sciadv.aaz1346.

Moore, T. E., Wallace, W. K., Bird, K. J., Karl, S. M., Mull, C. G. & Dillon, J. T. (1994). "Geology of northern Alaska". In.

Nanda, N. C. (2021). *Seismic data interpretation and evaluation for hydrocarbon exploration and production. A Practitioner's Guide.* Springer. ISBN: 978-3-319-79961-2. DOI: 10.1007/978-3-319-26491-2.

Nickel, J. C., Di Primio, R., Mangelsdorf, K., Stoddart, D. & Kallmeyer, J. (2012). "Characterization of microbial activity in pockmark fields of the SW-Barents

Sea". In: *Marine Geology* 332-334, pp. 152–162. ISSN: 0025-3227. DOI: 10.1016/j.margeo.2012.02.002.

Nielsen, T., Santis, L., Dahlgren, K. I. T., Kuijpers, A., Laberg, J., Nygård, A., Praeg, D. & Stoker, M. S. (2005). "A comparison of the NW European margin with other glaciated margins". In: *Marine and Petroleum Geology* 22.9-10, pp. 1149–1183. ISSN: 0264-8172. DOI: 10.1016/j.marpetgeo.2004.12.007.

Niessen, F., Hong, J. K., Hegewald, A., Matthiessen, J., Stein, R., Kim, H., Kim, S., Jensen, L., Jokat, W., Nam, S.-I. & Kang, S.-H. (2013). "Repeated Pleistocene glaciation of the East Siberian continental margin". In: *Nature Geoscience* 6.10, pp. 842–846. ISSN: 1752-0908. DOI: 10.1038/ngeo1904.

Nikishin, A., Petrov, E., Malyshev, N. & Ershova, V. (2017). "Rift systems of the Russian Eastern Arctic shelf and Arctic deep water basins: link between geological history and geodynamics". In: *Geodynamics & Tectonophysics* 8.1, pp. 11–43. ISSN: 2078-502X. DOI: 10.5800/GT-2017-8-1-0231.

Nikolskiy, P. A., Basilyan, A. E. & Zazhigin, V. S. (2017). "New data on the age of the glaciation in the New Siberian Islands (Russian Eastern Arctic)". In: *Doklady Earth Sciences* 475.1, pp. 748–752. ISSN: 1531-8354. DOI: 10.1134/S1028334X17070194.

Ó Cofaigh, C., Dowdeswell, J. A., Allen, C. S., Hiemstra, J. F., Pudsey, C. J., Evans, J. & J.A. Evans, D. (2005). "Flow dynamics and till genesis associated with a marine-based Antarctic palaeo-ice stream". In: *Quaternary Science Reviews* 24.5, pp. 709–740. ISSN: 0277-3791. DOI: 10.1016/j.quascirev.2004.10.006.

Ó Cofaigh, C., Taylor, J., Dowdeswell, J. A. & Pudsey, C. J. (2003). "Palaeo-ice streams, trough mouth fans and high-latitude continental slope sedimentation". In: *Boreas* 32.1, pp. 37–55. ISSN: 0300-9483. DOI: 10.1080/03009480310001858.

O´Regan, M., Backman, J., Barrientos, N., Cronin, T., Gemery, L., Kirchner, N., Mayer, L., Nilsson, J., Noormets, R., Pearce, C., Semilietov, I., Stranne, C. & Jakobsson, M. (2017). "De Long Trough: A newly discovered glacial trough on the East Siberian Continental Margin". In: *Climate of the Past Discussions*, pp. 1–28. DOI: 10.5194/cp-2017-56.

Ottesen, D., Dowdeswell, J. A. & Rise, L. (2005). "Submarine landforms and the reconstruction of fast-flowing ice streams within a large Quaternary ice sheet: the 2500-km-long Norwegian-Svalbard margin (57–80 N)". In: *GSA Bulletin* 117.7-8, pp. 1033–1050. ISSN: 0016-7606. DOI: 10.1130/B25577.1.

Ottesen, D. & Dowdeswell, J. A. (2006). "Assemblages of submarine landforms produced by tidewater glaciers in Svalbard". In: *Journal of Geophysical Research: Earth Surface* 111.F1. ISSN: 0148-0227. DOI: 10.1029/2005JF000330.

Ottesen, D. & Dowdeswell, J. A. (2009). "An inter-ice-stream glaciated margin: Submarine landforms and a geomorphic model based on marine-geophysical data from Svalbard". In: *Bulletin of the Geological Society of America* 121.11-12, pp. 1647–1665. ISSN: 0016-7606. DOI: 10.1130/B26467.1.

Park, K., Ohkushi, K., Cho, H. G. & Khim, B.-K. (2017). "Lithostratigraphy and paleoceanography in the Chukchi Rise of the western Arctic Ocean since the last glacial period". In: *Polar Science* 11, pp. 42–53. ISSN: 1873-9652. DOI: 10.1016/j.polar.2017.01.002.

Petrov, O., Morozov, A., Shokalsky, S., Kashubin, S., Artemieva, I. M., Sobolev, N., Petrov, E., Ernst, R. E., Sergeev, S. & Smelror, M. (2016). "Crustal structure and tectonic model of the Arctic region". In: *Earth-Science Reviews* 154, pp. 29–71. ISSN: 0012-8252. DOI: 10.1016/j.earscirev.2015.11.013.

Phrampus, B. J., Hornbach, M. J., Ruppel, C. D. & Hart, P. E. (2014). "Widespread gas hydrate instability on the upper U.S. Beaufort margin". In: *Journal of Geophysical Research B: Solid Earth* 119.12, pp. 8594–8609. ISSN: 2169-9313. DOI: 10.1002/2014JB011290.

Piper, D. J. W. & Normark, W. R. (2009). "Processes that initiate turbidity currents and their influence on turbidites: A marine geology perspective". In: *Journal of Sedimentary Research* 79.6, pp. 347–362. ISSN: 1527-1404. DOI: 10.2110/jsr.2009.046.

Piskarev, A., Poselov, V. & Kaminsky, V. (2018). *Geologic Structures of the Arctic Basin*. Springer. ISBN: 3319777424. DOI: 10.1007/978-3-319-77742-9.

Polyak, L., Darby, D. A., Bischof, J. F. & Jakobsson, M. (2007). "Stratigraphic constraints on late Pleistocene glacial erosion and deglaciation of the Chukchi margin, Arctic Ocean". In: *Quaternary Research* 67.2, pp. 234–245. ISSN: 0033-5894. DOI: 10.1016/j.yqres.2006.08.001.

Polyak, L., Edwards, M., Coakley, B. & Jakobsson, M. (2001). "Ice shelves in the Pleistocene Arctic Ocean inferred from deep-sea bedforms". In: *Nature* 410.6827, pp. 453–7. ISSN: 0028-0836. DOI: 10.1038/35068536.

Polyak, L., Niessen, F., Gataullin, V. & Gainanov, V. (2008). "The eastern extent of the Barents–Kara ice sheet during the Last Glacial Maximum based on seismic-reflection data from the eastern Kara Sea". In: *Polar Research* 27.2, pp. 162–174. ISSN: 0800-0395. DOI: 10.3402/polar.v27i2.6174.

Randall, D. A., Wood, R. A., Bony, S., Colman, R., Fichefet, T., Fyfe, J., Kattsov, V., Pitman, A., Shukla, J. & Srinivasan, J. (2007). "Climate models and their evaluation". In: *Climate change 2007: The physical science basis. Contribution of Working Group I to the Fourth Assessment Report of the IPCC (FAR)*. Cambridge University Press, pp. 589–662.

Rekant, P., Bauch, H. A., Schwenk, T., Portnov, A., Gusev, E., Spiess, V., Cherkashov, G. & Kassens, H. (2015). "Evolution of subsea permafrost landscapes in Arctic Siberia since the Late Pleistocene: a synoptic insight from acoustic data of the Laptev Sea". In: *arktos* 1.1, p. 11. ISSN: 2364-9461. DOI: 10.1007/s41063-015-0011-y.

Rembert, J. R. (2012). *MB-System: An Open Source Bathymetric Processing Solution*. Web Page.

Rise, L., Ottesen, D., Berg, K. & Lundin, E. (2005). "Large-scale development of the mid-Norwegian margin during the last 3 million years". In: *Marine and Petroleum Geology* 22.1, pp. 33–44. ISSN: 0264-8172. DOI: 10.1016/j.marpetgeo.2004.10.010.

Roberts, H. H., Hardage, B. A., Shedd, W. W. & Hunt Jesse, J. (2006). "Seafloor reflectivity—An important seismic property for interpreting fluid/gas expulsion geology and the presence of gas hydrate". In: *The Leading Edge* 25.5, pp. 620–628. ISSN: 1070-485X. DOI: 10.1190/1.2202667.

Robinson, A. H., Callow, B., Böttner, C., Yilo, N., Provenzano, G., Falcon-Suarez, I. H., Marín-Moreno, H., Lichtschlag, A., Bayrakci, G., Gehrmann, R., Parkes, L., Roche, B., Saleem, U., Schramm, B., Waage, M., Lavayssière, A., Li, J., Jedari-Eyvazi, F., Sahoo, S., Deusner, C., Kossel, E., Minshull, T. A., Berndt, C., Bull, J. M., Dean, M., James, R. H., Chapman, M., Best, A. I., Bünz, S., Chen, B., Connelly, D. P., Elger, J., Haeckel, M., Henstock, T. J., Karstens, J., Macdonald, C., Matter, J. M., North, L. & Reinardy, B. (2021). "Multiscale characterisation of chimneys/pipes: Fluid escape structures within sedimentary basins". In: *International Journal of Greenhouse Gas Control* 106, p. 103245. ISSN: 1750-5836. DOI: 10.1016/j.ijggc.2020.103245.

Romanovskii, N. N. & Hubberten, H.-W. (2001). "Results of permafrost modelling of the lowlands and shelf of the Laptev Sea Region, Russia". In: *Permafrost and Periglacial Processes* 12.2, pp. 191–202. ISSN: 1045-6740. DOI: 10.1002/ppp.387.

Rüther, D. C., Mattingsdal, R., Andreassen, K., Forwick, M. & Husum, K. (2011). "Seismic architecture and sedimentology of a major grounding zone system deposited by the Bjørnøyrenna Ice Stream during Late Weichselian deglaciation". In: *Quaternary Science Reviews* 30.19, pp. 2776–2792. ISSN: 0277-3791. DOI: 10.1016/j.quascirev.2011.06.011.

Rydningen, T. A., Laberg, J. S. & Kolstad, V. (2015). "Seabed morphology and sedimentary processes on high-gradient trough mouth fans offshore Troms, northern Norway". In: *Geomorphology* 246, pp. 205–219. ISSN: 0169-555X. DOI: 10.1016/j.geomorph.2015.06.007.

Rydningen, T. A., Laberg, J. S. & Kolstad, V. (2016). "Late Cenozoic evolution of high-gradient trough mouth fans and canyons on the glaciated continental margin offshore Troms, northern Norway—Paleoclimatic implications and sediment yield". In: *GSA Bulletin* 128.3-4, pp. 576–596. ISSN: 0016-7606. DOI: 10.1130/b31302.1.

Sættem, J., Poole, D. A. R., Ellingsen, L. & Sejrup, H. P. (1992). "Glacial geology of outer Bjørnøyrenna, southwestern Barents Sea". In: *Marine Geology* 103.1, pp. 15–51. ISSN: 0025-3227. DOI: 10.1016/0025-3227(92)90007-5.

Sarkar, S., Berndt, C., Minshull, T., Westbrook, G., Klaeschen, D., Masson, D., Chabert, A. & Thatcher, K. (2012). "Seismic evidence for shallow gas-escape features associated with a retreating gas hydrate zone offshore west Svalbard". In: *Journal*

of Geophysical Research (Solid Earth) 117, p. 9102. ISSN: 2169-9313. DOI: `10.1029/2011JB009126`.

Shakhova, N., Semiletov, I. & Panteleev, G. (2005). "The distribution of methane on the Siberian Arctic shelves: Implications for the marine methane cycle". In: *Geophysical Research Letters* 32.9. ISSN: 0094-8276. DOI: `10.1029/2005GL022751`.

Shakhova, N., Semiletov, I., Salyuk, A., Yusupov, V., Kosmach, D. & Gustafsson, Ö. (2010). "Extensive Methane Venting to the Atmosphere from Sediments of the East Siberian Arctic Shelf". In: *Science* 327.5970, pp. 1246–1250. ISSN: 1095-9203 (Electronic) 0036-8075 (Linking). DOI: `10.1126/science.1182221`.

Sheriff, R. E. & Geldart, L. P. (1995). *Exploration Seismology.* 2nd ed. Cambridge: Cambridge University Press. ISBN: 9780521468268. DOI: `DOI:10.1017/CBO9781139168359`.

Sherwood, K. W., Johnson, P. P., Craig, J. D., Zerwick, S. A., Lothamer, R. T., Thurston, D. K., Hurlbert, S. B., Miller, E. L., Grantz, A. & Klemperer, S. L. (2002). "Structure and stratigraphy of the Hanna Trough, U.S. Chukchi Shelf, Alaska". In: *Tectonic Evolution of the Bering Shelf-Chukchi Sea-Artic Margin and Adjacent Landmasses.* Vol. 360. Geological Society of America. ISBN: 9780813723600. DOI: `10.1130/0-8137-2360-4.39`.

Siegert, M. J. & Dowdeswell, J. A. (1996). "Topographic control on the dynamics of the Svalbard-Barents Sea ice sheet". In: *Global and Planetary Change* 12.1, pp. 27–39. ISSN: 0921-8181. DOI: `10.1016/0921-8181(95)00010-0`.

Solheim, A., Andersen, E. S., Elverhøi, A. & Fiedler, A. (1996). "Late Cenozoic depositional history of the western Svalbard continental shelf, controlled by subsidence and climate". In: *Global and Planetary Change* 12.1, pp. 135–148. ISSN: 0921-8181. DOI: `10.1016/0921-8181(95)00016-X`.

Spagnolo, M., Clark, C. D., Ely, J. C., Stokes, C. R., Anderson, J. B., Andreassen, K., Graham, A. G. C. & King, E. C. (2014). "Size, shape and spatial arrangement of mega-scale glacial lineations from a large and diverse dataset". In: *Earth Surface Processes and Landforms* 39.11, pp. 1432–1448. ISSN: 0197-9337. DOI: `10.1002/esp.3532`.

Stein, R., J, M., Niessen, F., Krylov, A., S-I, N. & Bazhenova, E. (2010). "Towards a better (litho-) stratigraphy and reconstruction of Quaternary Paleoenvironment in the Amerasian Basin (Arctic Ocean)". In: *Polarforschung* 79. ISSN: 03018202. DOI: `10013/epic.34884.d001`.

Stewart, M. A., Lonergan, L. & Hampson, G. (2013). "3D seismic analysis of buried tunnel valleys in the central North Sea: morphology, cross-cutting generations and glacial history". In: *Quaternary Science Reviews* 72, pp. 1–17. ISSN: 0277-3791. DOI: `10.1016/j.quascirev.2013.03.016`.

Stokes, C. R. & Clark, C. D. (1999). "Geomorphological criteria for identifying Pleistocene ice streams". In: *Annals of glaciology* 28, pp. 67–74. ISSN: 0260-3055. DOI: `10.3189/172756499781821625`.

Stokes, C. R., Clark, C. D., Darby, D. A. & Hodgson, D. A. (2005). "Late Pleistocene ice export events into the Arctic Ocean from the M'Clure Strait Ice Stream, Canadian Arctic Archipelago". In: *Global and Planetary Change* 49.3, pp. 139–162. ISSN: 0921-8181. DOI: `10.1016/j.gloplacha.2005.06.001`.

Stokes, C. R. & Tarasov, L. (2010). "Ice streaming in the Laurentide ice sheet : a first comparison between data-calibrated numerical model output and geological evidence". In: *Geophysical research letters.* 37.1, p. L01501. ISSN: 0094-8276. DOI: `10.1029/2009GL040990`.

Svendsen, J. I., Alexanderson, H., Astakhov, V. I., Demidov, I., Dowdeswell, J. A., Funder, S., Gataullin, V., Henriksen, M., Hjort, C., Houmark-Nielsen, M., Hubberten, H. W., Ingólfsson, Ó., Jakobsson, M., Kjær, K. H., Larsen, E., Lokrantz, H., Lunkka, J. P., Lyså, A., Mangerud, J., Matiouchkov, A., Murray, A., Möller, P., Niessen, F., Nikolskaya, O., Polyak, L., Saarnisto, M., Siegert, C., Siegert, M. J., Spielhagen, R. F. & Stein, R. (2004). "Late Quaternary ice sheet history of northern Eurasia". In: *Quaternary Science Reviews* 23.11, pp. 1229–1271. ISSN: 0277-3791. DOI: `10.1016/j.quascirev.2003.12.008`.

Taylor, J., Dowdeswell, J. A. & Kenyon, N. (2000). "Canyons and late Quaternary sedimentation on the North Norwegian margin". In: *Marine Geology* 166.1-4, pp. 1–9. ISSN: 0025-3227. DOI: `10.1016/S0025-3227(00)00010-4`.

Triezenberg, P., Hart, P. & Childs, J. (2016). *National Archive of Marine Seismic Surveys (NAMSS): A USGS Data Website of Marine Seismic Reflection Data within the U.S. Exclusive Economic Zone (EEZ): U.S. Geological Survey Data Release.* Dataset. DOI: `10.5066/F7930R7P`.

Tripati, A. & Darby, D. (2018). "Evidence for ephemeral middle Eocene to early Oligocene Greenland glacial ice and pan-Arctic sea ice". In: *Nature Communications* 9.1, p. 1038. ISSN: 2041-1723. DOI: `10.1038/s41467-018-03180-5`.

Vanneste, K., Uenzelmann-Neben, G. & Miller, H. (1995). "Seismic evidence for long-term history of glaciation on central East Greenland shelf south of Scoresby Sund". In: *Geo-Marine Letters* 15.2, pp. 63–70. ISSN: 1432-1157. DOI: `10.1007/BF01275408`.

Verschuur, D. J., Berkhout, A. J. & Wapenaar, C. P. A. (1992). "Adaptive surface-related multiple elimination". In: *GEOPHYSICS* 57.9, pp. 1166–1177. DOI: `10.1190/1.1443330`.

Verschuur, D. J. (2013). *Seismic multiple removal techniques: past, present and future.* EAGE publications Houten, The Netherlands, p. 211. ISBN: 978-9073834569.

Vogt, P., Taylor, P., Kovacs, L. & Johnson, G. (1979). "Detailed aeromagnetic investigation of the Arctic Basin". In: *Journal of Geophysical Research: Solid Earth* 84.B3, pp. 1071–1089. ISSN: 0148-0227.

Von Toll, E. G. (1897). "Fossil glaciers of the New Siberian Islands, their relationship to mammoth carcasses and to the glacial period". In: *Zapiski Russkogo Geograficheskogo Obshchestva po obshchey geografii* 32.1, pp. 1–139.

Vorren, T. O., Lebesbye, E., Andreassen, K. & Larsen, K. B. (1989). "Glacigenic sediments on a passive continental margin as exemplified by the Barents Sea". In: *Marine Geology* 85.2, pp. 251–272. ISSN: 0025-3227. DOI: `10.1016/0025-3227(89)90156-4`.

Vorren, T. O. & Laberg, J. S. (1997). "Trough mouth fans — palaeoclimate and ice-sheet monitors". In: *Quaternary Science Reviews* 16.8, pp. 865–881. ISSN: 0277-3791. DOI: `10.1016/S0277-3791(97)00003-6`.

Vorren, T. O., Laberg, J. S., Blaume, F., Dowdeswell, J. A., Kenyon, N. H., Mienert, J., Rumohr, J. A. N. & Werner, F. (1998). "The Norwegian–Greenland Sea Continental Margins: Morphology And Late Quaternary Sedimentary Processes And Environment". In: *Quaternary Science Reviews* 17.1, pp. 273–302. ISSN: 0277-3791. DOI: `10.1016/S0277-3791(97)00072-3`.

Waage, M., Portnov, A., Serov, P., Bünz, S., Waghorn, K. A., Vadakkepuliyambatta, S., Mienert, J. & Andreassen, K. (2019). "Geological controls on fluid flow and gas hydrate pingo development on the Barents Sea margin". In: *Geochemistry, Geophysics, Geosystems* 20.2, pp. 630–650. ISSN: 1525-2027. DOI: `10.1029/2018GC007930`.

Walder, J. S. & Fowler, A. (1994). "Channelized subglacial drainage over a deformable bed". In: *Journal of Glaciology* 40.134, pp. 3–15. ISSN: 0022-1430. DOI: `10.3189/S0022143000003750`.

Wang, R., Xiao, W., März, C. & Li, Q. (2013). "Late Quaternary paleoenvironmental changes revealed by multi-proxy records from the Chukchi Abyssal Plain, western Arctic Ocean". In: *Global and Planetary Change* 108, pp. 100–118. ISSN: 0921-8181. DOI: `10.1016/j.gloplacha.2013.05.017`.

Weigelt, E., Jokat, W. & Franke, D. (2014). "Seismostratigraphy of the Siberian sector of the Arctic Ocean and adjacent Laptev Sea Shelf". In: *Journal of Geophysical Research: Solid Earth* 119.7, pp. 5275–5289. ISSN: 2169-9313. DOI: `10.1002/2013jb010727`.

Wessel, P. & Smith, W. H. F. (1998). "New, improved version of generic mapping tools released". In: *Eos, Transactions American Geophysical Union* 79.47, pp. 579–579. ISSN: 0096-3941. DOI: `10.1029/98EO00426`.

Winkelmann, D., Jokat, W., Jensen, L. & Schenke, H.-W. (2010). "Submarine end moraines on the continental shelf off NE Greenland – Implications for Lateglacial dynamics". In: *Quaternary Science Reviews* 29.9, pp. 1069–1077. ISSN: 0277-3791. DOI: `10.1016/j.quascirev.2010.02.002`.

Winsborrow, M. C. M., Clark, C. D. & Stokes, C. R. (2010). "What controls the location of ice streams?" In: *Earth-Science Reviews* 103.1, pp. 45–59. ISSN: 0012-8252. DOI: `10.1016/j.earscirev.2010.07.003`.

Al-Yahya, K. M. (1991). "Application of the Partial Karhunen-Loeve Transform to Suppress Random Noise in Seismic Sections1". In: *Geophysical Prospecting* 39.1, pp. 77–93. ISSN: 0016-8025 1365-2478. DOI: `10.1111/j.1365-2478.1991.tb00302.x`.

Ye, L., Zhang, W., Wang, R., Yu, X. & Jin, L. (2020). "Ice events along the East Siberian continental margin during the last two glaciations: Evidence from clay minerals".

In: *Marine Geology* 428, p. 106289. ISSN: 0025-3227. DOI: 10.1016/j.margeo.2020.106289.

Yilmaz, Ö. (2001). *Seismic Data Analysis*. Investigations in Geophysics. Society of Exploration Geophysicists, p. 2065. ISBN: 978-1-56080-094-1 978-1-56080-158-0. DOI: 10.1190/1.9781560801580.

Zhang, Z., Yan, Q., Farmer, E. J., Li, C., Ramstein, G., Hughes, T., Jakobsson, M., O'regan, M., Zhang, R., Tan, N., Contoux, C., Dumas, C. & Guo, C. (2018). "Instability of Northeast Siberian ice sheet during glacials". In: *Clim. Past Discuss.* 2018, pp. 1–19. ISSN: 1814-9359. DOI: 10.5194/cp-2018-79.

Zhang, Z., Yan, Q., Zhang, R., Colleoni, F., Ramstein, G., Dai, G., Jakobsson, M., O'regan, M., Liess, S., Rousseau, D. D., Wu, N., Farmer, E. J., Contoux, C., Guo, C., Tan, N. & Guo, Z. (2020). "Rapid waxing and waning of Beringian ice sheet reconcile glacial climate records from around North Pacific". In: *Clim. Past Discuss.* 2020, pp. 1–25. ISSN: 1814-9359. DOI: 10.5194/cp-2020-38.
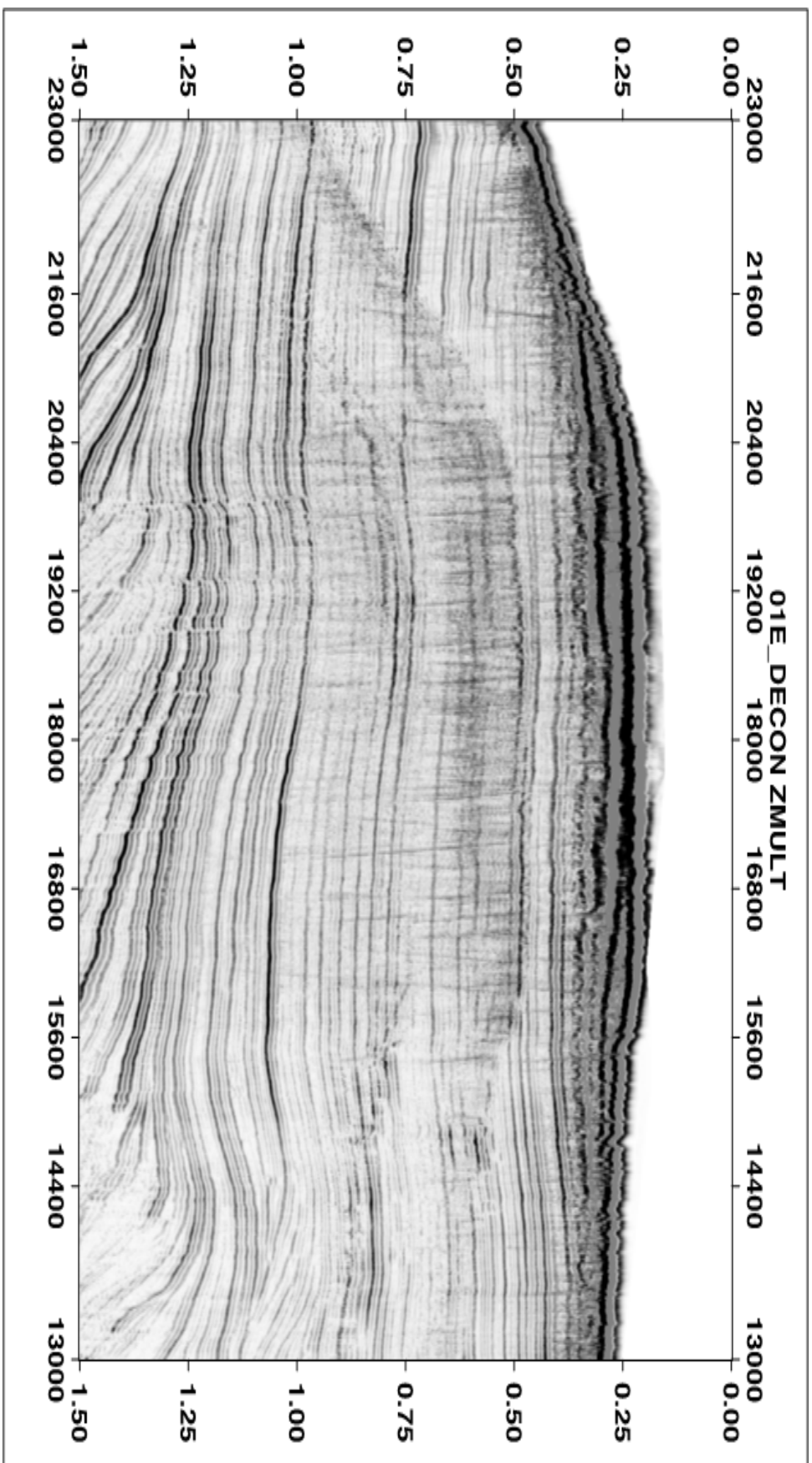
A. Appendix A

Figure A.1. – Stacked section of Line 01E with the applied multiple suppression methods De-convolution and f-k overcorrection filter.
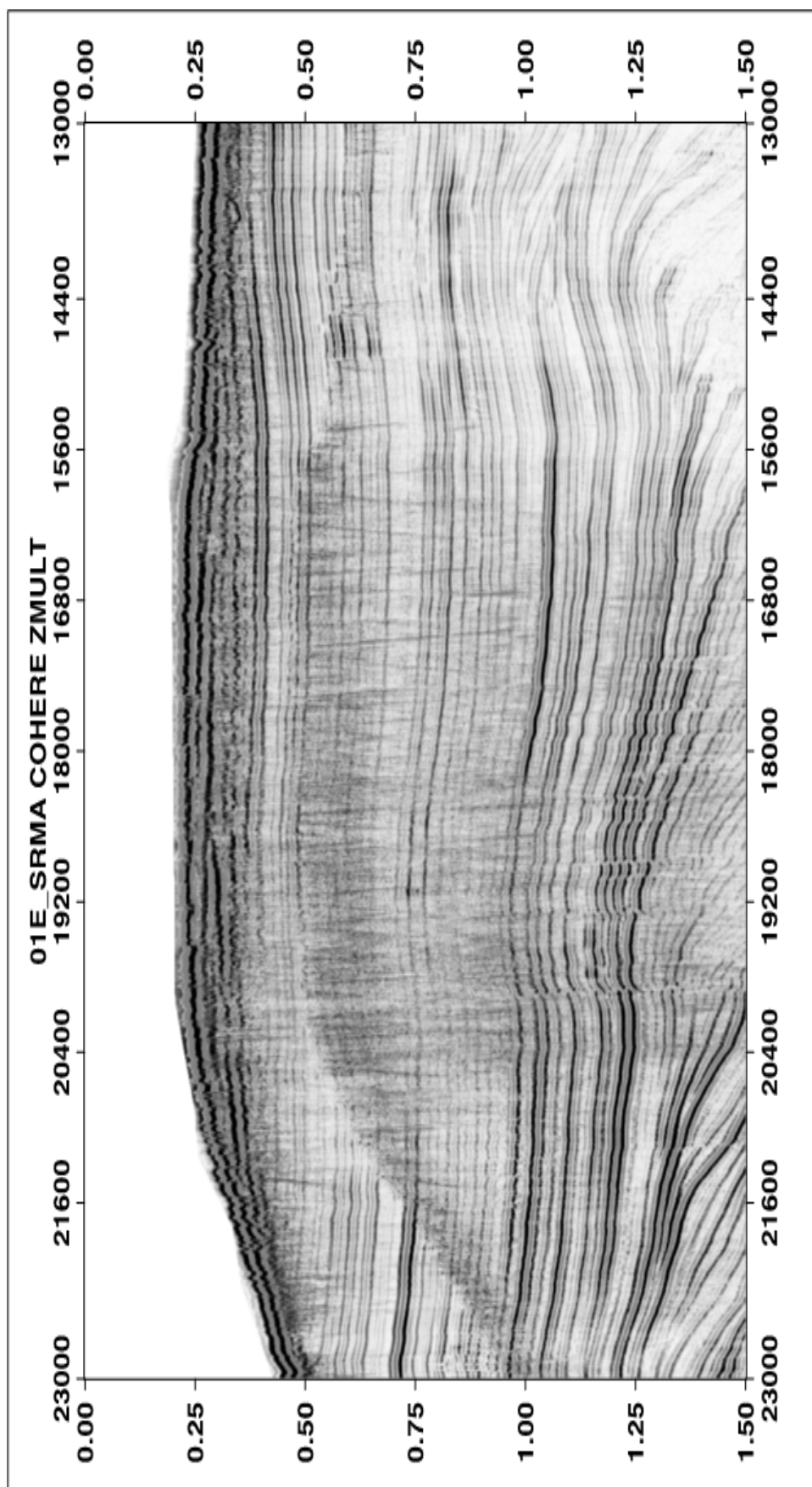
Figure A.2. – Stacked section of Line 01E with the applied multiple suppression methods SRMA, dip and f-k overcorrection filter.
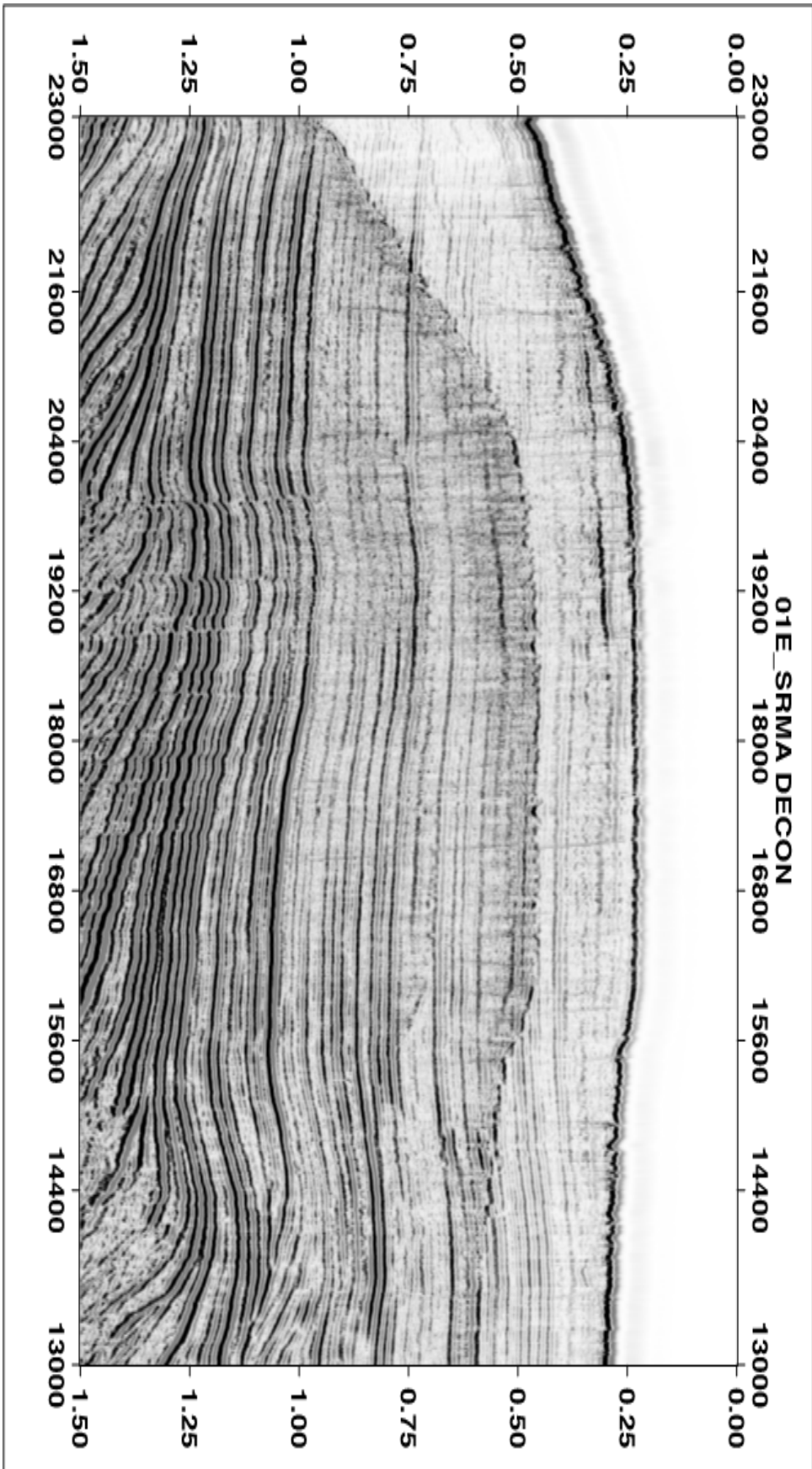
Figure A.3. – Stacked section of Line 01E with the applied multiple suppression methods SRMA and Deconvolution.
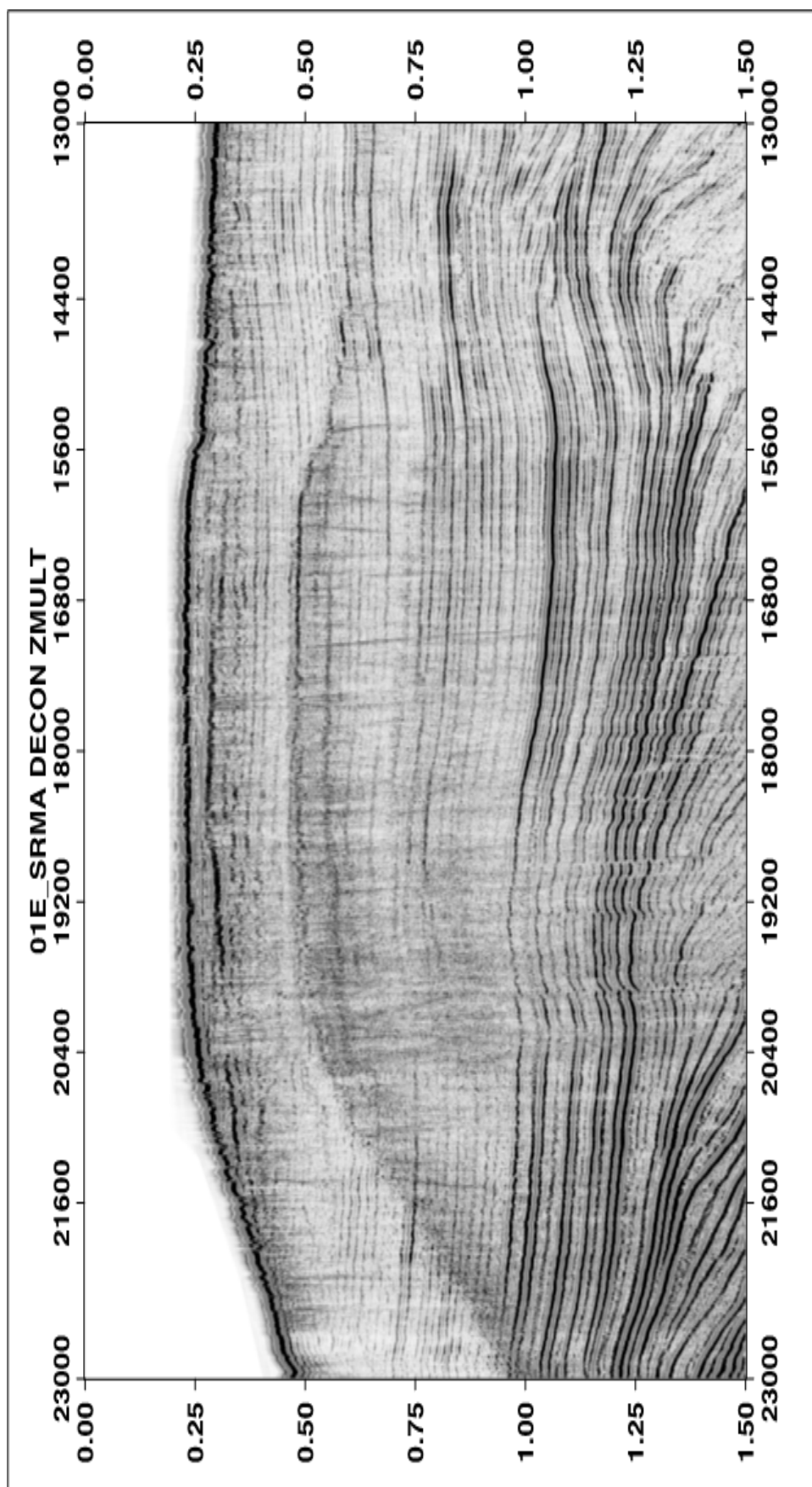
Figure A.4. – Stacked section of Line 01E with the applied multiple suppression methods SRMA, Deconvolution and f-k overcorrection filter.
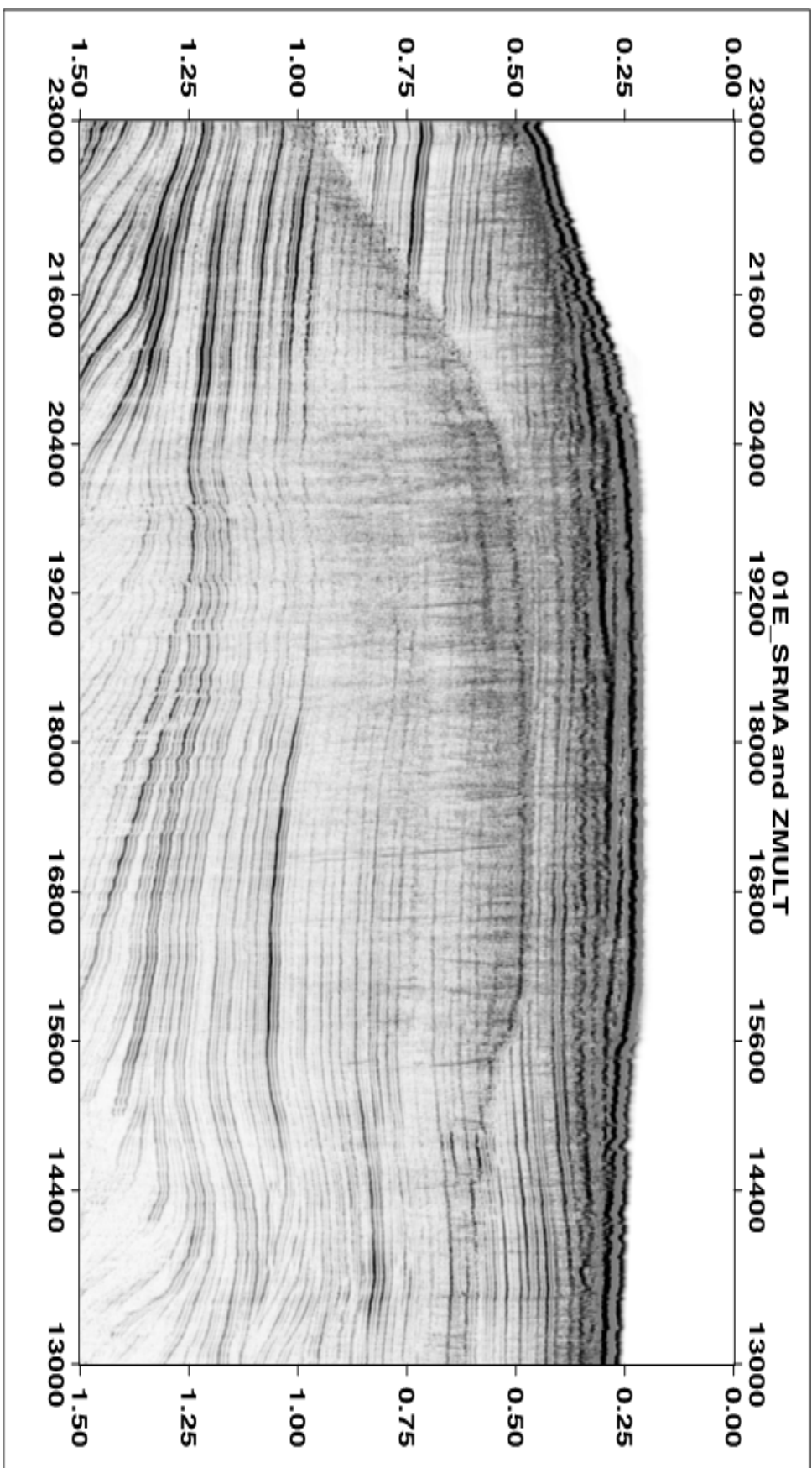
Figure A.5. – Stacked section of Line 01E with the applied multiple suppression methods SRMA and f-k overcorrection filter.